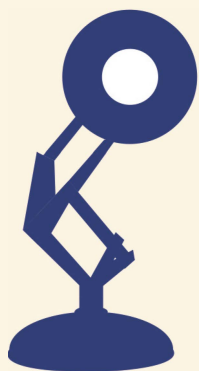


A stylized anatomical diagram of the prostate gland and associated structures. The diagram is composed of various shades of blue and yellow. The prostate gland is shown in a light blue color, with the ureters and vas deferens entering from the top. The ureters are shown as white structures with a grid-like pattern. The vas deferens are shown as dark blue lines. The diagram is set against a background of dark blue and light blue shapes, with a yellow area on the left side.

**J.G. Heetman**

NEW INSIGHTS IN  
THE DETECTION  
AND STAGING OF  
PROSTATE  
**CANCER**



NEW INSIGHTS IN  
THE DETECTION  
AND STAGING OF  
PROSTATE CANCER

**J.G. Heetman**

## **New Insights in the Detection and Staging of Prostate Cancer**

PhD thesis, Utrecht University, The Netherlands

©J.G. Heetman, Utrecht, 2024

All rights reserved. No part of this thesis may be reproduced or transmitted in any form or by any means without prior written permission from the author. The copyright of the papers that have been published or have been accepted for publication has been transferred to the respective journals.

The research presented in this thesis was financially supported by St. Antonius Onderzoeksfonds

Printing: ridderprint  
Cover design and layout: @evelienjagtman.com

ISBN: 978-94-6506-309-6

# NEW INSIGHTS IN THE DETECTION AND STAGING OF PROSTATE CANCER

**Nieuwe inzichten in het detecteren en stadiëren van prostaatkanker**

(met een samenvatting in het Nederlands)

## **Proefschrift**

ter verkrijging van de graad van doctor aan de  
Universiteit Utrecht  
op gezag van de  
rector magnificus, prof. dr. H.R.B.M. Kummeling,  
ingevolge het besluit van het College voor Promoties  
in het openbaar te verdedigen op

donderdag 19 september 2024 des ochtends te 10.15 uur

door

**Joris Gilles Heetman**

geboren op 21 januari 1993  
te Assen

**Promotor:**

Prof. dr. M.G.E.H. Lam

**Copromotoren:**

Dr. R.C.N. van den Bergh

Dr. H.H.E. van Melick

**Beoordelingscommissie:**

Prof. dr. P.J. van Diest

Prof. dr. ir. H.W.A.M. de Jong

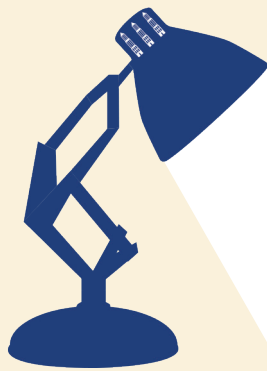
Prof. dr. L.M.O. de Kort (voorzitter)

Prof. dr. M.P.W. Intven

Prof. dr. A.N. Vis

# Contents

Chapter 1	General Introduction and Thesis Outline	7
<hr/>		
<b>Part I: The Detection of Clinically Significant Prostate Cancer</b>		
<hr/>		
Chapter 2:	Immunohistochemical and Histopathological Validation of <sup>18</sup> F-PSMA-1007 PET/CT for Intraprostatic Cancerous Lesions	35
Chapter 3:	The Additional Value of <sup>68</sup> Ga-PSMA PET/CT SUVmax in Predicting ISUP GG $\geq$ 2 and ISUP GG $\geq$ 3 Prostate Cancer in Biopsy	57
Chapter 4:	Gallium-68 Prostate-specific Membrane Antigen Positron Emission Tomography/Computed Tomography in Active Surveillance for Prostate Cancer Trial (PASPoRT)	75
Chapter 5:	Clinically Significant Prostate Cancer Diagnosis without Histological Proof: A Possibility in the Prostate-Specific Membrane Antigen Era?	93
<hr/>		
<b>Part II: The Adequate Staging of Prostate Cancer</b>		
<hr/>		
Chapter 6:	External Validation of Nomograms Including MRI Features for the Prediction of Side-specific Extraprostatic Extension	103
Chapter 7:	A Side-specific Nomogram for Extraprostatic Extension may Reduce The Positive Surgical Margin Rate in Radical Prostatectomy	127
Chapter 8:	Is Cribriform Pattern in Prostate Biopsy a Risk Factor for Metastatic Disease on <sup>68</sup> Ga-PSMA-11 PET/CT?	147
Chapter 9:	General Summary	163
Chapter 10:	General Discussion and Future Perspectives	169
<hr/>		
<b>Appendices</b>		
<hr/>		
	Dutch Summary – Nederlandse Samenvatting	189
	List of Publications	197
	Curriculum Vitae Auctoris	201
	Dankwoord	207





# CHAPTER 1

GENERAL INTRODUCTION  
AND THESIS OUTLINE



## Prostate Cancer

In 2021, over 13,500 patients in the Netherlands were diagnosed with prostate cancer (PCa), and more than 3,000 patients succumbed to the disease.<sup>1</sup> This discrepancy between incidence and mortality illustrates that not all forms of PCa significantly impact life expectancy, as the disease ranges from indolent to aggressive. Accurate detection and staging of PCa is crucial for providing patients with the best possible treatment, aiming to enhance both their life expectancy and quality of life on one side and avoiding unnecessary diagnosis and treatments on the other side. Multiple curative treatments are available for localised prostate cancer, each with a distinct impact on quality of life post-treatment.<sup>2</sup> However, selecting the optimal treatment is a challenging issue, as between 13% and 19% of patients experience treatment regret.<sup>3</sup>

### Expectant Management for Prostate Cancer

Historically, PCa was often diagnosed at an advanced, incurable stage.<sup>4,5</sup> Today, the diagnosis of PCa predominantly occurs at earlier stages, frequently initiated by elevated prostate-specific antigen (PSA) levels identified during routine check-ups, leading to the detection of localised prostate cancer.<sup>6</sup> Not only has early detection through screening increased the likelihood of curative outcomes, decreasing PCa-specific mortality on a population level, but it has also escalated the diagnosis of indolent cancers that may not impact the patient adversely if left undiscovered.<sup>7</sup>

To counteract the risk of unnecessary treatment-related morbidity in newly diagnosed patients, expectant management strategies such as watchful waiting (WW) and active surveillance (AS) are utilised. WW is a conservative approach for patients unlikely to benefit from curative treatment due to advanced age or comorbidities, delaying the commencement of palliative treatments such as hormonal therapy. Conversely, AS is intended to postpone unnecessary treatments and their side effects in men with clinically localised PCa and a life expectancy exceeding 10 years, while ensuring a timely curative intervention when this becomes necessary.<sup>8</sup>

AS demands intensive follow-up protocols, typically consisting of periodic repeat prostate biopsies (every 1–3 years) and PSA monitoring (every 3–6 months), which are crucial for identifying when the disease progresses to a stage necessitating active treatment.

Although there are no formal RCTs directly comparing AS with curative treatments, cohort studies investigating AS in low-risk PCa report a 10-year prostate cancer-specific survival rate between 96% and 100% for both low and intermediate-risk PCa.<sup>9</sup> Notably, 27.5% of patients on AS experience disease upgrading at 5 years follow up and switch to an active treatment.<sup>10</sup>

The current preference for managing low-risk and selected intermediate-risk PCa is AS, as recommended by European Association of Urology guidelines.<sup>11</sup> Advances in risk stratification, aided by magnetic resonance imaging (MRI) and targeted biopsies have led to a stage migration and broader inclusion criteria for AS.<sup>12-15</sup>

### **Prostatectomy**

Radical prostatectomy (RP) is the most commonly applied treatment for localised PCa; it has been shown to significantly increase life expectancy compared to expectant management in a randomised trial setting.<sup>16</sup> RP can be performed via open, laparoscopic, or robot-assisted (RARP) approaches. The evolution of this surgery began with the open technique of RP introduced by Young in 1904 through a perineal approach.<sup>17</sup> The retropubic approach, which gained popularity after Walsh and Donker's anatomical descriptions in 1982, allowed early control of the dorsal venous complex and preservation of the cavernous nerves, facilitating bilateral nerve-sparing procedures.<sup>18</sup>

An advancement came in 2002 with the introduction of the RARP using the da Vinci Surgical System®.<sup>19</sup> This method combines the minimally invasive benefits of laparoscopic RP with enhanced surgeon ergonomics and technical ease, particularly in the suture reconstruction of the vesicourethral anastomosis. A randomised phase 3 trial demonstrated RARP's superiority in terms of reduced admission times and blood loss compared to open RP, although no significant differences were observed in early (12 weeks) functional or oncological outcomes.<sup>20</sup> Subsequent analysis at 24 months confirmed these findings, revealing no significant disparities in functional outcomes between the approaches.<sup>21</sup> A systematic review and meta-analysis in 2016, including two small randomised controlled trials (RCTs) comparing RARP with laparoscopic RP (LRP), suggested higher rates of erectile function retention and continence in the RARP group.<sup>22</sup> However, a comprehensive Cochrane review, encompassing comparisons of either RARP or LRP with open RP, found no significant differences in oncological, urinary, and sexual function outcomes, though RARP and LRP were superior in reducing hospital stay durations and blood transfusion rates.<sup>23</sup> These findings have led to the current perspective that no single surgical approach is universally recommended in the guidelines. Nonetheless, RARP has become the preferred minimally invasive approach when available.

The outcomes post-prostatectomy are influenced by the surgeon's expertise and the hospital's volume of such procedures.<sup>24,25</sup> During RARP, the preservation of neurovascular bundles, which contain parasympathetic nerve branches of the pelvic plexus, can contribute to the retention of erectile function.<sup>18,26</sup>

## Radiotherapy

In the current landscape of PCa treatment, radiotherapy is considered one of the standards of care as a curative option. The standard approach in external beam radiation therapy (EBRT) now employs Intensity-modulated Radiotherapy (IMRT) and Volumetric Arc Therapy (VMAT), often augmented by Image-Guided Radiotherapy (IGRT). These advanced techniques mark a paradigm shift from traditional radiotherapy methods, offering precision targeting of cancer cells while minimising collateral damage to the surrounding tissues.<sup>27</sup>

Dose escalation is a pivotal aspect of contemporary radiotherapy for prostate cancer. Research indicates that higher radiation doses can have a significant impact on biochemical relapse.<sup>28</sup> The challenge, however, is to balance these escalated doses with the potential for increased treatment-related toxicity.

Radiotherapy is frequently combined with neoadjuvant or adjuvant hormone therapy. This combination has been definitively shown to be superior to radiotherapy alone, particularly for patients with high-risk PCa, and is debatable for those with intermediate-risk PCa.<sup>29,30</sup>

Moreover, brachytherapy, whether in low-dose-rate (LDR) or high-dose-rate (HDR) modalities, remains a key therapeutic option. It is employed as monotherapy for low-risk patients or in conjunction with EBRT for those at higher risk, delivering high biological doses directly to the tumour. The decision between LDR or HDR brachytherapy depends on various factors, including tumour characteristics and patient preferences, highlighting the necessity for personalised treatment planning.

Recent advancements in radiotherapy have introduced the concept of MR-guided adaptive RT. This innovative approach utilises real-time high-field (up to 1.5 T) MRI to monitor the prostate and adjacent tissues during EBRT sessions. It enables the adaptation of the radiotherapy plan in response to the movement and deformation of the prostate and the surrounding tissues, aiming to minimise radiation exposure to healthy tissues.<sup>31</sup> The integration of such cutting-edge techniques into standard care and their impact on patient outcomes remains an active field of research and development.

## Systematic Treatment of Metastatic Disease

Treatment in metastatic PCa is highly individualised, considering factors such as the volume of the disease, the patient's overall health, and the potential side effects. The basis of metastatic PCa treatment is Androgen Deprivation Therapy (ADT).<sup>32</sup> ADT reduces testosterone levels, which PCa cells rely on for growth. Luteinizing hormone-releasing hormone (LHRH) agonists and antagonists are commonly used.

The integration of chemotherapy, particularly docetaxel, into the treatment regimen for metastatic PCa has marked a significant advancement in the treatment of metastatic PCa. Clinical trials have demonstrated that adding docetaxel to ADT significantly improves overall survival, especially in patients with high-volume metastatic disease.<sup>33-35</sup>

The introduction of new Androgen receptor pathway inhibitors (ARPIs) such as abiraterone acetate, enzalutamide, and apalutamide has revolutionised the treatment landscape of metastatic PCa. Large-scale clinical trials have consistently shown that the addition of ARPIs to ADT significantly improves survival outcomes.<sup>36-38</sup> These agents block the androgen receptor signalling pathway more effectively, which is crucial for PCa cell growth. They are particularly effective in patients with newly diagnosed metastatic disease; this shows its benefits across various subgroups, including those with high and low disease volumes.

## Diagnosing Prostate Cancer

For the best treatment selection, an adequate diagnostic pathway is crucial, resulting in the proper grade and stage of the disease. The more accurately the aggressiveness and stage of the disease are identified during the diagnosis, the higher the likelihood of selecting the treatment option providing the best value in terms of oncological and health-related quality of life outcomes. The European Association of Urology risk groups of localised and locally advanced PCa are shown in Table 1.<sup>11</sup> These are based on the risk of biochemical recurrence after surgery.

**Table 1:** The European Association Urology risk group for biochemical recurrence of localised and locally advanced prostate cancer

Low-risk	Intermediate risk	High-risk	
PSA <0.10 ng/ml	PSA 10-20 ng/ml	PSA >20 ng/ml	Any PSA
And ISUP GG 1	Or ISUP GG 2/3	Or ISUP GG 4/5	any
And cT1-2	Or cT2b	Or cT2c	cT3-4 or cN+
Localised	Locally advanced		

PSA = Prostate-specific antigen, ISUP GG = International Society of Urologic Pathology Grade Group, cT = clinical T stadium

### Clinical T-stage

The clinical T (cT) stadium describes the primary tumour's size and extent. In PCa, digital rectal examination (DRE) is the conventional method for determining the cT of the tumour. DRE findings, such as the palpation of a nodule or evidence of extraprostatic extension (EPE), have been considered valuable for establishing the disease stage.<sup>5</sup> Since the inception of the first prostate cancer staging system, information regarding the primary tumour size assessed by DRE has been included as an essential component.<sup>5</sup> Over the years, staging systems have evolved, and cT is now an integral part of the widely accepted Tumour, Node, and Metastasis (TNM) classification of malignant tumours. Currently, the 8th Edition of the American Joint Committee on Cancer Staging Manual is utilised to define the cT category (Table 2).<sup>39</sup>

### Histological Grading of Prostate Cancer

Histological analysis can be performed on prostate needle biopsies. These can be performed systematically (applying a fixed pattern) or targeted on a legion. The Gleason grading system, introduced by Donald Gleason in 1966, revolutionised the grading of PCa by emphasising histological architecture.<sup>40</sup> His system is essential for predicting mortality rates and complements clinical tumour staging.<sup>41</sup> It entails assigning a primary score to

the most dominant tumour pattern (representing over 50% of the observed pattern) and a secondary score to the next most prevalent pattern (representing less than 50%). The sum of these two scores, which can range from 2 to 10, constitutes the Gleason score. The system has evolved: the 2005 and 2014 International Society of Urologic Pathology (ISUP) consensus meetings discontinued the use of Gleason patterns 1 and 2, limiting the grades to a range from 3 to 5, and they are combined in the ISUP Group Grade (GG) as can be seen in Table 3 and Figure 1.<sup>42,43</sup>

**Table 2:** Shows clinical T-stage following the definition of the American Joint Committee on Cancer

TX	<u>Primary tumour cannot be assessed</u>
T0	<u>No evidence of primary tumour</u>
T1	<u>Clinically inapparent tumour that is not palpable</u>
a	Tumour incidental histologic finding in 5% or less of tissue resected
b	Tumour incidental histologic finding in more than 5% of tissue resected
c	Tumour identified by needle biopsy found in one or both sides, but not palpable
T2	<u>Tumour is palpable and confined within prostate</u>
a	Tumour involves one-half of one side or less
b	Tumour involves more than one-half of one side but not both sides
c	Tumour involves both sides
T3	<u>Extraprostatic tumour that is not fixed or does not invade adjacent structures</u>
a	Extraprostatic extension (unilateral or bilateral)
b	Tumour invades seminal vesicle(s)
T4	<u>Tumour is fixed or invades adjacent structures other than seminal vesicles, such as external sphincter, rectum, bladder, levator muscles, and/or pelvic wall</u>

Another key histological aspect is the tumour's growth pattern, with the cribriform pattern (CP) being one of the four patterns in Gleason pattern 4 prostate cancer. CP is characterised by a sieve-like appearance under the microscope and is associated with a higher risk of metastatic recurrence and a shorter time to biochemical recurrence.<sup>44-48</sup> CP also correlates with an increased likelihood of positive lymph nodes during pelvic lymph node dissection.<sup>49</sup> Given its prognostic importance, the ISUP recommends reporting the presence of CP in both prostate biopsies and prostatectomy specimens, regardless of the ISUP GG.<sup>50,51</sup>



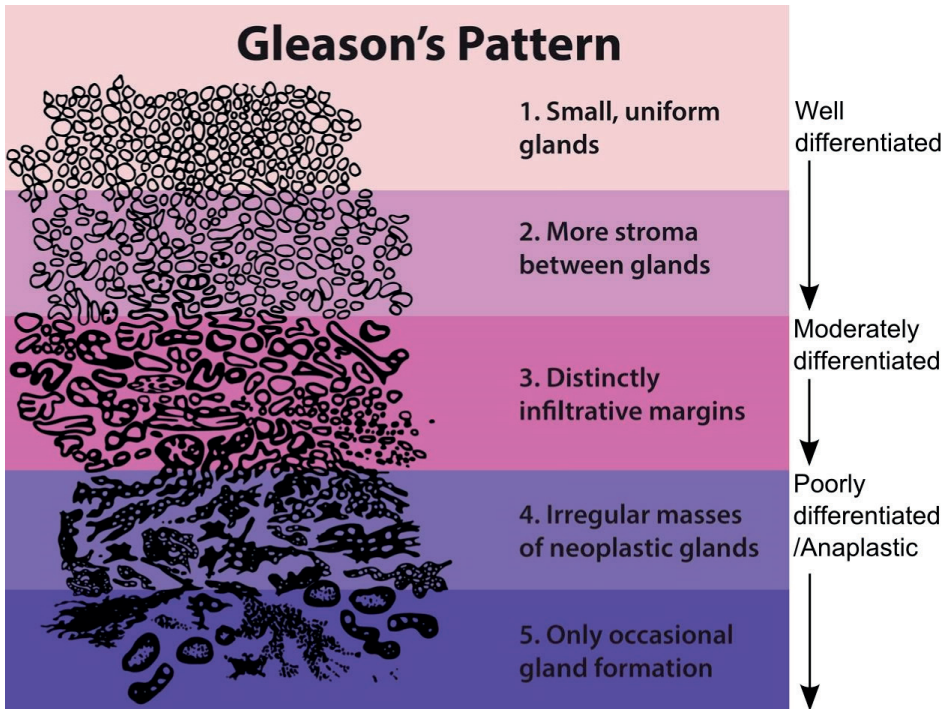


**Figure 1:** The International Society of Urological Pathology grading system

### Prostate-Specific Antigen

Prostate-specific antigen (PSA) was introduced by Wang *et al.* in 1979.<sup>52</sup> PSA is a serum marker that is specific to the prostate organ but not to cancer; thus, it can also be elevated in benign prostatic hyperplasia, prostatitis, and other non-malignant conditions. The widespread implementation of PSA testing in a screening setting has led to an increase in the diagnosis of PCa, particularly in detecting indolent disease at an early stage. Beyond its roles in screening and monitoring, PSA has proven to be a valuable prognostic indicator. For instance, high preoperative PSA levels are associated with an increased likelihood of extracapsular extension, seminal vesicle invasion, an elevated risk of biochemical progression following radical prostatectomy, and metastases.<sup>53</sup>

**Table 3:** The International Society of Urological Pathology (ISUP) grading system

ISUP Grade Group	Gleason scores	Definition
1	3+3=6	Only individual discrete well-formed glands
2	3+4=7	Predominantly well-formed glands with lesser component of poorly formed/fused/cribriform glands
3	4+3=7	Predominantly poorly formed/fused/cribriform glands with lesser component of well-formed glands
4	4+4=8 3+5=8 5+3=8	Only poorly formed/fused/cribriform glands Predominantly well-formed glands and lesser component lacking glands (or with necrosis) Predominantly lacking glands (or with necrosis) and lesser component of well-formed glands
5	4+5=9 5+4=9 5+5=10	Lacking gland formation (or with necrosis) with or without poorly formed/fused/cribriform glands

## Imaging in Prostate Cancer

Imaging plays a critical role in the detection and staging of PCa, from detecting abnormal lesions within the prostate to guiding biopsies and detecting metastatic disease. Due to the rapid development of new techniques, their effects on long-term outcomes are not always clear before they are adopted in clinical use.

### Transrectal Ultrasound

First introduced in the early 1970s, Transrectal Ultrasound (TRUS) has long been the established 'gold standard' for imaging of the prostate. PCa may sometimes present as a hypoechoic lesion on grayscale TRUS, as can be seen in Figure 2; however, the absence of such lesions does not preclude the disease. Furthermore, targeting hypoechoic lesions for biopsy has not shown a significant increase in the detection of PCa compared to sampling from isoechoic areas.<sup>54</sup> Owing to its limited sensitivity and specificity, TRUS alone is insufficient for a definitive PCa diagnosis; a biopsy remains indispensable. It is now mainly used for guiding biopsy cores during the diagnosis of PCa via needle biopsy.<sup>55</sup>

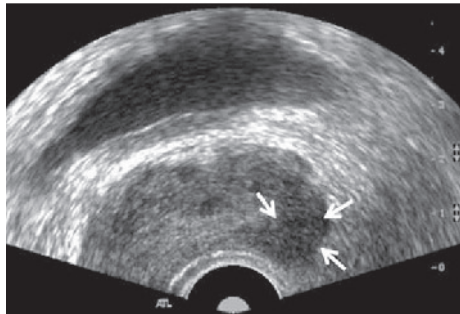


**Figure 2:** Transrectal Ultrasound of the prostate with prostate cancer

### Magnetic Resonance Imaging

In the early 1980s, the first study of Magnetic Resonance Imaging (MRI) of the prostate gland was conducted by Steyn and Smith, marking a pivotal moment in the imaging of PCa.<sup>56</sup> The initial technology was rudimentary, featuring a four-coil air-cored magnetic ring, with a static magnetic field of 0.04 T and thickness of 17.53 mm, which was used to distinguish between benign prostatic hyperplasia and prostate cancer. The advantage of high-field-strength magnets and phased-array coils has significantly enhanced image quality, improving the technique's accuracy in detecting clinical significant (cs) PCa aiding treatment planning, and detecting early recurrence.<sup>57</sup>

In the 1990s, the concept of multiparametric MRI (mpMRI) emerged, combining T2-weighted imaging, diffusion-weighted imaging (DWI), and dynamic contrast-enhanced MRI (DCE-MRI). The use of contrast in prostate MRI has evolved rapidly, with studies highlighting the utility of dynamic contrast enhancement in evaluating tumour margins.<sup>58</sup> However, the use of contrast is debatable, as biparametric (bp) MRI, which does not use contrast and thereby does not have a DCE series, is comparably effective in detecting EPE.<sup>59</sup> Figure 3 shows a patient with a suspicion of EPE on MRI.

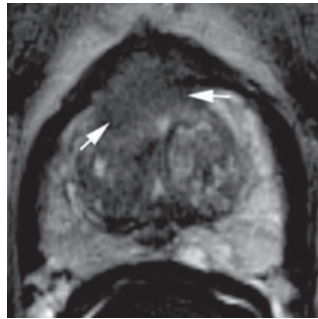


**Figure 3:** Extra prostatic extension of the transition zone on T2-weighted imaging from the Prostate Imaging –Reporting and Data System 2009 version 2.1 manual

The evolution of MRI technology has also led to advancements in coil design and magnetic field strength. Early prostate MRI studies used conventional body coils with limited anatomic resolution. In 1989, the development of an endorectal surface coil for use with a 1.5-T system greatly improved image quality, providing superior visualisation of prostate findings compared to images obtained with a body coil.<sup>60</sup> Technically, the endorectal coil significantly enhances the signal-to-noise ratio, yielding higher-resolution T2-weighted imaging and more accurate staging due to better delineation of the prostate capsule in a 1.5-T MRI. The necessity of endorectal coils for the more powerful 3-T MRI systems has not yet been conclusively proven.<sup>61–63</sup>

**Table 4:** Prostate Imaging-Reporting and Data System

PI-RADS 1	Clinically significant cancer highly unlikely
PI-RADS 2	Clinically significant cancer unlikely
PI-RADS 3	Clinically significant cancer equivocal
PI-RADS 4	Clinically significant cancer likely
PI-RADS 5	Clinically significant cancer highly likely

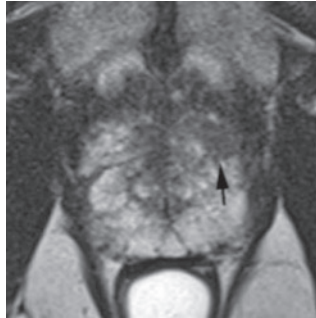


**Figure 4:** PI-RADS 4 lesion in peripheral zone on T2-weighted imaging from the Prostate Imaging –Reporting and Data System 2009 version 2.1 manual

Currently, mpMRI of the prostate is integral to the clinical pathway of PCa and is recommended before prostate biopsy according to the guidelines.<sup>11</sup> Reporting is standardised with the Prostate Imaging-Reporting and Data System (PI-RADS), as can be seen in Table 4, and an example of a PI-RADS 4 lesion is shown in Figure 4.<sup>64</sup>

### **Positron Emission Tomography/Computed Tomography**

Prostate-specific Membrane Antigen (PSMA) is a transmembrane protein overexpressed in most PCa.<sup>65</sup> Initially studied in neuronal tissue as N-acetyl-L-glutamate peptidase (NAALADase), PSMA increases the concentration of the excitatory neurotransmitter glutamate by splitting N-acetylaspartylglutamic acid into glutamate and N-Acetyl acetic acid. However, due to its hydrophilic nature, it was unsuitable for brain imaging as it could not cross the blood-brain barrier.<sup>66</sup> Later, PSMA was found to be present in prostate cells, with marked overexpression in most PCa. PSMA also has a role in PCa due to its folate hydrolase 1 function, cleaving folate from poly-g-glutamate folate to make it available for cellular metabolism.<sup>67</sup> High folate concentration is associated with increased tumour growth and invasiveness<sup>68</sup>

High PSMA expression in biopsy and RP specimens has been identified as an independent predictor of PCa recurrence following treatment with curative intent.<sup>69</sup> Furthermore, the level of PSMA expression in PCa is higher in castration-resistant PCa compared to metastatic hormone-sensitive PCa, and higher still compared to localised PCa. This gradient of PSMA expression across different PCa stages suggests that its level is proportional to tumour aggressiveness and patient outcomes.<sup>69</sup>

PSMA can be visualised using PSMA-Positron Emission Tomography/Computed Tomography (PSMA PET/CT), where PSMA is tagged with a radioactive tracer, as can be seen in Figure 5. A range of molecular ligands designed to target PSMA, conjugated with both diagnostic and therapeutic radionuclides, ushers in a new era for PCa imaging and treatment. Prominent

radioligands are  $^{68}\text{Ga}$ -PSMA-11,  $^{18}\text{F}$ -DCFPyL and  $^{18}\text{F}$ -rhPSMA-7.3. Their efficacy is supported by robust phase 3 clinical trials demonstrating superior performance, resulting in daily use of these tracers (Table 5).<sup>70-72</sup> However, their impact on disease-specific survival remains under investigation, with guidelines advocating cautious use.<sup>11</sup>

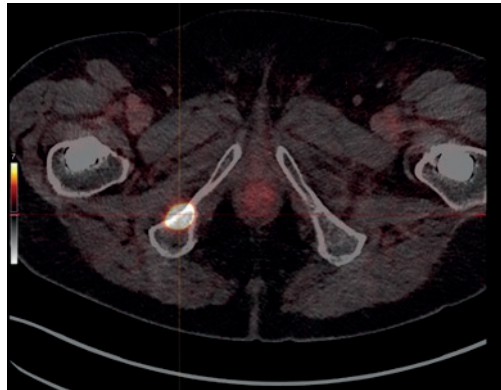


**Figure 5:** Bone metastases on PSMA PET/CT

**Table 5:** Phase 3 trials for PSMA PET/CT in the initial staging of patients suspected for metastatic prostate cancer

Radioligands	Author	Study
$^{68}\text{Ga}$ -PSMA-11	Hope 2021 <sup>70</sup>	Diagnostic Accuracy of $^{68}\text{Ga}$ -PSMA-11 PET for Pelvic Nodal Metastasis Detection Prior to Radical Prostatectomy and Pelvic Lymph Node Dissection: A Multicenter Prospective Phase 3 Imaging Trial.
$^{18}\text{F}$ -DCFPyL	Pienta 2021 <sup>71</sup>	A Phase 2/3 Prospective Multicenter Study of the Diagnostic Accuracy of Prostate Specific Membrane Antigen PET/CT with $^{18}\text{F}$ -DCFPyL in Prostate Cancer Patients (OSPREY)
$^{18}\text{F}$ -rhPSMA-7.3	Surasi 2023 <sup>72</sup>	Diagnostic Performance and Safety of Positron Emission Tomography with $^{18}\text{F}$ -rhPSMA-7.3 in Patients with Newly Diagnosed Unfavourable Intermediate- to Very-high-risk Prostate Cancer: Results from a Phase 3, Prospective, Multicentre Study (LIGHTHOUSE)

## The Role of Imaging in Diagnosis and Treatment Planning

The expansion of the use of imaging of the prostate itself and the potential dissemination in PCa has significantly impacted diagnosis, staging, treatment planning, and follow-up.

### Diagnosis of Prostate Cancer

In the Netherlands, the diagnostic pathway typically begins with a general practitioner noting an elevated PSA or abnormal DRE. Before undergoing a prostate biopsy, nearly all patients receive an MRI. The pre-biopsy MRI has led to a significant shift in biopsy strategy, allowing patients without risk factors and a negative MRI to safely omit biopsy, while those with suspected lesions receive targeted biopsies.<sup>72</sup> Current guidelines recommend performing systematic biopsies as well. However, recent research suggests that systematic biopsies could be omitted to reduce the number of procedures.<sup>73</sup> The precision of targeted biopsies guided by pre-biopsy MRI has led to an increase in the average Gleason score found as well as a stage migration, which consequently leads to a broadening of the criteria for AS.<sup>15,74</sup> Yet, this imaging technique is not foolproof, and a histological biopsy remains mandatory to confirm csPCa. In fact, 17% of biopsies for lesions with a maximum PI-RADS score of 5 confirm nonsignificant PCa or benign tissue.<sup>72</sup>

Although primarily indicated for staging lymph nodes and distant metastatic diseases, the clinical utility of PSMA PET/CT in detecting primary PCa is increasingly being researched. Figure 6 shows the PSMA activity in the prostate of a patient with PCa.

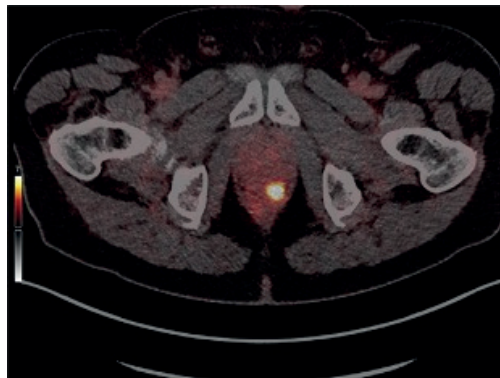


**Figure 6:** PSMA activity in the prostate on the PSMA PET/CT

Kalapara *et al.* observed a significantly higher median in the maximum standardised uptake value (SUVmax) of 6.40 (IQR 4.47–11.0) for ISUP GG 3–5 tumours compared to a median SUVmax of 3.14 (IQR 2.55–3.91) for benign and GG 1–2 tumours.<sup>75</sup> The PRIMARY trial

demonstrated the benefit of PSMA-PET/CT in detecting csPCa in the primary diagnostic setting. The study showed that local gland PSMA activity, defined as positive with an SUVmax of 4 or higher, in combination with MRI led to an improvement in the negative predictive value and sensitivity.<sup>76</sup> In a sub-analysis of the PRIMARY trial, Ptasznik *et al.* examined the combined results of MRI and PSMA PET/CT. All 53 patients with a PI-RADS score of 4 or 5 and an SUVmax greater than 8.7 were identified as having csPCa, defined as GG 2 or higher. The capabilities of this innovative molecular imaging modality may offer added value in the standard risk stratification pathway and in selecting patients for AS.<sup>80</sup> A general limitation of PET/CT in detecting intraprostatic cancer is the voxel size, which may cause lower SUVmax readings due to the partial-volume effect in smaller lesions, as depicted in Figure 6.<sup>81,82</sup> The impact of this on the detection of csPCa is not well understood.

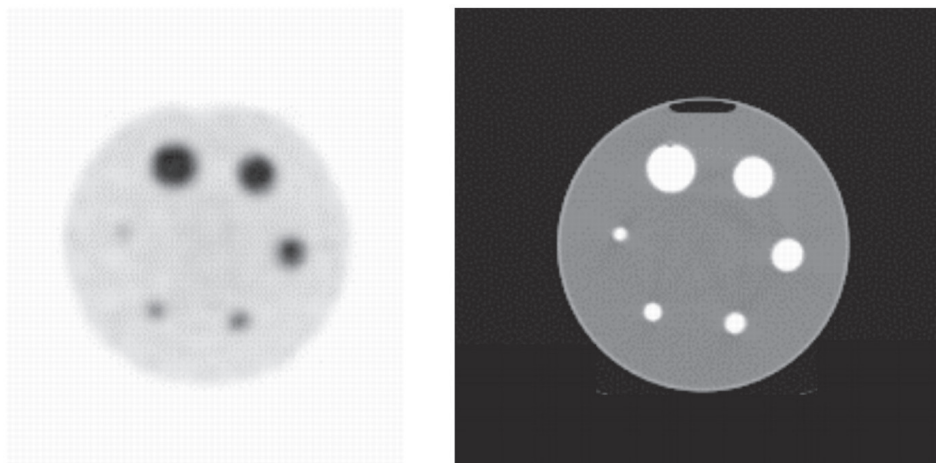


**Figure 7:** Transverse PET slice of 6 radioactive spheres with different diameters (10, 12, 16, 22, 28, and 34 mm) and filled with same radioactivity concentrations in uniform radioactive background (left) and corresponding CT slice (right). PVE makes apparent uptake decrease when sphere size decreases. This figure was originally published in JNM. Soret M, Bacharach SL, Buvat I. Partial-volume effect in PET tumor imaging. *J Nucl Med.* 2007 Jun;48(6):932-45© SNMMI.

### Local Staging and Treatment Planning

After detecting PCa, accurate staging is essential for selecting the optimal treatment for patients. Precise identification of extraprostatic extension (EPE) is particularly important when deciding on nerve-sparing RARP or devising the radiotherapy plan. However, one limitation of MRI is the detection of EPE. This challenge is critical because an incorrect assessment at this stage can lead to the risk of PSMs if a nerve-sparing prostatectomy is performed in patients with EPE. Despite MRI's high specificity for EPE detection (80–85%),



its per-prostate sensitivity remains low (57%), making MRI alone an unreliable predictor.<sup>83</sup> Therefore, guidelines advocate for nomogram-utilised approaches, incorporating MRI parameters for a more accurate EPE assessment.<sup>11,84</sup> The challenge with nomograms lies in determining the appropriate cut-off point for their use, their external validation, and their impact on patient outcomes.

While the nerve-sparing RARP can reduce the risk of erectile dysfunction, they are associated with an increased risk of positive surgical margins (PSM), which elevates the likelihood of disease recurrence and cancer-specific mortality.<sup>85,86</sup> Consequently, the European Association of Urology advises against nerve-sparing in cases with a high probability of extraprostatic extension (EPE).<sup>11</sup> Notably, EPE is present on only one side in most cases (85%), indicating that contralateral nerve-sparing could be an oncologically safe option.<sup>87</sup> The use of nomograms could help increase the number of nerve-sparing RARPs without increasing the risk of a PSM.

### **Screening for Metastatic Disease**

To select patients for curative treatment, accurate staging for potential lymph node invasion (LNI) or metastases is crucial. The proPSMA study demonstrated a higher sensitivity for PSMA PET/CT than for the combination of CT and bone scan in detecting either LNI or distant metastatic disease, at 85% (95% CI 74–96%) versus 38% (95% CI 23–31%), respectively.<sup>88</sup> Owing to the proPSMA trial and the phase 3 trials presented in Table 5, Dutch hospitals now employ PSMA PET/CT for patients at risk of LNI or metastatic disease. However, due to its cost and limited availability, it is essential to appropriately select patients who could benefit from additional staging imaging.

In summary, the new imaging modalities may importantly impact the diagnosis, staging, and treatment of PCa. Their specific role, however, needs to be further refined.

### **Thesis Objective and Structure**

The primary aim of this thesis is to explore how new imaging techniques can improve the detection and staging of prostate cancer, potentially refining patient selection for tailored treatment regimens. The focus will be on assessing the diagnostic efficacy of these methods and establishing optimal strategies for their clinical application. This thesis is structured into two main sections: Part I focuses on the detection of csPCa, while Part II addresses the appropriate staging of the disease.

#### **Part I: The Detection of Clinically Significant Prostate Cancer**

The advent of MRI has notably advanced the diagnostic process for csPCa, prompting recommendations for prostate MRI preceding biopsy.<sup>11</sup> Despite its advancements, MRI alone cannot verify csPCa without histological corroboration. PSMA PET/CT may also be able to

detect csPCa and may have additional value. **Chapter 2** examines the immunohistochemical and histopathological validation of PSMA PET/CT for intraprostatic lesions. Subsequently, **Chapter 3** deliberates on how combining local gland PSMA activity with MRI findings may improve csPCa prediction accuracy. **Chapter 4** assesses the value of this novel imaging modality in refining patient selection for AS, and **Chapter 5** discusses the necessity of prostate biopsy in the era of PSMA PET/CT.

## **Part II: The Adequate Staging of Prostate Cancer**

**Chapter 6** discusses the external validation of multiple nomograms within a European dataset, while **Chapter 7** investigates the impact of a nomogram predicting side-specific EPE on nerve-sparing and surgical margins at RARP. Accurate staging, including the evaluation of N and M stages, is crucial for patient selection for curative treatment. The emergence of PSMA PET/CT represents a significant advancement but also presents challenges, particularly concerning its cost and limited availability. As the demand for PSMA PET/CT scans grows, healthcare providers must navigate the complexities of its use. **Chapter 8** explores the potential of using CP presence in prostate biopsies as a criterion for selecting patients for staging PSMA PET/CT.

## References

- 1 Prostaatkanker. <https://iknl.nl/kankersoorten/prostaatkanker> (accessed 28 Nov2023).
- 2 Teunissen FR, Willigenburg T, Meijer RP, van Melick HHE, Verkooyen HM, van der Voort van Zyp JRN. The first patient-reported outcomes from the Utrecht Prostate Cohort (UPC): the first platform facilitating 'trials within cohorts' (TwiCs) for the evaluation of interventions for prostate cancer. *World J Urol* 2022. doi:10.1007/s00345-022-04092-2.
- 3 Fanshawe JB, Wai-Shun Chan V, Asif A, Ng A, Van Hemelrijck M, Cathcart P et al. Decision Regret in Patients with Localised Prostate Cancer: A Systematic Review and Meta-analysis. *Eur Urol Oncol* 2023; **6**: 456–466.
- 4 McClelland JC. THE EARLY DIAGNOSIS OF CANCER IN THE BLADDER, PROSTATE AND KIDNEY. *Can Med Assoc J* 1934; **31**: 165–167.
- 5 Mellinger GT. Carcinoma of the prostate. *J Lancet* 1963; **83**: 94–105.
- 6 Butler SS, Muralidhar V, Zhao SG, Sanford NN, Franco I, Fullerton ZH et al. Prostate cancer incidence across stage, NCCN risk groups, and age before and after USPSTF Grade D recommendations against prostate-specific antigen screening in 2012. *Cancer* 2020; **126**: 717–724.
- 7 Loeb S, Bjurlin MA, Nicholson J, Tammela TL, Penson DF, Carter HB et al. Overdiagnosis and overtreatment of prostate cancer. *Eur Urol* 2014; **65**: 1046–1055.
- 8 Bruinsma SM, Roobol MJ, Carroll PR, Klotz L, Pickles T, Moore CM et al. Expert consensus document: Semantics in active surveillance for men with localized prostate cancer - results of a modified Delphi consensus procedure. *Nat Rev Urol* 2017; **14**: 312–322.
- 9 Thomsen FB, Brasso K, Klotz LH, Røder MA, Berg KD, Iversen P. Active surveillance for clinically localized prostate cancer--a systematic review. *J Surg Oncol* 2014; **109**: 830–835.
- 10 Van Hemelrijck M, Ji X, Helleman J, Roobol MJ, van der Linden W, Nieboer D et al. Reasons for Discontinuing Active Surveillance: Assessment of 21 Centres in 12 Countries in the Movember GAP3 Consortium. *Eur Urol* 2019; **75**: 523–531.
- 11 Mottet N, van den Bergh RCN, Briers E, Van den Broeck T, Cumberbatch MG, De Santis M et al. EAU-EANM-ESTRO-ESUR-SIOG Guidelines on Prostate Cancer-2020 Update. Part 1: Screening, Diagnosis, and Local Treatment with Curative Intent. *Eur Urol* 2021; **79**: 243–262.
- 12 Kasivisvanathan V, Rannikko AS, Borghi M, Panebianco V, Mynderse LA, Vaarala MH et al. MRI-Targeted or Standard Biopsy for Prostate-Cancer Diagnosis. *N Engl J Med* 2018; **378**: 1767–1777.
- 13 Ahmed HU, El-Shater Bosaily A, Brown LC, Gabe R, Kaplan R, Parmar MK et al. Diagnostic accuracy of multi-parametric MRI and TRUS biopsy in prostate cancer (PROMIS): a paired validating confirmatory study. *Lancet* 2017; **389**: 815–822.
- 14 Ahdoot M, Wilbur AR, Reese SE, Lebastchi AH, Mehralivand S, Gomella PT et al. MRI-Targeted, Systematic, and Combined Biopsy for Prostate Cancer Diagnosis. *N Engl J Med* 2020; **382**: 917–928.
- 15 PRIAS project - Active surveillance -. <https://www.prias-project.org/> (accessed 22 Jun2022).
- 16 Bill-Axelson A, Holmberg L, Garmo H, Taari K, Busch C, Nordling S et al. Radical Prostatectomy or Watchful Waiting in Prostate Cancer - 29-Year Follow-up. *N Engl J Med* 2018; **379**: 2319–2329.
- 17 Hatzinger M, Hubmann R, Moll F, Sohn M. [The history of prostate cancer from the beginning to DaVinci]. *Aktuelle Urol* 2012; **43**: 228–230.
- 18 Walsh PC. The discovery of the cavernous nerves and development of nerve sparing radical retropubic prostatectomy. *J Urol* 2007; **177**: 1632–1635.

- 19 Binder J, Jones J, Bentas W, Wolfram M, Bräutigam R, Probst M et al. [Robot-assisted laparoscopy in urology. Radical prostatectomy and reconstructive retroperitoneal interventions]. *Urologe A* 2002; **41**: 144–149.
- 20 Yaxley JW, Coughlin GD, Chambers SK, Occhipinti S, Samaratunga H, Zajdlewicz L et al. Robot-assisted laparoscopic prostatectomy versus open radical retropubic prostatectomy: early outcomes from a randomised controlled phase 3 study. *Lancet* 2016; **388**: 1057–1066.
- 21 Coughlin GD, Yaxley JW, Chambers SK, Occhipinti S, Samaratunga H, Zajdlewicz L et al. Robot-assisted laparoscopic prostatectomy versus open radical retropubic prostatectomy: 24-month outcomes from a randomised controlled study. *Lancet Oncol* 2018; **19**: 1051–1060.
- 22 Allan C, Ilic D. Laparoscopic versus Robotic-Assisted Radical Prostatectomy for the Treatment of Localised Prostate Cancer: A Systematic Review. *Urol Int* 2016; **96**: 373–378.
- 23 Ilic D, Evans SM, Allan CA, Jung JH, Murphy D, Frydenberg M. Laparoscopic and robotic-assisted versus open radical prostatectomy for the treatment of localised prostate cancer. *Cochrane Database Syst Rev* 2017; **9**: CD009625.
- 24 Begg CB, Riedel ER, Bach PB, Kattan MW, Schrag D, Warren JL et al. Variations in morbidity after radical prostatectomy. *N Engl J Med* 2002; **346**: 1138–1144.
- 25 Gershman B, Meier SK, Jeffery MM, Moreira DM, Tollefson MK, Kim SP et al. Redefining and Contextualizing the Hospital Volume–Outcome Relationship for Robot-Assisted Radical Prostatectomy: Implications for Centralization of Care. *J Urol* 2017; **198**: 92–99.
- 26 Walz J, Epstein JI, Ganzer R, Graefen M, Guazzoni G, Kaouk J et al. A Critical Analysis of the Current Knowledge of Surgical Anatomy of the Prostate Related to Optimisation of Cancer Control and Preservation of Continence and Erection in Candidates for Radical Prostatectomy: An Update. *Eur Urol* 2016; **70**: 301–311.
- 27 Yu T, Zhang Q, Zheng T, Shi H, Liu Y, Feng S et al. The Effectiveness of Intensity Modulated Radiation Therapy versus Three-Dimensional Radiation Therapy in Prostate Cancer: A Meta-Analysis of the Literatures. *PLoS One* 2016; **11**: e0154499.
- 28 Dearnaley DP, Jovic G, Syndikus I, Khoo V, Cowan RA, Graham JD et al. Escalated-dose versus control-dose conformal radiotherapy for prostate cancer: long-term results from the MRC RT01 randomised controlled trial. *Lancet Oncol* 2014; **15**: 464–473.
- 29 Bolla M, Van Tienhoven G, Warde P, Dubois JB, Mirimanoff R-O, Storme G et al. External irradiation with or without long-term androgen suppression for prostate cancer with high metastatic risk: 10-year results of an EORTC randomised study. *Lancet Oncol* 2010; **11**: 1066–1073.
- 30 Preisser F, Cooperberg MR, Crook J, Feng F, Graefen M, Karakiewicz PI et al. Intermediate-risk Prostate Cancer: Stratification and Management. *Eur Urol Oncol* 2020; **3**: 270–280.
- 31 Teunissen FR, van der Voort van Zyp JRN, Wortel RC. Advances in erectile function-preserving radiotherapy for prostate cancer. *J Sex Med* 2023; **20**: 121–123.
- 32 Pagliarulo V, Bracarda S, Eisenberger MA, Mottet N, Schröder FH, Sternberg CN et al. Contemporary role of androgen deprivation therapy for prostate cancer. *Eur Urol* 2012; **61**: 11–25.
- 33 James ND, Sydes MR, Clarke NW, Mason MD, Dearnaley DP, Spears MR et al. Addition of docetaxel, zoledronic acid, or both to first-line long-term hormone therapy in prostate cancer (STAMPEDE): survival results from an adaptive, multiarm, multistage, platform randomised controlled trial. *Lancet* 2016; **387**: 1163–1177.
- 34 Sweeney CJ, Chen Y-H, Carducci M, Liu G, Jarrard DF, Eisenberger M et al. Chemohormonal Therapy in Metastatic Hormone-Sensitive Prostate Cancer. *N Engl J Med* 2015; **373**: 737–746.

- 35 Gravis G, Fizazi K, Joly F, Oudard S, Priou F, Esterni B et al. Androgen-deprivation therapy alone or with docetaxel in non-castrate metastatic prostate cancer (GETUG-AFU 15): a randomised, open-label, phase 3 trial. *Lancet Oncol* 2013; **14**: 149–158.
- 36 Davis ID, Martin AJ, Stockler MR, Begbie S, Chi KN, Chowdhury S et al. Enzalutamide with Standard First-Line Therapy in Metastatic Prostate Cancer. *N Engl J Med* 2019; **381**: 121–131.
- 37 Chi KN, Chowdhury S, Bjartell A, Chung BH, Pereira de Santana Gomes AJ, Given R et al. Apalutamide in Patients With Metastatic Castration-Sensitive Prostate Cancer: Final Survival Analysis of the Randomized, Double-Blind, Phase III TITAN Study. *J Clin Oncol* 2021; **39**: 2294–2303.
- 38 Fizazi K, Tran N, Fein L, Matsubara N, Rodriguez-Antolin A, Alekseev BY et al. Abiraterone plus Prednisone in Metastatic, Castration-Sensitive Prostate Cancer. *N Engl J Med* 2017; **377**: 352–360.
- 39 Buyyounouski MK, Choyke PL, McKenney JK, Sartor O, Sandler HM, Amin MB et al. Prostate cancer - major changes in the American Joint Committee on Cancer eighth edition cancer staging manual. *CA Cancer J Clin* 2017; **67**: 245–253.
- 40 Gleason DF. Classification of prostatic carcinomas. *Cancer Chemother Rep* 1966; **50**: 125–128.
- 41 Gleason DF. The Veterans Administration Cooperative Urological Research Group. Prediction of prognosis for prostatic adenocarcinoma by combined histological grading and clinical staging. *J Urol* 1974; **111**: 58–64.
- 42 Epstein JI, Allsbrook WC, Amin MB, Egevad LL, ISUP Grading Committee. The 2005 International Society of Urological Pathology (ISUP) Consensus Conference on Gleason Grading of Prostatic Carcinoma. *Am J Surg Pathol* 2005; **29**: 1228–1242.
- 43 Epstein JI, Egevad L, Amin MB, Delahunt B, Srigley JR, Humphrey PA et al. The 2014 International Society of Urological Pathology (ISUP) Consensus Conference on Gleason Grading of Prostatic Carcinoma: Definition of Grading Patterns and Proposal for a New Grading System. *Am J Surg Pathol* 2016; **40**: 244–252.
- 44 Kweldam CF, Wildhagen MF, Steyerberg EW, Bangma CH, van der Kwast TH, van Leenders GJLH. Cribriform growth is highly predictive for postoperative metastasis and disease-specific death in Gleason score 7 prostate cancer. *Mod Pathol* 2015; **28**: 457–464.
- 45 Dong F, Yang P, Wang C, Wu S, Xiao Y, McDougal WS et al. Architectural heterogeneity and cribriform pattern predict adverse clinical outcome for Gleason grade 4 prostatic adenocarcinoma. *Am J Surg Pathol* 2013; **37**: 1855–1861.
- 46 Hollemans E, Verhoef EI, Bangma CH, Rietbergen J, Roobol MJ, Helleman J et al. Clinical outcome comparison of Grade Group 1 and Grade Group 2 prostate cancer with and without cribriform architecture at the time of radical prostatectomy. *Histopathology* 2020; **76**: 755–762.
- 47 Hollemans E, Verhoef EI, Bangma CH, Rietbergen J, Osanto S, Pelger RCM et al. Cribriform architecture in radical prostatectomies predicts oncological outcome in Gleason score 8 prostate cancer patients. *Mod Pathol* 2021; **34**: 184–193.
- 48 Remmers S, Hollemans E, Nieboer D, Luiting HB, van Leenders GJLH, Helleman J et al. Improving the prediction of biochemical recurrence after radical prostatectomy with the addition of detailed pathology of the positive surgical margin and cribriform growth. *Ann Diagn Pathol* 2022; **56**: 151842.
- 49 Downes MR, Xu B, van der Kwast TH. Cribriform architecture prostatic adenocarcinoma in needle biopsies is a strong independent predictor for lymph node metastases in radical prostatectomy. *Eur J Cancer* 2021; **148**: 432–439.
- 50 van Leenders GJLH, van der Kwast TH, Grignon DJ, Evans AJ, Kristiansen G, Kweldam CF et al. The 2019 International Society of Urological Pathology (ISUP) Consensus Conference on Grading of Prostatic Carcinoma. *Am J Surg Pathol* 2020; **44**: e87–e99.

- 51 van der Kwast TH, van Leenders GJ, Berney DM, Delahunt B, Evans AJ, Iczkowski KA et al. ISUP Consensus Definition of Cribriform Pattern Prostate Cancer. *Am J Surg Pathol* 2021; **45**: 1118–1126.
- 52 Wang MC, Valenzuela LA, Murphy GP, Chu TM. Purification of a human prostate specific antigen. *Invest Urol* 1979; **17**: 159–163.
- 53 Freedland SJ, Hotaling JM, Fitzsimons NJ, Presti JC, Kane CJ, Terris MK et al. PSA in the new millennium: a powerful predictor of prostate cancer prognosis and radical prostatectomy outcomes--results from the SEARCH database. *Eur Urol* 2008; **53**: 758–764; discussion 765–766.
- 54 Onur R, Littrup PJ, Pontes JE, Bianco FJ. Contemporary impact of transrectal ultrasound lesions for prostate cancer detection. *J Urol* 2004; **172**: 512–514.
- 55 Heidenreich A, Bellmunt J, Bolla M, Joniau S, Mason M, Matveev V et al. EAU guidelines on prostate cancer. Part 1: screening, diagnosis, and treatment of clinically localised disease. *Eur Urol* 2011; **59**: 61–71.
- 56 Steyn JH, Smith FW. Nuclear magnetic resonance imaging of the prostate. *Br J Urol* 1982; **54**: 726–728.
- 57 Edelman RR. The history of MR imaging as seen through the pages of radiology. *Radiology* 2014; **273**: S181–200.
- 58 Mirowitz SA, Brown JJ, Heiken JP. Evaluation of the prostate and prostatic carcinoma with gadolinium-enhanced endorectal coil MR imaging. *Radiology* 1993; **186**: 153–157.
- 59 Christophe C, Montagne S, Bourrelier S, Roupret M, Barret E, Rozet F et al. Prostate cancer local staging using biparametric MRI: assessment and comparison with multiparametric MRI. *European Journal of Radiology* 2020; **132**: 109350.
- 60 Solari EL, Gafta A, Schachoff S, Bogdanović B, Villagrán Asiares A, Amiel T et al. The added value of PSMA PET/MR radiomics for prostate cancer staging. *Eur J Nucl Med Mol Imaging* 2021. doi:10.1007/s00259-021-05430-z.
- 61 Heijmink SWTPJ, Fütterer JJ, Hambrock T, Takahashi S, Scheenen TWJ, Huisman HJ et al. Prostate cancer: body-array versus endorectal coil MR imaging at 3 T--comparison of image quality, localization, and staging performance. *Radiology* 2007; **244**: 184–195.
- 62 Engelbrecht MR, Jager GJ, Laheij RJ, Verbeek ALM, van Lier HJ, Barentsz JO. Local staging of prostate cancer using magnetic resonance imaging: a meta-analysis. *Eur Radiol* 2002; **12**: 2294–2302.
- 63 Gawlitza J, Reiss-Zimmermann M, Thörmer G, Schaudinn A, Linder N, Garnov N et al. Impact of the use of an endorectal coil for 3 T prostate MRI on image quality and cancer detection rate. *Sci Rep* 2017; **7**: 40640.
- 64 Turkbey B, Rosenkrantz AB, Haider MA, Padhani AR, Villeirs G, Macura KJ et al. Prostate Imaging Reporting and Data System Version 2.1: 2019 Update of Prostate Imaging Reporting and Data System Version 2. *Eur Urol* 2019; **76**: 340–351.
- 65 Leek J, Lench N, Maraj B, Bailey A, Carr IM, Andersen S et al. Prostate-specific membrane antigen: evidence for the existence of a second related human gene. *Br J Cancer* 1995; **72**: 583–588.
- 66 Rowe SP, Gorin MA, Pomper MG. Imaging of Prostate-Specific Membrane Antigen with Small-Molecule PET Radiotracers: From the Bench to Advanced Clinical Applications. *Annu Rev Med* 2019; **70**: 461–477.
- 67 Pinto JT, Suffoletto BP, Berzin TM, Qiao CH, Lin S, Tong WP et al. Prostate-specific membrane antigen: a novel folate hydrolase in human prostatic carcinoma cells. *Clin Cancer Res* 1996; **2**: 1445–1451.
- 68 Yao V, Berkman CE, Choi JK, O’Keefe DS, Bacich DJ. Expression of prostate-specific membrane antigen (PSMA), increases cell folate uptake and proliferation and suggests a novel role for PSMA in the uptake of the non-polyglutamated folate, folic acid. *Prostate* 2010; **70**: 305–316.

- 69 Hupe MC, Philippi C, Roth D, Kümpers C, Ribbat-Idel J, Becker F et al. Expression of Prostate-Specific Membrane Antigen (PSMA) on Biopsies Is an Independent Risk Stratifier of Prostate Cancer Patients at Time of Initial Diagnosis. *Front Oncol* 2018; **8**: 623.
- 70 Hope TA, Eiber M, Armstrong WR, Juarez R, Murthy V, Lawhn-Heath C et al. Diagnostic Accuracy of 68Ga-PSMA-11 PET for Pelvic Nodal Metastasis Detection Prior to Radical Prostatectomy and Pelvic Lymph Node Dissection: A Multicenter Prospective Phase 3 Imaging Trial. *JAMA Oncol* 2021; **7**: 1635–1642.
- 71 Pienta KJ, Gorin MA, Rowe SP, Carroll PR, Pouliot F, Probst S et al. A Phase 2/3 Prospective Multicenter Study of the Diagnostic Accuracy of Prostate Specific Membrane Antigen PET/CT with 18F-DCFPyL in Prostate Cancer Patients (OSPREY). *J Urol* 2021; **206**: 52–61.
- 72 Surasi DS, Eiber M, Maurer T, Preston MA, Helfand BT, Josephson D et al. Diagnostic Performance and Safety of Positron Emission Tomography with 18F-rhPSMA-7.3 in Patients with Newly Diagnosed Unfavourable Intermediate- to Very-high-risk Prostate Cancer: Results from a Phase 3, Prospective, Multicentre Study (LIGHTHOUSE). *Eur Urol* 2023; **84**: 361–370.
- 73 Paulino Pereira LJ, Reesink DJ, de Bruin P, Gandaglia G, van der Hoeven EJRJ, Marra G et al. Outcomes of a Diagnostic Pathway for Prostate Cancer Based on Biparametric MRI and MRI-Targeted Biopsy Only in a Large Teaching Hospital. *Cancers (Basel)* 2023; **15**: 4800.
- 74 Vickers A, Carlsson SV, Cooperberg M. Routine Use of Magnetic Resonance Imaging for Early Detection of Prostate Cancer Is Not Justified by the Clinical Trial Evidence. *Eur Urol* 2020; **78**: 304–306.
- 75 Kalapara AA, Ballok ZE, Ramdave S, O’Sullivan R, Ryan A, Konety B et al. Combined Utility of 68Ga-Prostate-specific Membrane Antigen Positron Emission Tomography/Computed Tomography and Multiparametric Magnetic Resonance Imaging in Predicting Prostate Biopsy Pathology. *Eur Urol Oncol* 2022; **5**: 314–320.
- 76 Emmett L, Buteau J, Papa N, Moon D, Thompson J, Roberts MJ et al. The Additive Diagnostic Value of Prostate-specific Membrane Antigen Positron Emission Tomography Computed Tomography to Multiparametric Magnetic Resonance Imaging Triage in the Diagnosis of Prostate Cancer (PRIMARY): A Prospective Multicentre Study. *Eur Urol* 2021; **80**: 682–689.
- 77 Raveenthiran S, Yaxley WJ, Franklin T, Coughlin G, Roberts M, Gianduzzo T et al. Findings in 1,123 Men with Preoperative 68Ga-Prostate-Specific Membrane Antigen Positron Emission Tomography/Computerized Tomography and Multiparametric Magnetic Resonance Imaging Compared to Totally Embedded Radical Prostatectomy Histopathology: Implications for the Diagnosis and Management of Prostate Cancer. *J Urol* 2022; **207**: 573–580.
- 78 Uprimny C, Kroiss AS, Decristoforo C, Fritz J, von Guggenberg E, Kandler D et al. 68Ga-PSMA-11 PET/CT in primary staging of prostate cancer: PSA and Gleason score predict the intensity of tracer accumulation in the primary tumour. *Eur J Nucl Med Mol Imaging* 2017; **44**: 941–949.
- 79 Ptasznik G, Papa N, Kelly BD, Thompson J, Stricker P, Roberts MJ et al. High PSMA PET SUVmax in PI-RADS 4 or 5 men confers a high probability of significant prostate cancer. *BJU Int* 2022. doi:10.1111/bju.15736.
- 80 Bhanji Y, Rowe SP, Pavlovich CP. New imaging modalities to consider for men with prostate cancer on active surveillance. *World J Urol* 2022; **40**: 51–59.
- 81 Surti S, Kuhn A, Werner ME, Perkins AE, Kolthammer J, Karp JS. Performance of Philips Gemini TF PET/CT scanner with special consideration for its time-of-flight imaging capabilities. *J Nucl Med* 2007; **48**: 471–480.
- 82 Soret M, Bacharach SL, Buvat I. Partial-volume effect in PET tumor imaging. *J Nucl Med* 2007; **48**: 932–945.

- 83 de Rooij M, Hamoen EHJ, Witjes JA, Barentsz JO, Rovers MM. Accuracy of Magnetic Resonance Imaging for Local Staging of Prostate Cancer: A Diagnostic Meta-analysis. *Eur Urol* 2016; **70**: 233–245.
- 84 Sighinolfi MC, Rocco B. Re: EAU Guidelines: Prostate Cancer 2019. *European Urology* 2019; **76**: 871.
- 85 Nguyen LN, Head L, Witiuk K, Punjani N, Mallick R, Cnossen S et al. The Risks and Benefits of Cavernous Neurovascular Bundle Sparing during Radical Prostatectomy: A Systematic Review and Meta-Analysis. *J Urol* 2017; **198**: 760–769.
- 86 Soeterik TFW, van MHHE, Dijksman LM, Stomps S, Witjes JA, van BIPA. Nerve Sparing during Robot-Assisted Radical Prostatectomy Increases the Risk of Ipsilateral Positive Surgical Margins. *Journal of Urology* 2020; **204**: 91–95.
- 87 Ohori M, Kattan MW, Koh H, Maru N, Slawin KM, Shariat S et al. Predicting the presence and side of extracapsular extension: a nomogram for staging prostate cancer. *J Urol* 2004; **171**: 1844–1849; discussion 1849.
- 88 Hofman MS, Lawrentschuk N, Francis RJ, Tang C, Vela I, Thomas P et al. Prostate-specific membrane antigen PET-CT in patients with high-risk prostate cancer before curative-intent surgery or radiotherapy (proPSMA): a prospective, randomised, multicentre study. *Lancet* 2020; **395**: 1208–1216.

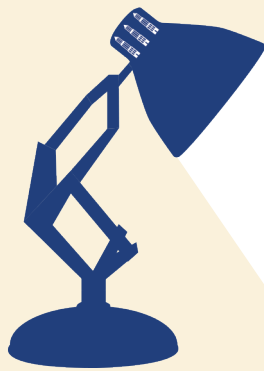






# PART I

THE DETECTION OF CLINICALLY  
SIGNIFICANT PROSTATE CANCER



# CHAPTER 2

## IMMUNOHISTOCHEMICAL AND HISTOPATHOLOGICAL VALIDATION OF $^{18}\text{F}$ -PSMA-1007 PET/CT FOR INTRAPROSTATIC CANCEROUS LESIONS

J.G. Heetman  
R. Hermsen  
L. Exterkate  
H.V.N. Küsters-Vandevelde  
L.J.M. Brouwer  
D.M. Somford  
R.C.N. van den Bergh  
J.P.A. van Basten

Prostate 2023 Oct;83(14):1332-1341. doi: 10.1002/pros.24595.

## Abstract

*Introduction:* Prostate-specific Membrane Antigen (PSMA) is overexpressed in prostate cancer (PCa). In this study, we aim to immunohistochemically and histopathological validate the fluorine-18 (<sup>18</sup>F)-PSMA-1007 positron emission tomography/computed tomography (PET/CT) for intraprostatic PCa lesions.

*Methods:* Between February 2019 and October 2020, patients with biopsy-proven, treatment-naïve intermediate-to-high-risk PCa undergoing a <sup>18</sup>F-PSMA-1007 PET/CT prior to robot-assisted radical prostatectomy (RARP) were prospectively enrolled. For all PCa lesions found on whole-mount histopathology, location, size, International Society of Urological Pathology (ISUP) Grade Group (GG), and immune reactive score (IRS) were assessed after PSMA staining. ISUP GG  $\geq 3$  PCa was defined as clinically significant(cs) PCa. All lesions were matched on PSMA PET/CT and SUVmax was measured.

*Results:* A total of 125 lesions were analysed in the 80 RARP specimens, of which 49 (40%) were csPCa and 76 (60%) non-csPCa (ncsPCa). Linear multivariable regressions showed that an increase in SUVmax significantly correlated with a higher ISUP GG ( $p$  values between 0.021 and 0.001) and a higher IRS ( $p = 0.017$ ). Logistic multivariable regression showed that csPCa significantly correlated with a higher SUVmax (odds ratio, OR: 1.17 [95% confidence interval, CI: 1.04–1.21,  $p = 0.005$ ]), an increase in tumour length (OR: 1.05 [95% CI 1.01–1.10,  $p = 0.020$ ]) and a higher IRS (OR; 1.24 [95% CI 1.07–1.47,  $p = 0.006$ ]). A SUVmax threshold of 4 would have resulted in one (2%) missed lesion with csPCa.

*Conclusion:* This prospective study revealed that <sup>18</sup>F-PSMA-1007 PET/CT SUVmax is correlated with the ISUP GG and IRS, and thereby could be a tool to characterize intraprostatic PCa lesions.

## Introduction

Prostate-specific Membrane Antigen (PSMA) is a transmembrane protein overexpressed in prostate cancer (PCa).<sup>1</sup> A high PSMA expression in biopsy and radical prostatectomy specimen is an independent predictor for PCa disease recurrence following treatment with curative intent.<sup>2</sup> PSMA-positron emission tomography/computed tomography (PSMA PET/CT) has first demonstrated its value in detecting metastatic disease in high-risk PCa patients.<sup>3,4</sup> Recent phase 3 studies have pushed the registration of the PSMA PET/CT for use in daily clinical practice as staging tool in biochemical recurrence setting and before radical prostatectomy and/or pelvic lymph node dissection.<sup>5-12</sup>

The guidelines currently recommend the use of multiparametric magnetic resonance imaging (mpMRI) for local staging and the primary detection of PCa, while the added value of the PSMA PET/CT in the context of primary PCa detection and local staging requires further investigation.<sup>13</sup> <sup>68</sup>Ga-PSMA-11 PET/CT was recently found to provide additional value before targeted biopsy, when combined with pre-biopsy MRI. It increased the sensitivity from 83% to 97%, and the negative predictive value from 72% to 91%, versus MRI alone.<sup>14</sup> A recent systematic review including five studies with a total of 459 patients showed a sensitivity of 91% and a negative predictive value of 81% for the combination of prebiopsy PSMA and MRI.<sup>15</sup> The standardised uptake value (SUV) of <sup>68</sup>Ga-PSMA-11 PET/CT was found to have a significant association with International Society of Urologic Pathology (ISUP) grade group (GG).<sup>16-18</sup>

There are multiple PSMA tracers that have been shown to be able to detect clinically significant (cs) PCa lesions.<sup>16,19,20</sup> <sup>68</sup>Ga-PSMA-HBED-CC was retrospectively immunohistochemically validated and an increase in PSMA expression resulted in a higher SUVmax.<sup>21</sup>

Fluorine-18 (<sup>18</sup>F)-based tracers are widely used in Europe for detecting lymph nodes and metastatic disease and have practical advantages over <sup>68</sup>Ga-based tracers. Besides the higher production capacity of a cyclotron produced radiopharmaceutical, the longer radioactive half-life of 110 versus 68 minutes makes central manufacturing for distribution on a larger scale possible. Furthermore, the higher spatial resolution of <sup>18</sup>F due to its lower positron energy of 0.65 MeV versus 1.9 MeV of <sup>68</sup>Ga and the lower urinary excretion with <sup>18</sup>F-PSMA-1007, may result in more accurate local staging.<sup>22</sup>

The ability of the <sup>18</sup>F-PSMA-1007 PET/CT to characterize intraprostatic PCa lesions remains unknown. The correlation of the PSMA immunohistochemical reactive score (IRS) of intraprostatic PCa lesions with <sup>18</sup>F-PSMA-1007 PET/CT SUVmax is undetermined. The IRS consists of the percentage of positive tumour cells and the staining intensity. Furthermore,

the performance of the PSMA PET/ CT in small intraprostatic PCa lesions is unclear. A known drawback of PET/CT is the voxel size as this may result in underestimation of the SUVmax for smaller lesions, due to the partial-volume effect.<sup>23,24</sup> The impact of this effect on the characterization of small intraprostatic csPCa lesions is unclear. Thereby the aim of this study is to analyse whether <sup>18</sup>F-PSMA-1007 PET/CT could serve as a tool to characterize intraprostatic PCa lesions.



## Methods

### Study Population

We performed a prospective study in patients with newly diagnosed intermediate- to high-risk biopsy-proven PCa (prostate-specific antigen  $\geq 10$  ng/mL or ISUP GG  $\geq 2$  or  $\geq$ clinical T2b stage) who have had an  $^{18}\text{F}$ -PSMA-1007 PET/CT before extended pelvic lymph node dissection (ePLND) with or without robot-assisted radical prostatectomy (RARP). Patients who did not receive RARP had their primary tumour treated with external beam radiotherapy. In this analysis, we evaluate the subgroup of patients who had undergone a RARP procedure. The study was approved by the institutional review board and is registered in The Netherlands Trial Registry (NTR7670). The primary outcome of the main study was the diagnostic accuracy of  $^{18}\text{F}$ -PSMA-1007 PET/CT in lymph node staging in primary PCa. The outcomes associated with the primary endpoints were independently documented, while a separate analysis comparing MRI and PSMA was conducted and the results were reported in a distinct article as secondary endpoints.<sup>6,25</sup> Current analysis aims to identify  $^{18}\text{F}$ -PSMA-1007 PET/CT characteristics of intraprostatic PCa lesions of the cohort of men undergoing RARP with concomitant ePLND.

All patients provided written informed consent. The indication for RARP with ePLND was set at the discretion of a local multidisciplinary tumour board and study eligibility did not impact treatment decision. Exclusion criteria for study participation were a history of prior treated PCa, unwillingness or inability to undergo a PSMA PET/CT, and no wish to undergo ePLND and/or RARP following counselling.

### Radical Prostatectomy

RARP with ePLND was performed by two experienced urological surgeons (J. P. A. vB and D. S., >500 procedures performed each) using the Da Vinci Xi Robotic System (Intuitive Surgical Inc.).

### Histopathological Evaluation

After at least 24-hour fixations in formaldehyde (10%), the RARP specimens were completely embedded. The apex and base were cut off by using the cone method and sagittally sliced.<sup>26</sup> Along the cutting edge, whole-mount slices were obtained at 4 mm intervals and embedded in whole-mount cassettes. Formalin-fixed and paraffin-embedded tissue blocks (FFPE) were cut at 3  $\mu\text{m}$  thickness versus 4  $\mu\text{m}$  for whole-mount slides and stained with hematoxylin and eosin (H&E). The microscopical evaluation was performed by a single uropathologist (H. V. N. K.-V.) with 15 years of experience.

On all pCa lesions, PSMA staining was performed on the slice with the highest tumour load. By the guidance of the H&E staining, the specific tumour area was cut out from an unstained 4- $\mu$ m-thick whole-mount FFPE tissue section and mounted on a Superfrost Plus slide. After deparaffinization and rehydration, antigen retrieval was performed by the EnVision™ FLEX Target Retrieval Solution for 30 min at a temperature of 97°C. Slides were stained with the Ready-to-Use FLEX Monoclonal Mouse Anti-Human PSMA of DAKO/Agilent, Clone 3E6, on a Dako Omnis immunostainer. Slides were incubated with the antibody for 27–30 min at a temperature of 32°C. The EnVision Flex Detection Kit (Dako/Agilent) was used for visualization.

The PSMA expression in each tumour was visually quantified by a single pathologist (H. V. N. K.-V.) and reported as the staining intensity score (0: no colour reaction; 1: mild; 2: moderate; 3: intense reaction) and the quantitative score (0: no positive cells, 1: 0%–10%, 2: 10%–50%, 3: 51%–80%, 4: >80% positive cells). Both these scores were multiplied, resulting in the IRS (0–12). For the analysis, the 0–12 scale was used.<sup>21</sup>

All tumours were delineated and ISUP GG was provided on whole-mount slides with the highest tumour load by the uropathologist and slides were placed on a score form in order of their anatomical location (base to apex).

### **<sup>18</sup>F-PSMA-1007 PET/CT**

<sup>18</sup>F-PSMA-1007 tracer was produced at the Radboud University Medical Centre translational medicine cyclotron facility. The reagent kit and PSMA-1007 precursor were obtained from ABX.

<sup>18</sup>F-PSMA-1007 PET/CT was performed on a Philips Gemini 64TF or a Siemens Biograph Vision 450. Images (skull base to mid-thigh) were acquired after intravenous injection of <sup>18</sup>F-PSMA-1007 (median 251 MBq, interquartile range [IQR]: 242–257) and median incubation time of 105 min (IQR: 97–119). Patients were prehydrated and were asked to void before scanning.

PET scans were performed with a 5 min/bed position of the pelvis (Philips) and flow motion at a scan speed of 1 mm/s (Siemens). PET image reconstruction was performed with a correction for attenuation, scatter, random coincidence, and time of flight. EARL-1 reconstructions were used for SUVmax measurements with Oasis Client® software.<sup>27</sup>

The score forms processed by a dedicated uropathologist (H. V. N. K.-V.) were matched to the PSMA PET/CT images by a nuclear medicine physician (R. H.) with >12 years of experience. Lesions were outlined on PSMA PET/CT and SUVmax values were measured. A noncontrast-enhanced low-dose CT was used for attenuation correction and anatomical correlation. When the delineated tumour was not distinguishable on PET/CT, an SUV measurement was done in the estimated region within the prostate.

### Statistical Analysis

A per lesion analysis was performed of PCa lesions with complete pathological information. A uni- and multivariable linear regression analysis were conducted on the correlation between the increase in SUVmax and ISUP GG, maximum tumour length, and IRS. The correlation between SUVmax, tumour length, and IRS and the presence of csPCa was tested using uni- and multivariable logistic regression. Two sensitivity curves were created to visualize the amount of missed PCa lesions for different SUVmax thresholds (from 1 to 10) one per ISUP GG and the other one with a distinction for csPCa and non-csPCa (ncsPCa). ISUP GG  $\geq 3$  PCa was defined as csPCa because active therapy is generally recommended for all these cases.<sup>13</sup> Furthermore, a scatterplot was created including all lesions on the y-axis SUVmax and on the x-axis tumour length. Tumour length was included to establish if there are possible missed lesions due to the voxel size of 4 mm. Statistical analysis was performed using R version 4.1.2 (R Foundation for Statistical Computing). All tests were two-sided, with a significance level set at  $p < 0.05$ .

## Results

### Baseline Characteristics per Lesion

A total of 99 patients were included, of whom 80 underwent a RARP, 37 (46%) of the patients were intermediate-risk and 43 (54%) were high-risk patients. The histopathological assessment of the radical prostatectomy specimens revealed 129 intraprostatic PCa lesions, of which two were excluded from the analysis due to one PSMA PET/ CT being performed in another centre and two ISUP GG 1 lesions being excluded from final analyses due to failure of PSMA staining. A total of 125 lesions remained evaluable for analysis. Baseline characteristics of all the intraprostatic PCa lesions, presented for ncsPCa and csPCa are shown in Table 1. Thirty-two tumours (26%) were graded as ISUP GG 1, 44 (35%) GG 2, 26 (21%) GG 3, 14 (11%) GG 4, and 9 (7%) GG 5. Figure 1 shows some examples of tumours delineated on histology and their corresponding axial <sup>18</sup>F-PSMA-1007 PET/CT slides. In Figure 2, boxplots are shown of the SUVmax, the tumour length measured on histology, and the IRS per ISUP GG. This figure shows an increase of SUVmax and IRS with higher ISUP GG groups, except for lesions with ISUP GG 5. The tumour length appears to increase with increasing ISUP GG.

### SUVmax

Univariable linear regression (Table 2) showed a significant correlation between SUVmax and ISUP GG ( $p = 0.021$  to  $<0.001$ ), tumour length ( $p = 0.010$ ), and IRS ( $p < 0.001$ ). In the multivariable linear regression analysis (Table 2), the ISUP GG 2–5 ( $p = 0.035$  to  $p < 0.001$ ) and the IRS ( $p = 0.017$ ) remained significant with a higher

### csPCa

The univariable logistic regression analysis showed a significant relation between SUVmax ( $p < 0.001$ ), tumour length ( $p < 0.001$ ), and IRS ( $p < 0.001$ ), as is shown in Table 3. In the multivariable logistic regression analysis, all these factors remained significant, resulting in a significant relation between csPCa and a higher SUVmax (odds ratio, OR: 1.11 [95% confidence interval, CI: 1.04–1.21,  $p = 0.005$ ]), a higher tumour length (OR: 1.05 [95% CI: 1.01–1.10,  $p = 0.020$ ]) and a higher IRS (OR: 1.24 [95% CI: 1.07–1.47,  $p = 0.006$ ]).

### SUVmax Threshold

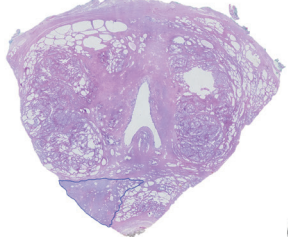
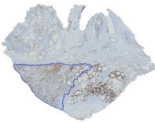
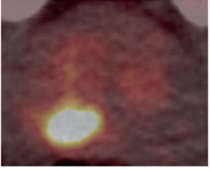
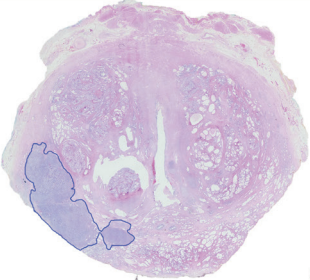
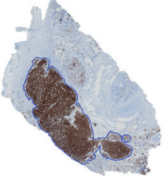
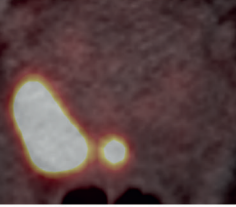
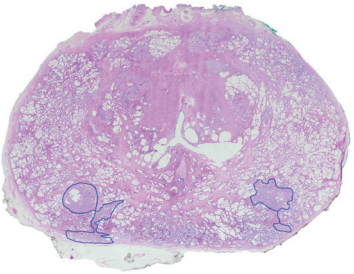
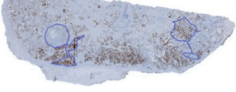
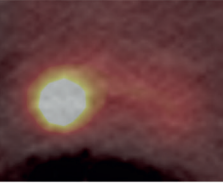
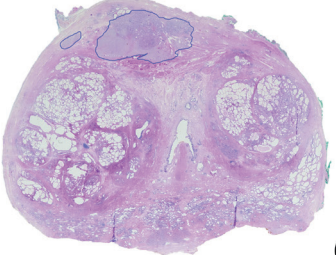
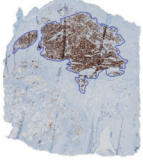
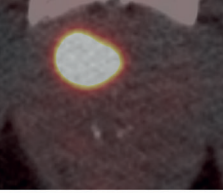
Figure 3 shows a sensitivity curve with the number of lesions with PCa for each SUVmax threshold. For csPCa, the lesion distribution below thresholds of 4, 5, and 6 was 3 (6%), 3 (10%), and 4 (10%), respectively. For ncsPCa, the distribution below the same thresholds was 23 (30%), 41 (54%), and 48 (63%), respectively. The threshold of 4 is shown in Figure 4. Figure 4 indicates that there are no lesions with csPCa smaller than the voxel size of 4 mm, the smallest lesions had a tumour length of 9 mm.

**Table 1:** Baseline characteristics of all the intraprostatic prostate cancer lesions, divided in non-clinically significant (ISUP Grade Group < 3) and clinically significant (ISUP Grade Group ≥3)

	Overall (n =125)	ncsPCa (n =76)	csPCa (n = 49)
SUVmax median (IQR)	7.0 (4.3, 12.0)	4.8 (3.8, 8.2)	11.2 (7.3, 19.7)
Max width or length (mm) median (IQR)	18.0 (12.0, 27.0)	15.0 (8.0, 22.5)	21.0 (16.0, 31.0)
IRS median (IQR)	8 (6, 12)	8 (4, 12)	12.0 (8, 12)
Q-score n (%)			
10-50% positive cells	12 (10%)	11 (14%)	1 (2%)
51-80%positive cells	24 (19%)	19 (14%)	5 (10%)
>80% positive cells	89 (71%)	46 (61%)	42 (88%)
SIS n (%)			
Mild reaction	13 (10%)	12 (16%)	1 (2%)
Moderate reaction	59 (47%)	42 (55%)	17 (35%)
Intense reaction	52 (42%)	22 (29%)	31 (63%)
ISUP Grade Group n (%)			
1	32 (26%)	32 (42%)	-
2	44 (35%)	44 (58%)	-
3	26 (21%)	-	26 (53%)
4	14 (11%)	-	14 (29%)
5	9 (7%)	-	9 (18%)

Note: Mean (IQR).

Abbreviations: csPCa, clinically significant prostate cancer; IQR, interquartile range; IRS, immune reactive score; ISUP, International Society of Urologic Pathology; ncsPCa, non-csPCa; Q score, quantitative score; SIS, staining intensity score; SUVmax, maximum standardised uptake value.

Tumours on H&E	PSMA staining	<sup>18</sup> F-PSMA-1007 PET/CT image
 <p>(A)</p>		
 <p>(B)</p>		
 <p>(C)</p>		
 <p>(D)</p>		

◀ **Figure 1:** Tumours on H&E (left) and PSMA-stained samples (middle) delineated in blue.

(A) High ISUP GG, low immune reactive score (IRS), and high SUVmax. Left: H&E stained whole mount section of the prostate shows an ISUP GG 4 in the peripheral zone at the right side midprostate. Note artifact of dissection at both posterolateral sides, caused by the use of intraoperative fresh-frozen section analysis of the posterolateral aspect of the prostate margin (NeuroSAFE technique). Middle: A low IRS of 4 in the tumour is visible after PSMA staining (Q score of 4 [ $>80\%$  positive cells], and a mild reaction SIS 1). Right: Intense uptake on PET/CT, SUVmax 19.8.

(B) High ISUP GG, IRS, and SUVmax. Left: A dense expansive growth pattern on the H&E section, ISUP GG 4, in the peripheral zone at the left side of the base of the prostate. Middle: Good overlap of H&E delineated tumour and PSMA staining. Mild artifacts caused by the NeuroSAFE technique. The maximum IRS of 12, resulted from  $>80\%$  positive cells and intense reaction (Q score 4, SIS 3, respectively). PET/CT on the right: A match of the lesion with histology, SUVmax of 53.1.

(C) Intermediate ISUP GG, low IRS, and high SUVmax. Left: Tumour of interest is located at the right posterolateral side midprostate, ISUP GG 3. Middle: The tumour shows heterogeneous PSMA reaction, resulting in a low IRS of 4, Q score 2 (10%–50% positive tumour cells), and SIS 2 (moderate reaction). There is a notable reaction to PSMA staining in the wall of normal prostate glands in the peripheral zone. On the right side, PET/CT shows a high SUVmax of 15.2. A second tumour is located in the left posterolateral peripheral zone with a low ISUP 2, IRS 4, and SUVmax of 4.7.

(D) Low ISUP GG, high IRS, and SUVmax. This case represents one of the outliers in the ISUP 2 group. Left: A tumour located in the anterior zone midprostate, invasive growth pattern, ISUP 2 GG, even after a second read by the pathologist. The middle shows an IRS of 12 which corresponds with a SUVmax value on the left of 35.1. CT, Computed Tomography; GG, group grade; H&E, hematoxylin and eosin; ISUP, International Society of Urological Pathology; PET, positron emission tomography; PSMA, prostate-specific membrane antigen; SIS, staining intensity score; SUVmax, maximum standardised uptake value.

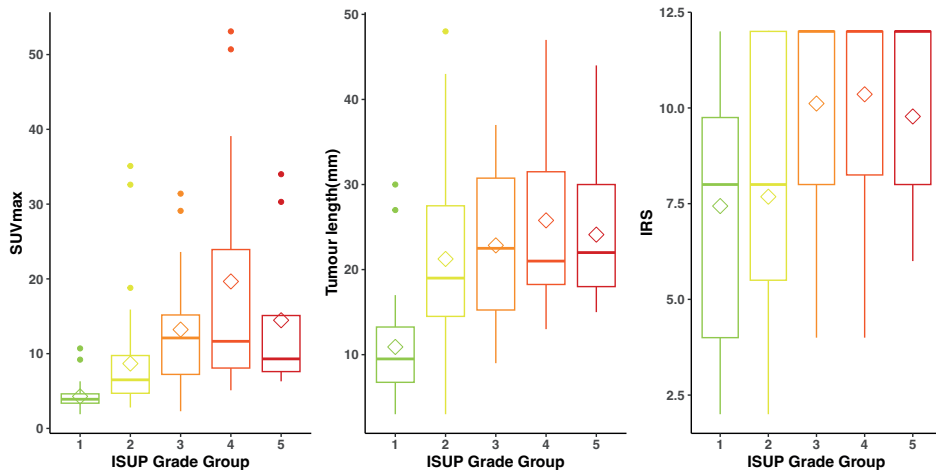


**Figure 2:** Boxplots showing SUVmax, histopathological tumour length, and immune reactive score (IRS) for different ISUP group grades (bar median, diamond mean). ISUP, International Society of Urological Pathology; SUVmax, maximum standardised uptake value.

**Table 2:** Univariable and multivariable linear regression analysis of the ISUP grade group, tumour length and IRS on the SUVmax

	Impact on SUVmax			
	Univariable		Multivariable	
	Beta (95% CI)	<i>p</i> -value	Beta (95% CI)	<i>p</i> -value
ISUP Grade Group				
1	Reference	-	-	-
2	4.4(0.68, 8.1)	0.021	4.3(0.31, 8.3)	0.035
3	8.9(4.7, 13.0)	<0.001	7.4(2.7, 12)	0.002
4	15.0(10.0, 21.0)	<0.001	14.0(8.0, 19.0)	<0.001
5	10.0(4.1, 16.0)	0.001	8.9(2.5, 15)	0.007
Tumour length (mm)	0.20(0.1, 0.4)	0.010	0.0(-0.2, 0.2)	>0.9
IRS	1.0(0.6, 1.5)	<0.001	0.6(0.1, 1.1)	0.017

CI, confidence interval; csPCa, clinically significant prostate cancer (defined as ISUP GG 3 or higher); GG, grade group; IRS, immune reactive score; ISUP, International Society of Urologic Pathology; ncsPCa, non-csPCa; OR, odds ratio; SUVmax, maximum standardised uptake value.



**Table 3:** Univariable and multivariable logistic regression analysis of the SUVmax, tumour length, and IRS on the presence of csPca (ISUP GG ≥ 3).

	Difference between ncsPca and csPca			
	Univariable		Multivariable	
	OR (95% CI)	p-value	OR (95% CI)	p-value
SUVmax	1.17(1.09, 1.27)	<b>&lt;0.001</b>	1.10(1.04, 1.21)	<b>0.005</b>
Tumour length (mm)	1.07(1.03, 1.12)	<b>&lt;0.001</b>	1.05(1.01, 1.10)	<b>0.020</b>
IRS	1.34(1.17, 1.5)	<b>&lt;0.001</b>	1.24(1.07, 1.47)	<b>0.006</b>

CI, confidence interval; csPca, clinically significant prostate cancer (defined as ISUP GG 3 or higher); GG, Grade Group; IRS, immune reactive score; ISUP, International Society of Urologic Pathology; ncsPca, non-csPca; OR, odds ratio; SUVmax, maximum standardised uptake value

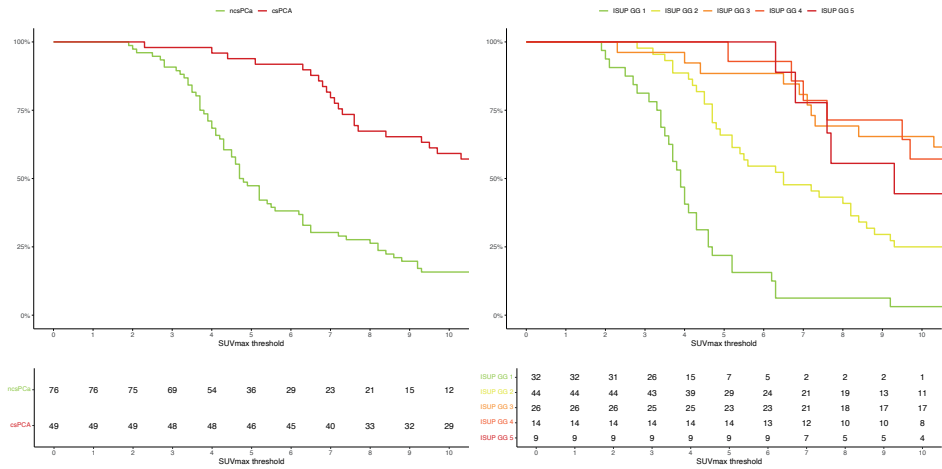


**Figure 3:** Sensitivity curve for different SUVmax thresholds for lesions with clinically significant prostate cancer (csPca) and nonclinically significant prostate cancer (ncsPca) on the left and on the right per ISUP group grade (GG). ISUP, International Society of Urological Pathology; SUVmax, maximum standardised uptake value.

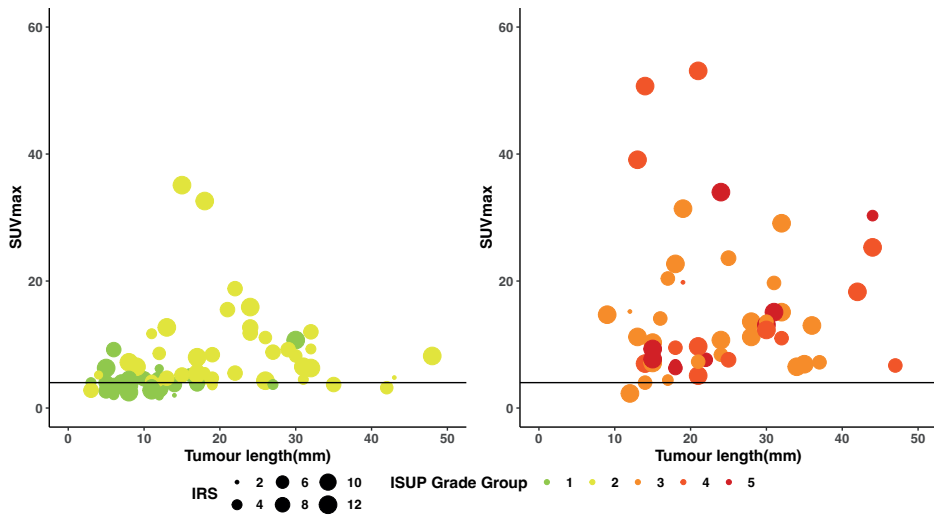


**Figure 4:** Scatter plot of all the intraprostatic lesions, on the left non-clinically significant prostate cancer and on right with clinically significant prostate cancer, with the intercept on SUVmax of 4.

## Discussion

To our knowledge, this is the largest prospective study that validates the  $^{18}\text{F}$ -PSMA-1007 tracer for the characterization of intraprostatic PCa. In this study, we found that histopathological characteristics of intraprostatic PCa lesions, in terms of ISUP GG and IRS, significantly correlate with SUVmax on the  $^{18}\text{F}$ -PSMA-1007 PET/CT regardless of tumour length.

Figure 2 shows an increase in SUVmax per ISUP GG except for ISUP GG 5. This pattern was also observed in the immunohistological results, which showed lower mean IRS within the ISUP GG 5 tumours compared to ISUP GG 4. This may possibly be caused by the loss of PSMA expression in ISUP GG 5 due to dedifferentiation. On the contrary, other studies have found a higher SUVmax in ISUP GG 5 compared to ISUP GG 4.<sup>17,18,28</sup> However, our cohort includes only a small number of ISUP GG 5 lesions and no firm conclusions can be drawn. As depicted in our results, a significant relation between SUVmax and IRS was established, Woythal *et al.* have also demonstrated with the  $^{68}\text{Ga}$ -PSMA-HBED-CC tracer.<sup>21</sup>

In the ISUP GG 2 cohort there were two notable outliers with a SUVmax > 30. Those were re-examined by the uropathologist and both remained ISUP GG 2, case d in Figure 1. This suggests that a low ISUP GG in histopathology is not always accompanied with a lower PSMA expression.

In the ISUP GG 2 cohort, there were two notable outliers with a SUVmax > 30. Those were re-examined by the uropathologist and both remained ISUP GG 2, as shown in Figure 1D. This suggests that a low ISUP GG in histopathology is not always accompanied by a lower PSMA expression.

Our results showed that missing csPCa due to the partial-volume effect is unlikely since all csPCa lesions in this cohort are substantially larger than the used voxel size. This is also confirmed by the result that tumour length does not seem to have a significant impact on the SUVmax value. Woythal *et al.* similarly found no relation between tumour size and SUVmax measurements.<sup>21</sup>

When applying a SUVmax threshold of 4 within this cohort, one csPCa lesion showed a SUVmax under the threshold. This csPCa lesion showed a maximum IRS of 12, a length of 12 mm, and ISUP GG 3. One would expect a higher SUVmax in this lesion due to the high IRS and sufficient tumour length. A possible explanation could be that the immunostaining was performed on the whole-mount slice with the highest amount of tumour load. Due to heterogeneity in PSMA expression, this could result in an overestimation of the PSMA expression in the total tumour and thereby could result in a lower-than-expected SUVmax below the threshold of 4.<sup>29</sup>

This study has several limitations. First, only patients undergoing RARP with ePLND were included, resulting in absence of patients with low-risk PCa. The study was initially designed and powered to assess the diagnostic accuracy of  $^{18}\text{F}$ -PSMA-1007 PET/CT for detection of lymph node metastases. Furthermore, only histological confirmed tumours were matched and then measured in the PET/CT images, resulting in no false positive lesions, which would be introduced when readings are blinded to all information. Thereby, only sensitivity at a certain threshold, but no specificity and receiver operating characteristic curve with area under the curve could be calculated. Of the few lesions with barely or no PSMA activity, SUVmax was measured within the region of the delineated tumour on whole-mount pathology. In these lesions, exact localisation was challenging which could have resulted in a slight under- or overestimation of already low SUVmax values. To a certain extent, the low-dose CT is helpful in matching the pathology results to the PET scan, but it lacks the ability to visualize intraprostatic anatomy. Unlike CT, MRI provides more structural information on the prostatic tissue, facilitating accurate localisation of histopathologically proven with the absence of low SUVmax. Therefore, the PET/MRI might aid the exact localisation and the SUVmax measurements might be more accurate, $^{68}\text{Ga}$ -PSMA PET/MRI has shown excellent results for the detection of PCa.<sup>30</sup> However, the availability of these expensive scanners is limited, and the imaging quality of the incorporated MRI still has room for improvement. Software merging the information of state-of-the-art mpMRI with PSMA PET/CT can mimic these excellent results.<sup>31</sup>

In our opinion, future research should explore additional parameters and radiomics beyond SUVmax in PSMA PET/CT for the characterization of intraprostatic PCa lesions. In the PRIMARY trial and PEDAL trial, patterns of activity were predictors of a higher chance of csPCa.<sup>32,33</sup> Tracer uptake velocity and wash-out is an interesting area of research and may result in a better ability to detect intraprostatic lesions with PCa.<sup>34</sup> On the other hand, these protocols are time-consuming.

Furthermore, additional information on PSMA PET/CT, like SUVmax as investigated in our study, could be included in a model to predict the presence or absence of csPCa in both the prebiopsy as well as active surveillance setting. The combination of PI-RADS with SUVmax thresholds has shown promising results in predicting csPCa.<sup>18,35</sup> In addition, future research may involve prospective assessment of prebiopsy  $^{18}\text{F}$ -PSMA-1007 PET/CT either independent or in conjunction with mpMRI or PET/MRI, aiming to evaluate its efficacy in the detection and prediction of csPCa, as well as its potential role in guiding biopsy procedures. The PRIMARY trial showed the additional value of the  $^{68}\text{Ga}$ -PSMA-11 tracer in detecting cancerous intraprostatic lesions for targeted biopsy.<sup>14</sup> This may also apply to the  $^{18}\text{F}$ -PSMA-1007 tracer. Lastly, the incorporation of additional PSMA information in magnetic resonance-guided radiotherapy could possibly enhance guidance and precision in treatment planning.

## Conclusion

Our results demonstrate that a higher ISUP GG and IRS are significantly associated with a higher SUVmax on  $^{18}\text{F}$ -PSMA-1007 PET/CT. Furthermore, lesions with csPCa have a higher IRS and a higher SUVmax versus lesions with ncsPCa. Therefore, this study suggests that the  $^{18}\text{F}$ -PSMA-1007 could be a potential asset in the characterization and identification of intraprostatic PCa lesions.

## References

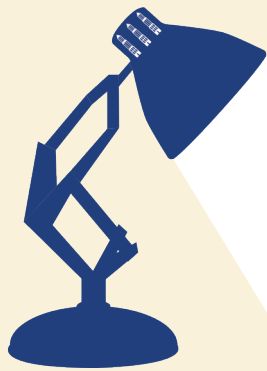
- 1 Leek J, Lench N, Maraj B, Bailey A, Carr IM, Andersen S *et al.* Prostate-specific membrane antigen: evidence for the existence of a second related human gene. *Br J Cancer* 1995; **72**: 583–588.
- 2 Hupe MC, Philippi C, Roth D, Kümpers C, Ribbat-Idel J, Becker F *et al.* Expression of Prostate-Specific Membrane Antigen (PSMA) on Biopsies Is an Independent Risk Stratifier of Prostate Cancer Patients at Time of Initial Diagnosis. *Front Oncol* 2018; **8**: 623.
- 3 Perera M, Papa N, Roberts M, Williams M, Udovicich C, Vela I *et al.* Gallium-68 Prostate-specific Membrane Antigen Positron Emission Tomography in Advanced Prostate Cancer-Updated Diagnostic Utility, Sensitivity, Specificity, and Distribution of Prostate-specific Membrane Antigen-avid Lesions: A Systematic Review and Meta-analysis. *Eur Urol* 2020; **77**: 403–417.
- 4 Hofman MS, Lawrentschuk N, Francis RJ, Tang C, Vela I, Thomas P *et al.* Prostate-specific membrane antigen PET-CT in patients with high-risk prostate cancer before curative-intent surgery or radiotherapy (proPSMA): a prospective, randomised, multicentre study. *Lancet* 2020; **395**: 1208–1216.
- 5 van Kalmthout LWM, van Melick HHE, Lavalaye J, Meijer RP, Kooistra A, de Klerk JMH *et al.* Prospective Validation of Gallium-68 Prostate Specific Membrane Antigen-Positron Emission Tomography/Computerized Tomography for Primary Staging of Prostate Cancer. *J Urol* 2020; **203**: 537–545.
- 6 Hermesen R, Wedick EBC, Vinken MJM, van Kalmthout LWM, Küsters-Vandeveldel HVN, Wijers CHW *et al.* Lymph node staging with fluorine-18 prostate specific membrane antigen 1007-positron emission tomography/computed tomography in newly diagnosed intermediate- to high-risk prostate cancer using histopathological evaluation of extended pelvic node dissection as reference. *Eur J Nucl Med Mol Imaging* 2022; **49**: 3929–3937.
- 7 Jansen BHE, Bodar YJL, Zwezerijnen GJC, Meijer D, van der Voorn JP, Nieuwenhuijzen JA *et al.* Pelvic lymph-node staging with 18F-DCFPyL PET/CT prior to extended pelvic lymph-node dissection in primary prostate cancer - the SALT trial. *Eur J Nucl Med Mol Imaging* 2021; **48**: 509–520.
- 8 Hope TA, Eiber M, Armstrong WR, Juarez R, Murthy V, Lawhn-Heath C *et al.* Diagnostic Accuracy of 68Ga-PSMA-11 PET for Pelvic Nodal Metastasis Detection Prior to Radical Prostatectomy and Pelvic Lymph Node Dissection: A Multicenter Prospective Phase 3 Imaging Trial. *JAMA Oncol* 2021; **7**: 1635–1642.
- 9 Pienta KJ, Gorin MA, Rowe SP, Carroll PR, Pouliot F, Probst S *et al.* A Phase 2/3 Prospective Multicenter Study of the Diagnostic Accuracy of Prostate Specific Membrane Antigen PET/CT with 18F-DCFPyL in Prostate Cancer Patients (OSPREY). *J Urol* 2021; **206**: 52–61.
- 10 Olivier P, Giraudet A-L, Skanjeti A, Merlin C, Weinmann P, Rudolph I *et al.* Phase III Study of 18F-PSMA-1007 Versus 18F-Fluorocholine PET/CT for Localization of Prostate Cancer Biochemical Recurrence: A Prospective, Randomized, Crossover Multicenter Study. *J Nucl Med* 2023; **64**: 579–585.
- 11 Morris MJ, Rowe SP, Gorin MA, Saperstein L, Pouliot F, Josephson D *et al.* Diagnostic Performance of 18F-DCFPyL-PET/CT in Men with Biochemically Recurrent Prostate Cancer: Results from the CONDOR Phase III, Multicenter Study. *Clin Cancer Res* 2021; **27**: 3674–3682.
- 12 Jani AB, Ravizzini GC, Gartrell BA, Siegel BA, Twardowski P, Saltzstein D *et al.* Diagnostic Performance and Safety of 18F-rhPSMA-7.3 Positron Emission Tomography in Men With Suspected Prostate Cancer Recurrence: Results From a Phase 3, Prospective, Multicenter Study (SPOTLIGHT). *J Urol* 2023; : 101097JU00000000000003493.

- 13 Mottet N, van den Bergh RCN, Briers E, Van den Broeck T, Cumberbatch MG, De Santis M *et al.* EAU-EANM-ESTRO-ESUR-SIOG Guidelines on Prostate Cancer-2020 Update. Part 1: Screening, Diagnosis, and Local Treatment with Curative Intent. *Eur Urol* 2021; **79**: 243–262.
- 14 Emmett L, Buteau J, Papa N, Moon D, Thompson J, Roberts MJ *et al.* The Additive Diagnostic Value of Prostate-specific Membrane Antigen Positron Emission Tomography Computed Tomography to Multiparametric Magnetic Resonance Imaging Triage in the Diagnosis of Prostate Cancer (PRIMARY): A Prospective Multicentre Study. *Eur Urol* 2021; **80**: 682–689.
- 15 Kawada T, Yanagisawa T, Rajwa P, Sari Motlagh R, Mostafaei H, Quhal F *et al.* Diagnostic Performance of Prostate-specific Membrane Antigen Positron Emission Tomography-targeted biopsy for Detection of Clinically Significant Prostate Cancer: A Systematic Review and Meta-analysis. *Eur Urol Oncol* 2022; : S2588-9311(22)00064–5.
- 16 Raveenthiran S, Yaxley WJ, Franklin T, Coughlin G, Roberts M, Gianduzzo T *et al.* Findings in 1,123 Men with Preoperative 68Ga-Prostate-Specific Membrane Antigen Positron Emission Tomography/Computerized Tomography and Multiparametric Magnetic Resonance Imaging Compared to Totally Embedded Radical Prostatectomy Histopathology: Implications for the Diagnosis and Management of Prostate Cancer. *J Urol* 2022; **207**: 573–580.
- 17 Uprimny C, Kroiss AS, Decristoforo C, Fritz J, von Guggenberg E, Kendler D *et al.* 68Ga-PSMA-11 PET/CT in primary staging of prostate cancer: PSA and Gleason score predict the intensity of tracer accumulation in the primary tumour. *Eur J Nucl Med Mol Imaging* 2017; **44**: 941–949.
- 18 Kalapara AA, Ballok ZE, Ramdave S, O’Sullivan R, Ryan A, Konety B *et al.* Combined Utility of 68Ga-Prostate-specific Membrane Antigen Positron Emission Tomography/Computed Tomography and Multiparametric Magnetic Resonance Imaging in Predicting Prostate Biopsy Pathology. *Eur Urol Oncol* 2022; **5**: 314–320.
- 19 Bodar YJL, Zwezerijnen BGJC, van der Voorn PJ, Jansen BHE, Smit RS, Kol SQ *et al.* Prospective analysis of clinically significant prostate cancer detection with [18F]DCFPyL PET/MRI compared to multiparametric MRI: a comparison with the histopathology in the radical prostatectomy specimen, the ProStaPET study. *Eur J Nucl Med Mol Imaging* 2022; **49**: 1731–1742.
- 20 Malaspina S, Taimen P, Kallajoki M, Oikonen V, Kuisma A, Ettala O *et al.* Uptake of 18F-rhPSMA-73 in Positron Emission Tomography Imaging of Prostate Cancer: A Phase 1 Proof-of-Concept Study. *Cancer Biother Radiopharm* 2022; **37**: 205–213.
- 21 Woythal N, Arsenic R, Kempkensteffen C, Miller K, Janssen J-C, Huang K *et al.* Immunohistochemical Validation of PSMA Expression Measured by 68Ga-PSMA PET/CT in Primary Prostate Cancer. *Journal of Nuclear Medicine* 2018; **59**: 238–243.
- 22 Pattison DA, Debowski M, Gulhane B, Arnfield EG, Pelecanos AM, Garcia PL *et al.* Prospective intra-individual blinded comparison of [18F]PSMA-1007 and [68 Ga]Ga-PSMA-11 PET/CT imaging in patients with confirmed prostate cancer. *Eur J Nucl Med Mol Imaging* 2022; **49**: 763–776.
- 23 Surti S, Kuhn A, Werner ME, Perkins AE, Kolthammer J, Karp JS. Performance of Philips Gemini TF PET/CT scanner with special consideration for its time-of-flight imaging capabilities. *J Nucl Med* 2007; **48**: 471–480.
- 24 Soret M, Bacharach SL, Buvat I. Partial-Volume Effect in PET Tumor Imaging. *Journal of Nuclear Medicine* 2007; **48**: 932–945.
- 25 Exterkate L, Hermsen R, Küsters-Vandeveldel HVN, Prette JF, Baas DJH, Somford DM *et al.* Head-to-Head Comparison of 18F-PSMA-1007 Positron Emission Tomography/Computed Tomography and Multiparametric Magnetic Resonance Imaging with Whole-mount Histopathology as Reference in Localisation and Staging of Primary Prostate Cancer. *European Urology Oncology* 2023; **0**. doi:10.1016/j.euo.2023.04.006.

- 26 Samaratunga H, Montironi R, True L, Epstein JI, Griffiths DF, Humphrey PA *et al.* International Society of Urological Pathology (ISUP) Consensus Conference on Handling and Staging of Radical Prostatectomy Specimens. Working group 1: specimen handling. *Mod Pathol* 2011; **24**: 6–15.
- 27 Aide N, Lasnon C, Veit-Haibach P, Sera T, Sattler B, Boellaard R. EANM/EARL harmonization strategies in PET quantification: from daily practice to multicentre oncological studies. *Eur J Nucl Med Mol Imaging* 2017; **44**: 17–31.
- 28 Hong J-J, Liu B, Wang Z-Q, Tang K, Ji X-W, Yin W-W *et al.* The value of 18F-PSMA-1007 PET/CT in identifying non-metastatic high-risk prostate cancer. *EJNMMI Res* 2020; **10**: 138.
- 29 Rüschoff JH, Ferraro DA, Muehlematter UJ, Laudicella R, Hermanns T, Rodewald A-K *et al.* What's behind 68Ga-PSMA-11 uptake in primary prostate cancer PET? Investigation of histopathological parameters and immunohistochemical PSMA expression patterns. *Eur J Nucl Med Mol Imaging* 2021; **48**: 4042–4053.
- 30 Margel D, Bernstine H, Groshar D, Ber Y, Nezir O, Segal N *et al.* Diagnostic Performance of 68Ga Prostate-specific Membrane Antigen PET/MRI Compared with Multiparametric MRI for Detecting Clinically Significant Prostate Cancer. *Radiology* 2021; **301**: 379–386.
- 31 Arslan A, Karaarslan E, Güner AL, Sağlıcan Y, Tuna MB, Özışık O *et al.* Comparison of MRI, PSMA PET/CT, and Fusion PSMA PET/MRI for Detection of Clinically Significant Prostate Cancer. *J Comput Assist Tomogr* 2021; **45**: 210–217.
- 32 Emmett LM, Papa N, Buteau J, Ho B, Liu V, Roberts M *et al.* The PRIMARY Score: Using intra-prostatic PSMA PET/CT patterns to optimise prostate cancer diagnosis. *J Nucl Med* 2022; : jnumed.121.263448.
- 33 Wong L. PEDAL: a phase III study comparing diagnostic accuracy of mpMRI prostate to 18F-DCPyL PSMA PET/CT. *Presented at the 37th annual European Association of Urology Congress, Amsterdam, The Netherlands, 2022.*
- 34 Schmuck S, Mamach M, Wilke F, von Klot CA, Henkenberens C, Thackeray JT *et al.* Multiple Time-Point 68Ga-PSMA I&T PET/CT for Characterization of Primary Prostate Cancer: Value of Early Dynamic and Delayed Imaging. *Clin Nucl Med* 2017; **42**: e286–e293.
- 35 Heetman JG, Wever L, Paulino Pereira LJ, van den Bergh RCN. Clinically Significant Prostate Cancer Diagnosis Without Histological Proof: A Possibility in the Prostate-specific Membrane Antigen Era? *European Urology Open Science* 2022; **44**: 30–32.







# CHAPTER 3

## THE ADDITIONAL VALUE OF $^{68}\text{Ga}$ -PSMA PET/CT SUVMAX IN PREDICTING ISUP GG $\geq 2$ AND ISUP GG $\geq 3$ PROSTATE CANCER IN BIOPSY

J.G. Heetman  
L.J. Paulino Pereira  
J.C. Kelder  
T.F.W. Soeterik  
L. Wever  
J. Lavalaye  
E.J.R.J van der Hoeven  
M.G.E.H. Lam  
H.H.E. van Melick  
R.C.N. van den Bergh

## Abstract

*Background:* Prebiopsy magnetic resonance imaging (MRI) increases the detection rate of clinically significant prostate cancer (csPCa). Prostate-specific membrane antigen-positron emission tomography/computed tomography (PSMA PET/CT) maximum standardized uptake value (SUVmax) of the prostate may offer additional value in predicting the likelihood of csPCa in biopsy.

*Methods:* A single-center cohort study involving patients with biopsy-proven PCa who underwent both MRI and PSMA PET/CT between 2020 and 2021. Logistic regression models were developed for International Society of Urological Pathology (ISUP) Grade Group (GG)  $\geq 2$  and GG  $\geq 3$  using noninvasive prebiopsy parameters: age, (log-)prostate-specific antigen (PSA) density, PI-RADS 5 lesion presence, extraprostatic extension (EPE) on MRI, and SUVmax of the prostate. Models with and without SUVmax were compared using Likelihood ratio tests and area under the curve (AUC). DeLong's test was used to compare the AUCs.

*Results:* The study included 386 patients, with 262 (68%) having ISUP GG  $\geq 2$  and 180 (47%) having ISUP GG  $\geq 3$ . Including SUVmax significantly improved both models' goodness of fit ( $p < 0.001$ ). The GG  $\geq 2$  model had a higher AUC with SUVmax 89.16% (95% confidence interval [CI]: 86.06%–92.26%) than without 87.34% (95% CI: 83.93%–90.76%) ( $p = 0.026$ ). Similarly, the GG  $\geq 3$  model had a higher AUC with SUVmax (82.51% 95% CI: 78.41%–86.6%) than without 79.33% (95% CI: 74.84%–83.83%) ( $p = 0.003$ ). The SUVmax inclusion improved the GG  $\geq 3$  model's calibration at higher probabilities.

*Conclusion:* SUVmax of the prostate on PSMA PET/CT potentially improves diagnostic accuracy in predicting the likelihood of csPCa in prostate biopsy.

## Introduction

Over a million prostate biopsies are performed annually for histological confirmation of PCa, yet this invasive procedure is unpleasant and carries the risk of complications, such as infection.<sup>1,2</sup> The integration of prebiopsy magnetic resonance imaging (MRI) has demonstrated an increased percentage of cancers labelled as clinically significant (cs)PCa.<sup>3</sup> However, MRI has limitations in accurately detecting csPCa, as 17% of biopsies performed in men with Prostate Imaging-Reporting and Data System (PI-RADS) maximum score 5 lesions yield nonsignificant PCa or benign tissue.<sup>1</sup> Therefore, PI-RADS 5 lesions are far from perfect predictors for csPCa.

The PRIMARY trial recently demonstrated the benefit of prostate-specific membrane antigen-positron emission tomography/computed tomography (PSMA PET/CT) in detecting csPCa in the primary diagnostic setting. The study showed that local gland PSMA activity, defined as positive with a maximum standardised uptake value (SUVmax) of 4 or higher, in combination with MRI did not lead to an improvement of the overall positive predictive value, but instead a reduction was found, probably due to the low SUVmax threshold used. As expected at such a low threshold, an improvement in negative predictive value and sensitivity was found.<sup>4</sup> Kalapara *et al.* observed a significantly higher median SUVmax of 6.40 (interquartile range [IQR] 4.47–11.0) for International Society of Urological Pathology (ISUP) Grade Group (GG) 3–5 tumours compared to a median SUVmax of 3.14 (IQR 2.55–3.91) for benign and GG 1–2 tumours.<sup>5</sup> In a subanalysis of the PRIMARY trial conducted by Ptasznik *et al.*, all 53 patients with a PI-RADS score of 4 or 5 and an SUVmax greater than 8.7 were identified as having csPCa, defined as a GG of 2 or higher.<sup>6</sup>

Given the findings, integrating local gland PSMA activity, treated as a continuous variable, with MRI results could enhance the accuracy in predicting csPCa. Therefore, the aim of this study is to assess the potential added value of the prostate's SUVmax on PSMA-PET/CT in predicting the likelihood of csPCa in biopsy.

## Materials and Methods

### Data Source and Patient Selection

This study included a retrospective cohort of patients diagnosed with clinically significant prostate cancer (csPCa) who received staging PSMA PET/CT at a Dutch teaching hospital (locally registered under Z22.053) between 2020 and 2021. Additionally, patients from a prospective study (PSMA in Active Surveillance for Prostate Cancer Trial; NL69880.100.19) were included.<sup>7</sup> The latter cohort primarily consisted of low-risk patients diagnosed with prostate cancer who were eligible for active surveillance. These patients received PSMA PET/CT as part of the PASPoRT protocol. In the PASPoRT study, patients underwent rebiopsy if the PSMA revealed new lesions that were not previously visualized on MRI. The biopsy results obtained before the PSMA-targeted biopsy were used in this study to ensure the comparability between the two cohorts. All patients included in the study had undergone both PSMA PET/CT and prostate MRI without prior treatment for biopsy-confirmed prostate cancer.

### MRI Protocol

All patients underwent a prebiopsy 3-Tesla biparametric MRI (Magnetom Skyra; Siemens Nederland B.V.) The scanner used a body coil. Sequences consisted of sagittal, coronal, and axial T2-weighted images and axial diffusion-weighted images. MRI scans were evaluated by experienced uro-radiologists (>1000 prostate MRI) using the PI-RADS v2.1 classification.<sup>8</sup>

### PSMA Protocol

The <sup>68</sup>Ga-PSMA was prepared using a GMP-grade <sup>68</sup>Ge/<sup>68</sup>Ga generator and a semiautomated synthesis module (Eckert & Ziegler and ITG). The dose of <sup>68</sup>Ga-PSMA was 1.5 MBq/kg. Patients received 10 mg of furosemide at the time of radiotracer injection. PET images were acquired 60 min postinjection. Low-dose CT was performed directly following PET imaging. Scans were acquired using a Biograph mCT 40 scanner (Siemens) or a Gemini TF 64 slice scanner (Philips). Scans were evaluated by experienced nuclear medicine physicians according to the prevailing European Association of Nuclear Medicine (EANM) guidelines.<sup>9</sup>

### Biopsy Protocol

The prostate biopsy cores were acquired via a transrectal or transperineal approach by an experienced onco-urologist. Cognitive targeted biopsy<sup>10</sup> was performed if a suspicious lesion (PI-RADS $\geq$ 3) was seen on the prebiopsy MRI. At least three targeted cores were performed on each MRI. Most patients also received systematic biopsy cores. A dedicated uropathologist examined the biopsy cores, according to the prevailing International Society of Urologic Pathology (ISUP) guidelines.<sup>11</sup>

### Missing Data

Missing data patterns were explored using response matrix and correlation plots. Missing data were handled by using multivariate imputation by chained equations including pooling using Rubin's rules.<sup>12</sup>

### Model Building and Performance

The aim was to ascertain the added value of the SUVmax of the prostate in predicting clinically significant prostate cancer (csPCa) at biopsy. Models for predicting csPCa in prostate biopsies were developed using multivariable logistic regression, two different endpoints were used: ISUP GG  $\geq 2$ , which is the most used definition for csPCa, and ISUP GG  $\geq 3$ , which is PCa for which active surveillance is generally considered no option and active therapy is indicated according to current guidelines. The models to predict ISUP GG  $\geq 2$  and GG  $\geq 3$  included the following variables: age (years), log (PSA density (ng/mL/mL)), EPE on the MRI, the presence of a PI-RADS 5 lesion, and SUVmax. These variables were chosen from the literature as they have known impact on the aggressiveness of PCa.<sup>1,13-15</sup> Both models were compared to models without SUVmax to assess the potential additional predictive value. Likelihood ratio tests were performed to compare the goodness of fit of models with and without the SUVmax of the prostate. Discrimination, which refers to the ability of a model to distinguish a patient with or without ISUP GG 2 or GG 3 or higher, was quantified using the area under the receiver operating characteristic curve (AUC), and DeLong's test was used to compare the AUC between models with and without SUVmax of the prostate. Calibration, which refers to the agreement between observed endpoints and predictions, was assessed using a calibration slope with a locally estimated scatterplot smoothing curve. All the analyses were performed with R version 4.2.2.

## Results

### Baseline Characteristics

Table 1 shows the baseline characteristics. A total of 386 patients were included for model development, of which 262 (68%) had an ISUP GG  $\geq 2$ , and 180 (47%) had an ISUP GG  $\geq 3$  or more. Out of the 352 patients with suspected lesions on MRI, 288 (82%) underwent targeted biopsy and systematic biopsy, and 64 (18%) received only targeted biopsy.

**Table 1:** Baseline characteristics

	Overall ( <i>n</i> = 386)
Age (years) median (IQR)	70 (65, 74)
PSA (ng/mL) median (IQR)	8.0 (5.2, 13.2)
PSAD (ng/mL/mL) median (IQR)	0.17 (0.12, 0.30)
unknown	6
MRI T-stadium <i>n</i> (%)	
T0	34 (9%)
T2	226 (59%)
T3	123 (32%)
T4	3 (1%)
PI-RADS <i>n</i> (%)	
1	13 (3%)
2	21 (5%)
3	27 (7%)
4	147 (35%)
5	188 (49%)
Biopsy type <i>n</i> (%)	
Systematic	34 (9%)
Systematic and targeted	288 (75%)
Only targeted	64 (17%)
ISUP Grade Group <i>n</i> (%)	
1	124 (32%)
2	82 (21%)
3	69 (18%)
4	83 (22%)
5	28 (7%)
SUVmax median (IQR)	6.5 (4.1, 11.1)

Abbreviations: IQR, interquartile range; ISUP, International Society of Urologic Pathology; MRI, magnetic resonance imaging; PI-RADS, Prostate Imaging-Reporting and Data System; PSA, prostate-specific antigen; PSAD, prostate-specific antigen density; SUVmax, maximum standardised uptake value.



**Model GG  $\geq$  2**

Table 2 shows that the patients with an ISUP GG  $\geq$  2 versus ISUP GG  $<$  2 in biopsy were significantly older ( $p < 0.001$ ), had a higher logPSA density ( $p < 0.001$ ), a higher SUVmax ( $p < 0.001$ ), had more frequent PI-RADS 5 lesions on MRI ( $p < 0.001$ ) and more often EPE on MRI ( $p < 0.001$ ). In Table 3 the multivariable logistic regression models are shown. The goodness of fit increased significantly with addition of SUVmax ( $\chi^2 = 24.75$ ,  $df = 1$ ,  $p < 0.001$ ). The models with SUVmax had a higher AUC of 89.16% (95% CI: 86.06%–92.26% versus 87.34% (95% CI: 83.93%–90.76%) for the model without SUVmax ( $p = 0.026$ ). Figure 1 shows the calibration slope for the models with and without SUVmax displaying a similar curve, with a better prediction for the model with SUVmax from a predicted probability between 0.55 and 0.75.

**Model GG  $\geq$  3**

Patients whose biopsy results showed an ISUP GG  $\geq$  3 were found to be significantly older ( $p < 0.001$ ), had higher logPSA density ( $p < 0.001$ ), a higher SUVmax ( $p < 0.001$ ), more frequent a PI-RADS 5 lesion on MRI ( $p < 0.001$ ), and more often EPE on MRI ( $p < 0.001$ ) compared to those with ISUP GG  $<$  3. Table 3 displays the multivariable logistic regression model. The goodness of fit increased significantly with the inclusion of SUVmax ( $\chi^2 = 23.54$ ,  $df = 1$ ,  $p < 0.001$ ). The model that included SUVmax had a higher AUC with a value of 82.5% (95% CI: 78.41%–86.6%) compared to 79.33% (95% CI: 74.84%–83.83%) for the model without SUVmax ( $p = 0.003$ ). Figure 1 shows that the calibration slope for the models with SUVmax had a better predictive performance from a predicted probability of 0.45 and higher.

**Table 2:** The variables used for the model for the two different definitions of clinically significant prostate cancer

Age(years) (IQR)

log(PSA-D ×100) (ng/mL/mL) (IQR)

MRI EPE

PI-RADS 5

SUVmax (IQR)

Abbreviations: EPE, extraprostatic extension; ISUP GG, International Society of Urologic Pathology Grade Group; IQR, interquartile range; MRI, magnetic resonance imaging; PI-RADS, Prostate Imaging-Reporting and Data System;

**Table 3:** The multivariable logistic regression models for the two different definitions of clinically significant prostate cancer with and without SUVmax of the prostate

	ISUP GG ≥ 2			
	SUVmax		without SUVmax	
	OR (95% CI)	p-value	OR (95% CI)	p-value
Age(years)	1.1 (1.0, 1.1)	0.005	1.1 (1.0, 1.1)	<0.001
log(PSA-D ×100) (ng/mL/mL)	5.8 (3.1, 11.7)	<0.001	8.6 (4.8, 16.6)	
MRI EPE		0.002		<0.001
No	Reference		Reference	
yes	5.8 (2.0, 18.5)		6.2 (2.2, 18.8)	
PI-RADS 5		0.4		0.072
No	Reference		Reference	
Yes	1.4 (0.6, 3.0)		2.0 (1.0, 4.2)	
SUVmax	1.2 (1.1, 1.4)	<0.001	-	-

Abbreviations: CI, confidence interval; EPE, extraprostatic extension; ISUP GG, International Society of Urologic Pathology Grade Group; MRI, magnetic resonance imaging;

N = 386			N = 386		
ISUP GG < 2 (n = 124)	ISUP GG ≥ 2 (n = 262)	p-value <sup>a</sup>	ISUP GG <3 (n = 206)	ISUP GG ≥ 3 (n = 180)	p-value <sup>a</sup>
68 (62, 72)	72 (67, 75)	<b>&lt;0.001</b>	69 (64, 73)	72 (68, 75)	<b>&lt;0.001</b>
2.56 (2.20, 2.77)	3.04 (2.71, 3.61)	<b>&lt;0.001</b>	2.71 (2.30, 3.00)	3.14 (2.71, 3.64)	<b>&lt;0.001</b>
7 (6%)	119 (45%)	<b>&lt;0.001</b>	35 (17%)	88 (49%)	<b>&lt;0.001</b>
23 (19%)	165 (63%)	<b>&lt;0.001</b>	60 (30%)	128 (71%)	<b>&lt;0.001</b>
4.1 (3.3, 5.5)	8.9 (5.4, 15.4)	<b>&lt;0.001</b>	5.0 (3.6, 7.1)	10.1 (6.4, 17.1)	<b>&lt;0.001</b>

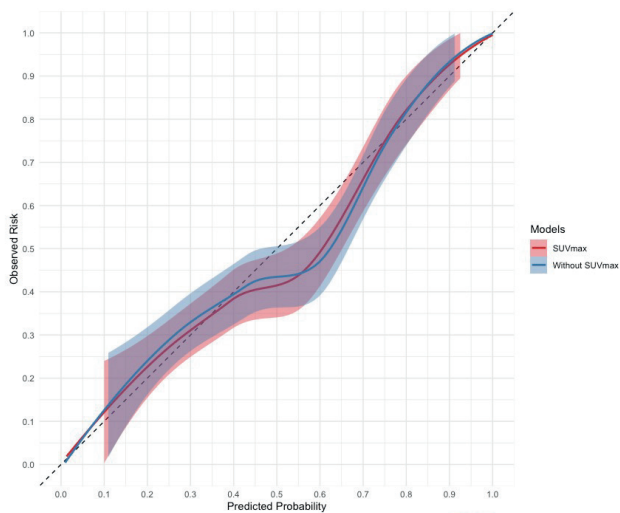
PSAD, prostate-specific antigen density; SUVmax, maximum standardised uptake value.

<sup>a</sup>Wilcoxon rank sum test; Pearson's  $\chi^2$  test.

ISUP GG ≥ 3			
SUVmax		without SUVmax	
OR (95% CI)	p-value	OR (95% CI)	p-value
1.1 (1.0, 1.1)	<b>0.005</b>	1.1 (1.0, 1.1)	<b>0.002</b>
1.5 (1.0, 2.2)	0.069	2.3 (1.6, 3.3)	0.069
	0.3		0.2
Reference 1.4 (0.7, 2.8)		Reference 1.6 (0.8, 3.1)	
	<b>0.003</b>		<b>&lt;0.001</b>
Reference 2.7 (1.4, 5.2)		Reference 3.1 (1.7, 5.9)	
1.1 (1.1, 1.2)	<b>&lt;0.001</b>	-	-

OR, odds ratio; PI-RADS, Prostate Imaging-Reporting and Data System; PSAD, prostate-specific antigen density; SUVmax, maximum standardised uptake value.

## ISUP GG $\geq 2$



## ISUP GG $\geq 3$

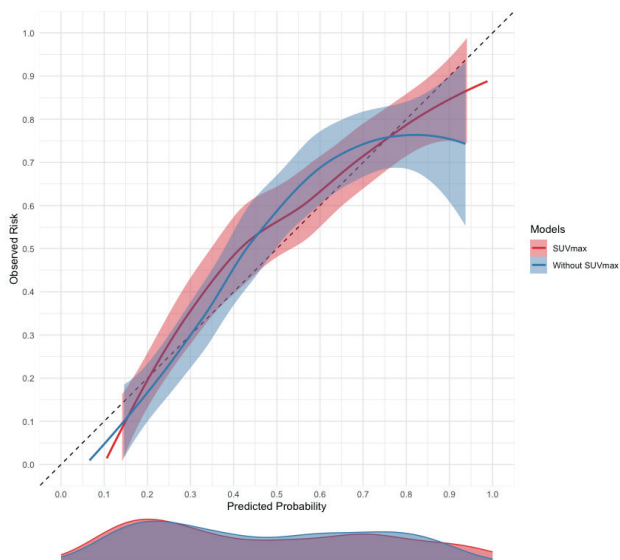


**Figure 1:**

The calibration curve with a LOESS (Locally Estimated Scatterplot Smoothing) curve for the predicted and observed probabilities in multivariable logistic regression models. These models are for two different definitions of clinically significant prostate cancer, with and without the SUVmax of the prostate. The model with ISUP GG  $\geq 2$ , shown at the top, demonstrates a minimal increase in predictive value.

In contrast, the model with ISUP GG  $\geq 3$ , presented at the bottom, exhibits better predictive performance from a predicted probability of 0.45 and higher, when including SUVmax. ISUP GG, International Society of Urologic Pathology Grade Group; SUVmax, maximum standardised uptake value.

## Discussion

This study evaluated the added value of PSMA PET/CT SUVmax of the prostate in predicting ISUP GG  $\geq 2$  and ISUP GG  $\geq 3$  on prostate biopsy, compared to conventional parameters. SUVmax significantly improved the predictive value of both models, particularly enhancing calibration for GG  $\geq 3$ . This emphasizes the benefit of SUVmax in identifying patients with a high probability of GG  $\geq 3$ .

These findings add to the growing body of evidence supporting the role of local gland PSMA activity in the characterization of PCa. In addition to the PRIMARY study, which concluded that with the combination of a negative MRI and an SUVmax below the cut-off point of 4, a prostate biopsy could be safely omitted due to the minimal likelihood of csPCa, this study illustrates the opposite: that SUVmax could be used to identify patients with a very high probability of csPCa.<sup>4</sup> The outcomes of this study reinforce the findings of Ptasznik *et al.*, wherein all patients with a PI-RADS score of 4 or 5 and a SUVmax above 8.7 had GG  $\geq 2$ .<sup>6</sup> Additionally, our findings support the use of a combination of PSMA PET/CT and MRI results in counselling patients, as presented by Meissner *et al.*, who are unwilling to undergo prostate biopsy. In their series of cases, radical prostatectomy was performed on 25 patients who showed a high suspicion on MRI (PI-RADS 4 or 5) and PSMA PET/CT (PET score  $\geq 4$  on a 5-point Likert scale and SUVmax  $\geq 4.0$ ) without prior biopsy, with histological confirmation of GG 2 or higher in all cases.<sup>16</sup> In addition to the <sup>68</sup>Ga tracer, other PSMA tracers, like <sup>18</sup>F-PSMA-1007 and <sup>18</sup>F-DCFPyL, have proven effective in detecting intraprostatic lesions with csPCa.<sup>17,18</sup> However, a practical issue to consider is the variation in SUV values between various PSMA ligands, with <sup>18</sup>F-based tracers generally having higher SUVmax values than <sup>68</sup>Ga-based tracers. Hence, SUVmax values cannot be universally exchanged between centres using different PSMA tracers, necessitating the development of tracer-specific predictive models.<sup>19,20</sup>

This study is not without limitations. A primary limitation is the lack of external validation, which may affect the generalizability of our findings. Furthermore, only MRI-targeted biopsies were used in 18% of patients with positive MRI results, thereby increasing the potential for undersampling. The study's reliance on biopsy histology could be interpreted as a surrogate outcome, introducing a possible source of bias. A centralised review was not conducted for pathology and imaging results, which might introduce a risk of misclassification and potentially compromise the accuracy of our findings. In contrast to the PRIMARY trial, our cohort underwent PSMA PET/CT postdiagnosis of PCa. This is because performing PSMA PET/CT in patients suspected of prostate cancer is not recommended by the guidelines.<sup>4,21</sup> This limitation means that PSMA active lesions were not targeted in biopsies, and no patients without prostate cancer were included. While universally

administering PSMA PET/CT to all patients suspected of PCa may not be economically viable, it might be feasible for high-risk groups. For these groups, who are likely to need staging imaging, an upfront PSMA PET/CT could be conducted without incurring additional costs. Furthermore, the PRIMARY score was not provided for the scans used in this study. The PRIMARY score was developed as a subanalysis of the PRIMARY study to identify high-risk patterns and locations of PSMA activity within the prostate. In this scoring system, 8.5% of the 47 patients with a PRIMARY score of 1 had  $GG \geq 2$ , increasing to 100% of the 43 patients with a PRIMARY score of 5.<sup>22</sup> This score shows promise but has not yet been externally validated. Lastly, the combination of the prospective and retrospective cohorts is a limitation, although by taking the biopsy results before PSMA PET/CT in the prospective group, this risk was minimized.

Although this study has methodological limitations, the inclusion of a large patient population, including patients in whom PSMA PET/CT was performed with ISUP  $GG < 2$  on biopsy, can be considered a major strength. This is because limited data is available on the value of PSMA PET/CT in patients with an ISUP  $GG < 2$ . Although the results in this study should be interpreted with caution, they provide clinically relevant pilot data regarding the value of PSMA PET/CT SUVmax of the prostate for csPCa detection at initial diagnosis.

This model serves as a proof of concept and has not yet been externally validated. Therefore, future directions include the development and external validation of models that incorporate the SUVmax of the prostate for predicting csPCa in a larger, multicentre cohort. Such an approach could yield more robust models with potential clinical applicability. Additionally, due to the increase in the number of patients, it may be possible to include more parameters, such as additional PSMA parameters like tumour volume on PSMA PET/CT or patterns of tracer distribution.<sup>22,23</sup> Vetrone *et al.* discovered that a higher tumour volume on PSMA PET/CT was indicative of the presence of a cribriform growth pattern, which is associated with an increased likelihood of positive lymph nodes during pelvic lymph node dissection, a risk of metastatic recurrence, and a shorter time to biochemical recurrence.<sup>24-27</sup> Furthermore, should more advanced statistical methods, like machine learning, be utilized for model development, this could potentially result in a model with higher predictive value. Moreover, the clinical implementation of models that include SUVmax is an interesting area of research. These models could be used not only for the prediction of csPCa but also to predict the chance of biopsy error and for counselling patients who refuse prostate biopsy. Finally, if these prediction tools with noninvasive parameters become more precise, it may be possible to predict other aspects of PCa, including the Gleason score, biomarkers, or the presence of cribriform growth. If that happens in the future, it may result in a real “virtual biopsy”.<sup>28</sup>

Starting therapy based on the suspicion of PCa without histological confirmation remains controversial. This approach is possible for other malignancies like renal cell carcinoma, where histological proof is only needed in the presence of radiologically indeterminate renal masses.<sup>29</sup> However, our results highlight the benefit of SUVmax in identifying patients with a high probability of GG  $\geq$  3. This could make a diagnostic pathway without biopsy viable in the future for selected cases of very high-risk PCa. A reduction in the number of patients indicated for biopsy could possibly result in less morbidity and discomfort for patients and a reduction in costs for society.<sup>2</sup> Nonetheless, to consider omitting a biopsy, near-perfect specificity is essential. This is because the minor inconvenience of a prostate biopsy is outweighed by the potential side effects and complications of unnecessary active PCa treatment.<sup>2,30,31</sup>

## Conclusion

Our study demonstrated that the inclusion of PSMA PET/CT SUVmax of the prostate improves models predicting biopsy results with an ISUP Grade Group of 2 or higher and 3 or higher. Therefore, it could potentially be useful for predicting the risk of clinically significant prostate cancer on biopsy.

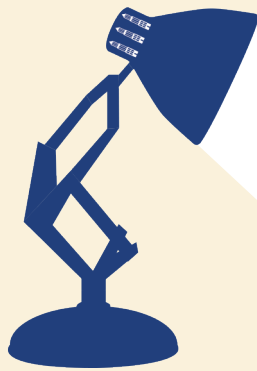


## References

- 1 Kasivisvanathan V, Rannikko AS, Borghi M, Panebianco V, Mynderse LA, Vaarala MH *et al.* MRI-Targeted or Standard Biopsy for Prostate-Cancer Diagnosis. *N Engl J Med* 2018; **378**: 1767–1777.
- 2 Tan J-L, Papa N, Hanegbi U, Snow R, Grummet J, Mann S *et al.* Predictors of erectile dysfunction after transperineal template prostate biopsy. *Investig Clin Urol* 2021; **62**: 159–165.
- 3 Drost FH, Osses DF, Nieboer D, Steyerberg EW, Bangma CH, Roobol MJ *et al.* Prostate MRI, with or without MRI-targeted biopsy, and systematic biopsy for detecting prostate cancer. *Cochrane Database Syst Rev* 2019; **2019**: CD012663.
- 4 Emmett L, Buteau J, Papa N, Moon D, Thompson J, Roberts MJ *et al.* The Additive Diagnostic Value of Prostate-specific Membrane Antigen Positron Emission Tomography Computed Tomography to Multiparametric Magnetic Resonance Imaging Triage in the Diagnosis of Prostate Cancer (PRIMARY): A Prospective Multicentre Study. *Eur Urol* 2021; **80**: 682–689.
- 5 Kalapara AA, Ballok ZE, Ramdave S, O’Sullivan R, Ryan A, Konety B *et al.* Combined Utility of 68Ga-Prostate-specific Membrane Antigen Positron Emission Tomography/Computed Tomography and Multiparametric Magnetic Resonance Imaging in Predicting Prostate Biopsy Pathology. *Eur Urol Oncol* 2022; **5**: 314–320.
- 6 Ptasznik G, Papa N, Kelly BD, Thompson J, Stricker P, Roberts MJ *et al.* High PSMA PET SUVmax in PI-RADS 4 or 5 men confers a high probability of significant prostate cancer. *BJU Int* 2022. doi:10.1111/bju.15736.
- 7 Heetman JG, Lavalaye J, Polm PD, Soeterik TFW, Wever L, Paulino Pereira LJ *et al.* Gallium-68 Prostate-specific Membrane Antigen Positron Emission Tomography/Computed Tomography in Active Surveillance for Prostate Cancer Trial (PASPoRT). *European Urology Oncology* 2023. doi:10.1016/j.euo.2023.05.004.
- 8 Turkbey B, Rosenkrantz AB, Haider MA, Padhani AR, Villeirs G, Macura KJ *et al.* Prostate Imaging Reporting and Data System Version 2.1: 2019 Update of Prostate Imaging Reporting and Data System Version 2. *Eur Urol* 2019; **76**: 340–351.
- 9 Ceci F, Oprea-Lager DE, Emmett L, Adam JA, Bomanji J, Czernin J *et al.* E-PSMA: the EANM standardized reporting guidelines v1.0 for PSMA-PET. *Eur J Nucl Med Mol Imaging* 2021; **48**: 1626–1638.
- 10 Wegelin O, Exterkate L, van der Leest M, Kummer JA, Vreuls W, de Bruin PC *et al.* The FUTURE Trial: A Multicenter Randomised Controlled Trial on Target Biopsy Techniques Based on Magnetic Resonance Imaging in the Diagnosis of Prostate Cancer in Patients with Prior Negative Biopsies. *Eur Urol* 2019; **75**: 582–590.
- 11 van Leenders GJLH, van der Kwast TH, Grignon DJ, Evans AJ, Kristiansen G, Kweldam CF *et al.* The 2019 International Society of Urological Pathology (ISUP) Consensus Conference on Grading of Prostatic Carcinoma. *Am J Surg Pathol* 2020; **44**: e87–e99.
- 12 Van Buuren S, Groothuis-Oudshoorn K. Multivariate Imputation by Chained Equations in R. *Journal of statistical software* 2011; **45**: 1–67.
- 13 Nordström T, Akre O, Aly M, Grönberg H, Eklund M. Prostate-specific antigen (PSA) density in the diagnostic algorithm of prostate cancer. *Prostate Cancer Prostatic Dis* 2018; **21**: 57–63.
- 14 Ahdoot M, Wilbur AR, Reese SE, Lebastchi AH, Mehralivand S, Gomella PT *et al.* MRI-Targeted, Systematic, and Combined Biopsy for Prostate Cancer Diagnosis. *N Engl J Med* 2020; **382**: 917–928.
- 15 Boschheidgen M, Schimmöller L, Arsov C, Ziayee F, Morawitz J, Valentin B *et al.* MRI grading for the prediction of prostate cancer aggressiveness. *Eur Radiol* 2022; **32**: 2351–2359.

- 16 Meissner VH, Rauscher I, Schwamborn K, Neumann J, Miller G, Weber W *et al.* Radical Prostatectomy Without Prior Biopsy Following Multiparametric Magnetic Resonance Imaging and Prostate-specific Membrane Antigen Positron Emission Tomography. *Eur Urol* 2021; : S0302-2838(21)02194-1.
- 17 Hong J-J, Liu B, Wang Z-Q, Tang K, Ji X-W, Yin W-W *et al.* The value of 18F-PSMA-1007 PET/CT in identifying non-metastatic high-risk prostate cancer. *EJNMMI Res* 2020; **10**: 138.
- 18 Bodar YJL, Zwezerijnen BGJC, van der Voorn PJ, Jansen BHE, Smit RS, Kol SQ *et al.* Prospective analysis of clinically significant prostate cancer detection with [18F]DCFPyL PET/MRI compared to multiparametric MRI: a comparison with the histopathology in the radical prostatectomy specimen, the ProStaPET study. *Eur J Nucl Med Mol Imaging* 2022; **49**: 1731-1742.
- 19 Dietlein M, Kobe C, Kuhnert G, Stockter S, Fischer T, Schomäcker K *et al.* Comparison of [(18)F] DCFPyL and [ (68)Ga]Ga-PSMA-HBED-CC for PSMA-PET Imaging in Patients with Relapsed Prostate Cancer. *Mol Imaging Biol* 2015; **17**: 575-584.
- 20 Piron S, Verhoeven J, Vanhove C, De Vos F. Recent advancements in 18F-labeled PSMA targeting PET radiopharmaceuticals. *Nucl Med Biol* 2022; **106-107**: 29-51.
- 21 Mottet N, van den Bergh RCN, Briers E, Van den Broeck T, Cumberbatch MG, De Santis M *et al.* EAU-EANM-ESTRO-ESUR-SIOG Guidelines on Prostate Cancer-2020 Update. Part 1: Screening, Diagnosis, and Local Treatment with Curative Intent. *Eur Urol* 2021; **79**: 243-262.
- 22 Emmett LM, Papa N, Buteau J, Ho B, Liu V, Roberts M *et al.* The PRIMARY Score: Using intra-prostatic PSMA PET/CT patterns to optimise prostate cancer diagnosis. *J Nucl Med* 2022; : jnumed.121.263448.
- 23 Wong L. PEDAL: a phase III study comparing diagnostic accuracy of mpMRI prostate to 18F-DCPyL PSMA PET/CT. *Presented at the 37th annual European Association of Urology Congress, Amsterdam, The Netherlands, 2022.*
- 24 Vetrone L, Mei R, Bianchi L, Giunchi F, Farolfi A, Castellucci P *et al.* Histology and PSMA Expression on Immunohistochemistry in High-Risk Prostate Cancer Patients: Comparison with 68Ga-PSMA PET/CT Features in Primary Staging. *Cancers (Basel)* 2023; **15**: 1716.
- 25 Kweldam CF, Wildhagen MF, Steyerberg EW, Bangma CH, van der Kwast TH, van Leenders GJLH. Cribriform growth is highly predictive for postoperative metastasis and disease-specific death in Gleason score 7 prostate cancer. *Mod Pathol* 2015; **28**: 457-464.
- 26 Hollemans E, Verhoef EI, Bangma CH, Rietbergen J, Osanto S, Pelger RCM *et al.* Cribriform architecture in radical prostatectomies predicts oncological outcome in Gleason score 8 prostate cancer patients. *Mod Pathol* 2021; **34**: 184-193.
- 27 Downes MR, Xu B, van der Kwast TH. Cribriform architecture prostatic adenocarcinoma in needle biopsies is a strong independent predictor for lymph node metastases in radical prostatectomy. *Eur J Cancer* 2021; **148**: 432-439.
- 28 Murray JM, Wiegand B, Hadaschik B, Herrmann K, Kleesiek J. Virtual Biopsy: Just an AI Software or a Medical Procedure? *J Nucl Med* 2022; **63**: 511-513.
- 29 Ljungberg B, Albiges L, Abu-Ghanem Y, Bedke J, Capitanio U, Dabestani S *et al.* European Association of Urology Guidelines on Renal Cell Carcinoma: The 2022 Update. *Eur Urol* 2022; : S0302-2838(22)01676-1.
- 30 Teunissen FR, Willigenburg T, Meijer RP, van Melick HHE, Verkooijen HM, van der Voort van Zyp JRN. The first patient-reported outcomes from the Utrecht Prostate Cohort (UPC): the first platform facilitating 'trials within cohorts' (TwICs) for the evaluation of interventions for prostate cancer. *World J Urol* 2022. doi:10.1007/s00345-022-04092-2.
- 31 Romito I, Giannarini G, Rossanese M, Mucciardi G, Simonato A, Ficarra V. Incidence of Rectal Injury After Radical Prostatectomy: A Systematic Review and Meta-analysis. *Eur Urol Open Sci* 2023; **52**: 85-99.





# CHAPTER 4

## GALLIUM-68 PROSTATE-SPECIFIC MEMBRANE ANTIGEN POSITRON EMISSION TOMOGRAPHY/ COMPUTED TOMOGRAPHY IN ACTIVE SURVEILLANCE FOR PROSTATE CANCER TRIAL (PASPORT)

J.G. Heetman

J. Lavalaye

P.D. Polm

T.F.W. Soeterik

L. Wever

L.J. Paulino Pereira

E.J.R.J. van der Hoeven

H.H.E. van Melick

R.C.N. van den Bergh

## Abstract

*Background:* The use of clinical parameters, including prebiopsy magnetic resonance imaging (MRI), to decide between active surveillance (AS) and active therapy for prostate cancer (PCa) leads to imperfect selection. Additional prostate-specific membrane antigen (PSMA) positron emission tomography/computed tomography (PET/CT) imaging may improve risk stratification.

*Objective:* To study risk stratification and patient selection for AS with the addition of PSMA PET/CT to standard practice.

*Design, setting, and participants:* A single-centre prospective cohort study (NL69880.100.19) enrolled patients recently diagnosed with PCa who started AS. At diagnosis, all participants had undergone prebiopsy MRI and targeted biopsy for visualised lesions. Patients underwent an additional [68Ga]-PSMA PET/CT and targeted biopsy of all PSMA lesions with a maximum standardised uptake value (SUVmax) of 24 not covered by previous biopsies.

*Outcome measurements and statistical analysis:* The primary outcome was the number needed to scan (NNS) to detect one patient with upgrading. The study was powered to detect an NNS of 10. Regarding secondary outcomes, univariate logistic regressions analyses were performed on all patients and on the patients who received additional PSMA targeted biopsies on the likelihood of upgrading.

*Results and limitations:* A total of 141 patients were included. Additional PSMA targeted biopsies were performed in 45 (32%) patients. In 13 (9%) patients, upgrading was detected: nine grade group (GG) 2, two GG 3, one GG 4, and one GG 5. The NNS was 11 (95% confidence interval 6–18). Of all participants, PSMA PET/CT and targeted biopsies yielded upgrading most frequently in patients with negative MRI (Prostate Imaging Reporting and Data System [PI-RADS] 1–2). Of patients who received additional PSMA targeted biopsies, upgrading was most frequently found in those with higher prostate-specific antigen density and negative MRI. Limitations included the lack of comparison with standard repeat biopsy, no central review of MRI, and possibility of biopsy sampling error.

*Conclusion:* PSMA PET/CT can further improve PCa risk stratification and selection for AS patients diagnosed after MRI and targeted biopsies.

*Patient summary:* Prostate-specific membrane antigen positron emission tomography/computed tomography and additional targeted prostate biopsies can identify more aggressive prostate cancer cases previously missed in patients recently started with expectant management for favourable-risk prostate cancer.

## Introduction

Active surveillance (AS) for low-risk and selected intermediate-risk prostate cancer (PCa) is the preferred treatment strategy, as recommended by the European guidelines.<sup>1</sup> Recently, using magnetic resonance imaging (MRI) and targeted biopsies, risk stratification of PCa has improved.<sup>2-4</sup> Owing to the resulting stage shift, the inclusion criteria for AS have expanded.<sup>5</sup> However, systematic biopsy may still detect clinically significant prostate cancer (csPCa) in patients with negative MRI (Prostate Imaging Reporting and Data System [PI-RADS] 1-2), and International Society of Urologic Pathology (ISUP) grade group (GG) upgrading between biopsy and prostatectomy specimen still occurs after MRI and targeted biopsies.<sup>3,6-8</sup>

Recently, prebiopsy prostate-specific membrane antigen (PSMA) positron emission tomography/computed tomography (PET/CT) has been discovered to provide added value in the primary diagnosis and local risk stratification of PCa when combined with prebiopsy MRI. This combination has increased the sensitivity and negative predictive value of csPCa detection from 83% to 97% and from 72% to 91%, respectively, compared with using MRI alone.<sup>9</sup> Additionally, the standardised uptake value (SUV) of PSMA PET/CT was found to have a significant positive association with ISUP GG.<sup>10,11</sup> The abilities of this new molecular imaging modality may also have additional value when added to the standard pathway of risk stratification and selection of patients for AS.<sup>12</sup>

The current study aims to prospectively assess whether additional PSMA PET/CT with additional targeted biopsies in lesions previously not covered by biopsy can result in a higher ISUP GG (upgrading) in patients recently started with AS, and thus result in better risk stratification and patient selection for AS.

## Method

### Data Source and Patient Selection

The prospective cohort study PSMA in Active Surveillance for PRostate Cancer Trial (PASPoRT; NL69880.100.19) was powered to detect GG upgrading (GG 1 to 22 or GG 2 to 23) in 10% of participants. This was estimated considering that after MRI and targeted biopsy 17% of patients have ISUP GG upgrading in prostatectomy.<sup>13</sup> This study was powered for precision with a 95% confidence interval (CI) with a width of 10%. This resulted in a sample size of 141 patients. The study was funded by the research fund of the Sint Antonius Hospital. Candidates were recently (<6 mo) diagnosed with PCa and started AS following the prevailing Prostate Cancer Research International: Active Surveillance (PRIAS) inclusion protocol.<sup>5</sup> At diagnosis, all participants had undergone prebiopsy MRI. Informed consent was obtained from all candidates. The study enrolment started in May 2020 and stopped in December 2021.

### MRI Protocol

All patients underwent prebiopsy 3-Tesla biparametric MRI (Magnetom Skyra; Siemens Nederland B.V., The Hague, The Netherlands). The scanner used a body coil. Sequences consisted of sagittal, coronal, and axial T2-weighted images and axial diffusion-weighted images. MRI scans were performed in four hospital locations of a regional oncological collaboration and evaluated using the PI-RADS version 2.1 classification.<sup>14</sup> All MRI scans were evaluated by one of three experienced urologists (>1000 MRI prostate scans) prior to the tumour board meeting.

### PSMA PET/CT Protocol

The radiotracer [68Ga]-PSMA was prepared using a GMP- grade <sup>68</sup>Ge/<sup>68</sup>Ga generator and a semiautomated synthesis module (Eckert & Ziegler, Berlin, Germany, and ITG, Munich, Germany). The dose of [68Ga]-PSMA was 1.5 MBq/kg. Patients received 10 mg of furosemide at the time of radiotracer injection. PET images were acquired 60 min after the injection. Low-dose CT was performed directly following PET imaging. Scans were made using a Biograph mCT 40 scanner (Siemens, Erlangen, Germany) or a Gemini TF 64 slice scanner (Philips, Best, The Netherlands). All scans were performed in one centre. Reports were generated by two experienced nuclear medicine physicians (>1000 PSMA cases), according to the prevailing European Association of Nuclear Medicine guidelines.<sup>15</sup>

### Biopsy Protocol

At diagnosis, cognitive targeted biopsy were performed if a suspected area (PI-RADS 3–4–5) was seen on the prebiopsy MRI.<sup>16</sup> For systematic biopsies, a volume-dependent approach was applied conforming to the local protocol: eight cores for a prostate of <40 cc, ten for 40–60 cc, and 12 for >60 cc. PSMA PET/CT images were reviewed in the local multi-



disciplinary tumour board, including a radiologist, a nuclear physician, and a urologist. The PSMA intraprostatic activity was compared with the prebiopsy MRI. Additional targeted biopsies were advised when a new lesion was visualised on PSMA PET/CT (defined as the maximum standardised uptake value [SUVmax] of 24) or when a previously visualised MRI lesion showed such high activity on PSMA PET/CT that previously performed biopsies were deemed unrepresentative by the tumour board.

The prostate needle biopsy cores were acquired via a transrectal or transperineal approach by an experienced oncurologist. At least three targeted cores were performed of each MRI and/or PSMA lesion. A dedicated uropathologist examined the prostate biopsy and, if performed, prostatectomy specimens according to the prevailing ISUP guidelines.<sup>17</sup> Immunohistochemistry was performed on all biopsy cores.

### **Outcomes and Statistical Analysis**

Our primary outcome was the percentage of upgrading due to the addition of PSMA targeted biopsy following PSMA PET/CT. Analyses were performed using a single-proportion test with a Wilson score interval. The number of upgrading will be expressed in a number needed to scan (NNS) to detect one patient with upgrading. In addition, two exploratory univariate logistic regression analyses were conducted to assess the likelihood of biopsy upgrading. The first analysis was conducted on all participants and included variables that were available prior to PSMA PET/CT, including age, prostate-specific antigen (PSA) density x 100, MRI (negative [PI-RADS 1–2] vs positive [PI-RADS 3–5]), systematic biopsy performed (yes/no), and ISUP GG. This analysis was performed to explore the indication for an additional PSMA PET/CT scan. Furthermore, an exploratory univariate logistic regression analysis was conducted in the patients who received additional PSMA targeted biopsy, using previously mentioned variables and the SUVmax of PSMA PET/CT. This analysis was performed to explore the indication for additional PSMA targeted biopsy. Lastly, an analysis of per intraprostatic lesion detected by PSMA PET/CT was performed to visualise the relation between SUVmax and ISUP GG.

Data were collected using REDcap hosted at our institution.<sup>18</sup> Analyses were performed using R version 4.2.2 (R Foundation for Statistical Computing, Vienna, Austria). All tests were two sided, with a significance level set at  $p < 0.05$ .

## Results

### Baseline Characteristics and Primary Outcome

Baseline characteristics are presented in Table 1, grouped by patients who received additional targeted biopsy and by patients with GG upgrading after PSMA targeted biopsy. Of the 141 patients included, 126 (89%) had GG 1 and 15 (11%) had GG 2 before PSMA PET/CT. PSMA PET/CT was performed at a median of 2.0 (interquartile range [IQR] 1.0, 4.0) mo after the start of AS. In one patient, the prostate showed no pathological PSMA activity; however, the SUVmax could not be generated due to a malfunction of the scanner. PSMA targeted biopsies were performed in 45 (32%) of the 141 patients included. These additional biopsies were taken in 41 (91%) patients due to a new lesion on PSMA PET/CT and in four (9%) patients due to an SUVmax considered to be discrepant with the ISUP GG found previously. Upgrading was observed in 13 (9%) patients, resulting in an NNS of 11 (95% CI 6–18). Of the 13 patients with upgrading, nine had GG 2, two had GG 3, one had GG 4, and one had GG 5 after PSMA targeted biopsy. Detailed characteristics of these 13 patients are shown in Supplementary Table 1. Figure 1 shows an example of a patient with previously undetected lesions probably not sampled by biopsy, who was upgraded after PSMA PET/CT and additional targeted biopsy. Of the patients with upgrading, six remained under AS and seven underwent a radical curative treatment: two received radiotherapy and five underwent a robot-assisted radical prostatectomy. In three (60%) of the patients who received radical prostatectomy, the biopsy GG was concordant with the prostatectomy specimen. In two patients downgrading was observed, in one from GG 3 to GG 2 and the other from GG 4 to GG 3; both had GG 1 before PSMA PET/CT. One patient without upgrading switched to active treatment after PSMA targeted biopsy due to the presence of a cribriform growth pattern.

Two patients underwent surgery after PSMA PET/CT without additional targeted biopsy, one because the patient preferred active treatment and the other due to a positive lymph node on PSMA PET/CT. Pelvic lymph node dissection showed no histological positive nodes. No GG upgrading was observed in the prostatectomy specimen.

**Table 1:** Characteristics of all the patients, patients who received additional target biopsy, and patients who were upgraded

	No additional targeted biopsy performed (n = 96)	Additional targeted biopsy performed (n = 45)	Upgrading (n = 13)
Age (yr), median (IQR)	67 (63, 71)	70 (63, 73)	70 (63, 72)
PSA (ng/ml), median (IQR)	5.4 (4.0, 7.8)	5.8 (4.8, 7.4)	5.0 (4.8, 7.4)
PSA density (ng/ml/ml) , median(IQR)	0.13 (0.10, 0.17)	0.13 (0.08, 0.17)	0.16 (0.14, 0.18)
PI-RADS, n(%)			
1	5 (5)	3 (7)	2 (15)
2	10 (10)	8 (18)	4 (31)
3	12 (12)	6 (13)	0
4	55 (57)	19 (42)	5 (38)
5	14 (15)	9 (20)	2 (15)
Systematic biopsy performed, n(%)	79 (82)	42 (93)	12 (92)
If performed, number of systematic biopsies, median (IQR)	8 (8, 10)	8 (7, 10)	8 (8, 10)
ISUP GG before PSMA PET/CT, n(%)			
1	85 (89)	41 (89)	12 (92)
2	11 (11)	4 (11)	1 (8)
SUVmax (ng/ml/ml), median (IQR)	3.6 (3.3, 4.5)	5.5 (4.8, 6.9)	6.2 (5.1, 9.6)
ISUP GG PSMA-target biopsy, n(%)			
Benign	-	17 (38)	0
1		13 (29)	0
2		11 (24)	9 (69)
3		2 (4)	2 (15)
4		1 (2)	1 (8)
5		1 (2)	1 (8)
Time between diagnosis and PSMA-PET/CT (mo), median(IQR)	2.0 (1.0, 4.0)	2.0 (1.0, 5.0)	2.0 (1.0, 8.0)
Time between MRI and PSMA-PET/CT (mo), median(IQR)	3.0 (2.0, 6.0)	5.0 (2.0, 8.0)	6.0 (3.0, 11.0)

IQR = Interquartile Range, PSA = Prostate Specific Antigen, PSAD = Prostate Specific Antigen Density, PI-RADS = Prostate Imaging-Reporting and Data System, ISUP GG= International Society of Urologic Pathology Grade Group, PSMA-PET/CT = Prostate-specific Membrane Antigen Positron Emission Tomography Computed Tomography, SUV = Standardised Uptake Value

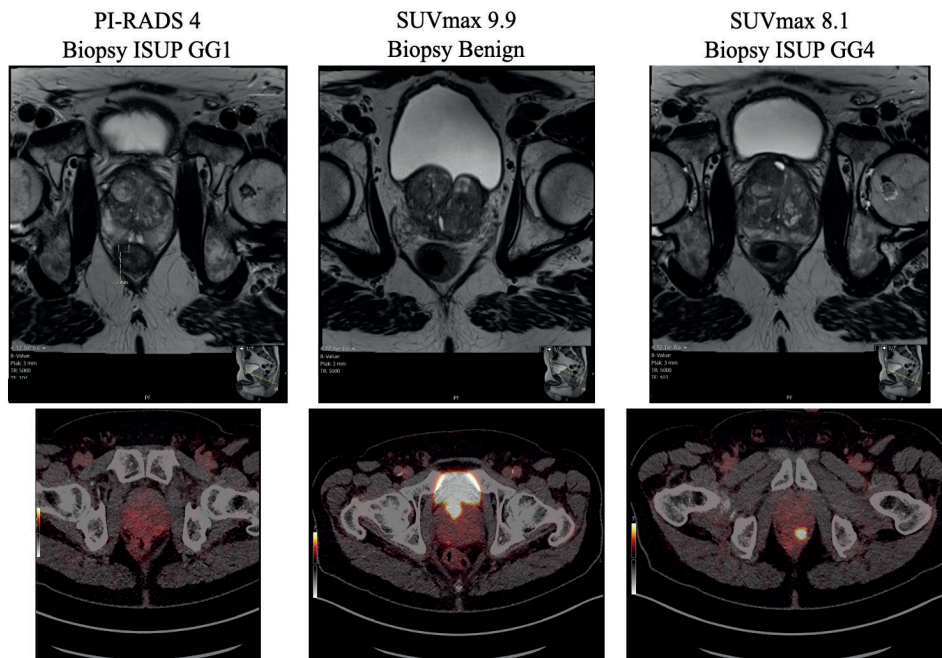


**Figure 1:** (A) Patient (patient 11; Supplementary Table 1) with upgrading after PSMA PET/CT, MRI showed a PI-RADS 4 lesion with targeted biopsy resulting in ISUP GG 1 (left). (B) PSMA PET/CT revealed two new lesions: one ventral in the basis of the prostate (middle) and one dorsal in the apex of the prostate (right). Additional targeted biopsy of the ventral lesion showed no prostate cancer and ISUP GG 4 in the second lesion. The patient was treated with a radical prostatectomy, showing ISUP GG 3.

ISUP GG = International Society of Urologic Pathology grade group; MRI = magnetic resonance imaging; PET/CT = positron emission tomography/computed tomography; PI-RADS = Prostate Imaging Reporting and Data System; PSMA = prostate-specific membrane antigen; SUVmax = maximum standardised uptake value.

### Secondary Outcomes

Table 2 presents the results of the two exploratory univariate analyses, examining the likelihood of upgrading in all 141 patients, as well as in the 45 patients who underwent targeted biopsy following PSMA PET/CT. The first analysis revealed that only negative MRI (PI-RADS 1-2) was significantly correlated with upgrading after PSMA targeted biopsy in all patients (odds ratio [OR] 4.63, 95% CI 1.36–15.4,  $p = 0.012$ ). Among the 45 patients who received additional biopsy, both PSA density (OR 1.16, 95% CI 1.02–1.34,  $p = 0.031$ ) and negative MRI (OR 4.63, 95% CI 1.10–20.9,  $p = 0.038$ ) were significantly correlated with upgrading after PSMA targeted biopsy.

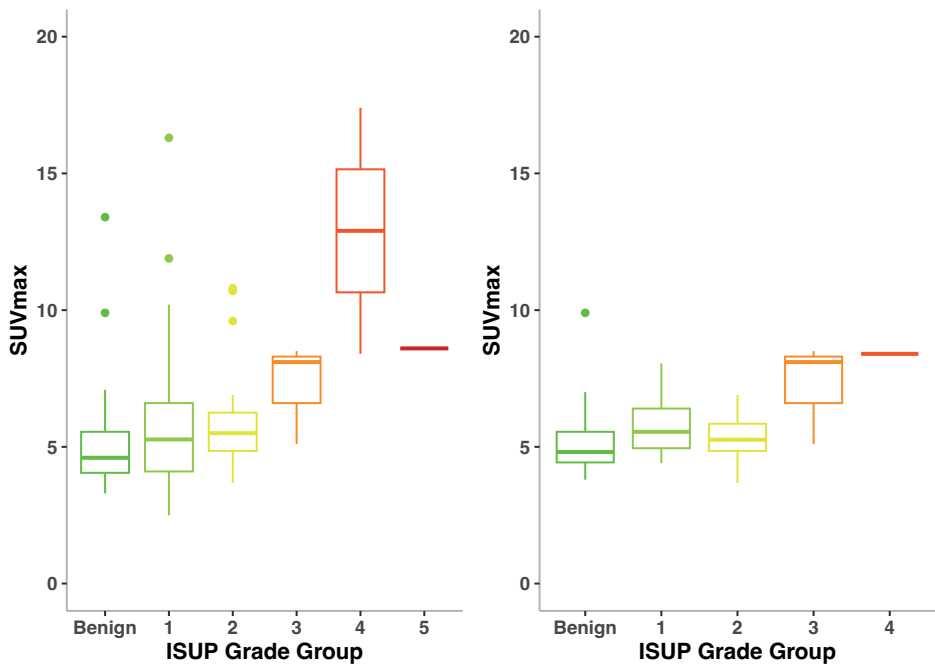


**Figure 2:** Boxplots of the SUVmax of (A) all 115 PSMA lesions with biopsy information per ISUP Grade Group and (B) the 51 lesions with SUVmax  $\geq 4$  not visualised by MRI. ISUP = International Society of Urologic Pathology; MRI = magnetic resonance imaging; PSMA = prostate-specific membrane antigen; SUVmax = maximum standardised uptake value.

The PSMA PET/CT scan detected 162 intraprostatic lesions, of which 100 (62%) had an SUVmax of 24. Of these, seven patients (7%) had no targeted biopsy information due to the following reasons: one patient refused to undergo biopsy (SUVmax 5.2), one patient chose immediate radical treatment (SUVmax 4.5), two patients had a more active lesion that was already covered by MRI targeted biopsy (SUVmax 4.2 and 5.4), one patient had a lesion with diffuse activity (SUVmax 4), and in two patients the lesion was considered to be sufficiently covered by systematic biopsy (SUVmax 4.2 and 5.2). Fifty-one lesions with an SUVmax of  $\geq 4$  were not previously visualised by MRI. Of the 162 intraprostatic lesions detected by PSMA PET/CT, no biopsy was performed in 47 (29%) lesions with a median SUVmax of 3.5 (IQR 3.3, 3.9). Of the 115 lesions with biopsy information, 35 were benign, 55 were GG 1, 19 were GG 2, three were GG 3, two were GG 4, and one was GG 5. In Figure 2, two box plots are shown. The first boxplot represents the SUVmax per GG of all PSMA lesions with biopsy information. The second boxplot shows the 51 lesions with SUVmax 24 that were not visualised by MRI, showing an increase of the SUVmax per GG except in the one with GG 5.

**Table 2:** Exploratory univariate logistic regression analyses for the likelihood of upgrading in all 141 patients and the 45 patients who received additional PSMA targeted biopsy

	All patients (n =141)			Patients that received additional biopsy (n =45)		
	OR	95% CI	p-value	OR	95%	p-value
Age (years)	1.05	0.96, 1.16	0.3	1.03	0.93, 1.14	0.6
PSA density*100 (ng/ml/ml)	1.11	1.00, 1.25	0.063	1.16	1.02, 1.34	<b>0.031</b>
PI-RADS			<b>0.012</b>			<b>0.038</b>
3-4-5	Reference	-		Reference	-	
1-2	4.63	1.36, 15.4		4.63	1.10, 20.9	
Systematic biopsy performed			0.5			0.5
Yes	Reference	-		Reference	-	
No	0.48	0.03, 2.65		1.25	0.06, 14.3	
ISUP GG before PSMA			0.7			0.9
1	Reference	-		Reference	-	
2	0.68	0.04, 3.86		0.81	0.04, 7.04	
SUVmax	-	-	-	1.26	1.02, 1.69	0.054

OR = Odds Ratio, CI = Confidence Interval, PSAD = Prostate Specific Antigen Density, PI-RADS = Prostate Imaging-Reporting and Data System, ISUP GG= International Society of Urologic Pathology Grade Group, PSMA-PET/CT = Prostate-specific Membrane Antigen Positron Emission Tomography Computed Tomography, SUV = Standardised Uptake Value

## Discussion

We studied whether the addition of PSMA PET/CT combined with additional targeted biopsy in patients selected for AS after MRI could result in improved risk stratification and patient selection. The NNS to detect biopsy upgrading in one patient was 11 (95% CI 6–18). PSMA PET/CT and additional targeted biopsy most frequently resulted in upgrading for patients with negative MRI findings. Furthermore, in patients who underwent PSMA targeted biopsy, upgrading was more commonly observed in those with a higher PSA density and negative MRI. Notably, in the subset of patients with a PSA density of  $\geq 0.15$  ng/ml/ml and negative MRI, we observed biopsy upgrading in five out of 14 patients, resulting in an NNS of 2.8. Further research is needed to validate these findings that may be used to improve risk stratification in this patient population.

Our results are in line with those found in the PRIMARY trial, where the addition of PSMA PET/CT resulted in a higher detection of csPCa.<sup>9</sup> Similar to the PRIMARY trial, the cost-benefit ratio of an additional PSMA PET/CT scan is disputable. The 9% upgrading found in our study should be seen in the perspective of 17% patients with upgrading after prostatectomy after diagnosis with MRI and targeted biopsy, suggesting that PSMA corrects for an important portion of understaging.<sup>13</sup> However, additional PSMA targeted biopsy may lead to a further stage shift. Following a combination of MRI targeted and systematic biopsy, 21% of patients experienced downgrading.<sup>3</sup> In the current cohort, 40% of the patients who underwent prostatectomy had downgrading, suggesting that the addition of PSMA targeted biopsy may possibly increase the proportion of downgrading. Additional PSMA PET/CT may result in unjustified exclusion for AS.

The increase in SUVmax per ISUP GG in our cohort is in concordance with the studies of prostatectomy specimens and biopsy information.<sup>10,11</sup> Contrary to the results in the systematic review of Kawada *et al.*<sup>19</sup>, PSMA PET/CT was of no additional value in patients with PI-RADS 3; this could be due to the limited number of patients with PI-RADS 3 in our cohort.

This study has some limitations. Firstly, there was no central review of the MRI scans, possibly resulting in missed lesions on MRI. In retrospect, some of the new PSMA lesions were already visible on MRI but had not been reported by the radiologist. This illustrates the well-known difficulty of prostate MRI assessment.<sup>20</sup> Secondly, only 32% of the patients received rebiopsy after PSMA PET/CT. Standard rebiopsy of all the participants could have resulted in upgrading due to a correction for the previous biopsy error. Furthermore, upgrading in additional targeted biopsy can be considered a surrogate outcome, since no prostatectomy specimen was available for all the patients. Therefore, upgrading may have

been a result of truly newly identified and biopsied lesions, identification of lesions on PSMA PET/ CT that were initially missed during the MRI assessment, or biopsy targeting error at diagnosis. Additionally, lesions with SUVmax < 4 did not undergo immediate rebiopsy, and a small number of lesions with an SUVmax of  $\geq 4$  were not targeted by biopsy, resulting in a possible underestimation of the patients with upgrading. Furthermore, a certain degree of subjectivity may have been introduced for the cases in whom the tumour board had decided that previous biopsies were unrepresentative due to high activity on PSMA PET/CT. Besides, in an ideal study design, the standard AS and PSMA AS protocols would have been compared in a randomised approach. Lastly, our sample size was too small to reliably identify subgroups of patients in whom upgrading was most frequent after PSMA PET/CT.

Future directions may involve personalising the use of PSMA PET/CT in AS protocols and creating a tool to predict which patients would benefit from additional PSMA PET/ CT. Furthermore, the results of MRI and PSMA can be combined to predict csPCa. The study by Kalapara *et al.*<sup>11</sup> and a subanalysis from the PRIMARY trial showed promising results when combining PI-RADS and SUVmax.<sup>21</sup> These results are in line with the data from our own centre.<sup>22</sup> Lastly will we provide further analyses as follow-up of this cohort.

We plan to conduct further analyses as a follow-up to this cohort study, with the aim of obtaining more definitive data on the benefits or disadvantages of PSMA PET/CT in AS and impact on long-term oncological outcomes.

This study supports the use of PSMA PET/CT to detect intraprostatic lesions in patients with low-risk or favourable intermediate-risk PCa. However, due to high costs and limited availability, PSMA PET/CT cannot be offered to all patients starting AS. If its value becomes clearer, PSMA PET/CT may be used in highly selected cases to improve patient selection for AS, potentially leading to a revised protocol with fewer follow-up visits. The inclusion of more PCa patients in AS could reduce costs and improve quality of life.<sup>23,24</sup>



## Conclusion

The addition of PSMA PET/CT to targeted biopsy in patients who recently started with AS and had MRI at diagnosis resulted in upgrading in 9% of the patients. Therefore, this study provides evidence that PSMA PET/CT has a role in the risk stratification of patient selection for AS.

## References

- 1 Mottet N, van den Bergh RCN, Briers E, Van den Broeck T, Cumberbatch MG, De Santis M *et al.* EAU-EANM-ESTRO-ESUR-SIOG Guidelines on Prostate Cancer-2020 Update. Part 1: Screening, Diagnosis, and Local Treatment with Curative Intent. *Eur Urol* 2021; **79**: 243–262.
- 2 Ahmed HU, El-Shater Bosaily A, Brown LC, Gabe R, Kaplan R, Parmar MK *et al.* Diagnostic accuracy of multi-parametric MRI and TRUS biopsy in prostate cancer (PROMIS): a paired validating confirmatory study. *Lancet* 2017; **389**: 815–822.
- 3 Ahdoot M, Wilbur AR, Reese SE, Lebastchi AH, Mehralivand S, Gomella PT *et al.* MRI-Targeted, Systematic, and Combined Biopsy for Prostate Cancer Diagnosis. *N Engl J Med* 2020; **382**: 917–928.
- 4 Kasivisvanathan V, Rannikko AS, Borghi M, Panebianco V, Mynderse LA, Vaarala MH *et al.* MRI-Targeted or Standard Biopsy for Prostate-Cancer Diagnosis. *N Engl J Med* 2018; **378**: 1767–1777.
- 5 PRIAS project - Active surveillance -. <https://www.prias-project.org/> (accessed 22 Jun2022).
- 6 Feuer Z, Meng X, Rosenkrantz AB, Kasivisvanathan V, Moore CM, Huang R *et al.* Application of the PRECISION Trial Biopsy Strategy to a Contemporary Magnetic Resonance Imaging-Targeted Biopsy Cohort-How Many Clinically Significant Prostate Cancers are Missed? *J Urol* 2021; **205**: 740–747.
- 7 Wenzel M, Preisser F, Wittler C, Hoeh B, Wild PJ, Tschäbunin A *et al.* Correlation of MRI-Lesion Targeted Biopsy vs. Systematic Biopsy Gleason Score with Final Pathological Gleason Score after Radical Prostatectomy. *Diagnostics* 2021; **11**: 882.
- 8 Luzzago S, Petralia G, Maresca D, Sabatini I, Cordima G, Brescia A *et al.* Pathological findings at radical prostatectomy of biopsy naïve men diagnosed with MRI targeted biopsy alone without concomitant standard systematic sampling. *Urol Oncol* 2020; **38**: 929.e11-929.e19.
- 9 Emmett L, Buteau J, Papa N, Moon D, Thompson J, Roberts MJ *et al.* The Additive Diagnostic Value of Prostate-specific Membrane Antigen Positron Emission Tomography Computed Tomography to Multiparametric Magnetic Resonance Imaging Triage in the Diagnosis of Prostate Cancer (PRIMARY): A Prospective Multicentre Study. *Eur Urol* 2021; **80**: 682–689.
- 10 Uprimny C, Kroiss AS, Decristoforo C, Fritz J, von Guggenberg E, Kandler D *et al.* 68Ga-PSMA-11 PET/CT in primary staging of prostate cancer: PSA and Gleason score predict the intensity of tracer accumulation in the primary tumour. *Eur J Nucl Med Mol Imaging* 2017; **44**: 941–949.
- 11 Kalapara AA, Ballok ZE, Ramdave S, O'Sullivan R, Ryan A, Konety B *et al.* Combined Utility of 68Ga-Prostate-specific Membrane Antigen Positron Emission Tomography/Computed Tomography and Multiparametric Magnetic Resonance Imaging in Predicting Prostate Biopsy Pathology. *Eur Urol Oncol* 2022; **5**: 314–320.
- 12 Bhanji Y, Rowe SP, Pavlovich CP. New imaging modalities to consider for men with prostate cancer on active surveillance. *World J Urol* 2022; **40**: 51–59.
- 13 Schoots IG, Nieboer D, Giganti F, Moore CM, Bangma CH, Roobol MJ. Is magnetic resonance imaging-targeted biopsy a useful addition to systematic confirmatory biopsy in men on active surveillance for low-risk prostate cancer? A systematic review and meta-analysis. *BJU Int* 2018; **122**: 946–958.
- 14 Turkbey B, Rosenkrantz AB, Haider MA, Padhani AR, Villeirs G, Macura KJ *et al.* Prostate Imaging Reporting and Data System Version 2.1: 2019 Update of Prostate Imaging Reporting and Data System Version 2. *Eur Urol* 2019; **76**: 340–351.
- 15 Ceci F, Oprea-Lager DE, Emmett L, Adam JA, Bomanji J, Czernin J *et al.* E-PSMA: the EANM standardized reporting guidelines v1.0 for PSMA-PET. *Eur J Nucl Med Mol Imaging* 2021; **48**: 1626–1638.

- 16 Wegelin O, Exterkate L, van der Leest M, Kummer JA, Vreuls W, de Bruin PC *et al.* The FUTURE Trial: A Multicenter Randomised Controlled Trial on Target Biopsy Techniques Based on Magnetic Resonance Imaging in the Diagnosis of Prostate Cancer in Patients with Prior Negative Biopsies. *Eur Urol* 2019; **75**: 582–590.
- 17 van Leenders GJLH, van der Kwast TH, Grignon DJ, Evans AJ, Kristiansen G, Kweldam CF *et al.* The 2019 International Society of Urological Pathology (ISUP) Consensus Conference on Grading of Prostatic Carcinoma. *Am J Surg Pathol* 2020; **44**: e87–e99.
- 18 Harris PA, Taylor R, Minor BL, Elliott V, Fernandez M, O’Neal L *et al.* The REDCap consortium: Building an international community of software platform partners. *J Biomed Inform* 2019; **95**: 103208.
- 19 Kawada T, Yanagisawa T, Rajwa P, Sari Motlagh R, Mostafaei H, Quhal F *et al.* Diagnostic Performance of Prostate-specific Membrane Antigen Positron Emission Tomography-targeted biopsy for Detection of Clinically Significant Prostate Cancer: A Systematic Review and Meta-analysis. *Eur Urol Oncol* 2022; : S2588-9311(22)00064–5.
- 20 Rosenkrantz AB, Ginocchio LA, Cornfeld D, Froemming AT, Gupta RT, Turkbey B *et al.* Interobserver Reproducibility of the PI-RADS Version 2 Lexicon: A Multicenter Study of Six Experienced Prostate Radiologists. *Radiology* 2016; **280**: 793–804.
- 21 Ptasznik G, Papa N, Kelly BD, Thompson J, Stricker P, Roberts MJ *et al.* High PSMA PET SUVmax in PI-RADS 4 or 5 men confers a high probability of significant prostate cancer. *BJU Int* 2022. doi:10.1111/bju.15736.
- 22 Heetman JG, Wever L, Paulino Pereira LJ, van den Bergh RCN. Clinically Significant Prostate Cancer Diagnosis Without Histological Proof: A Possibility in the Prostate-specific Membrane Antigen Era? *European Urology Open Science* 2022; **44**: 30–32.
- 23 Teunissen FR, Willigenburg T, Meijer RP, van Melick HHE, Verkooijen HM, van der Voort van Zyp JRN. The first patient-reported outcomes from the Utrecht Prostate Cohort (UPC): the first platform facilitating ‘trials within cohorts’ (TwiCs) for the evaluation of interventions for prostate cancer. *World J Urol* 2022. doi:10.1007/s00345-022-04092-2.
- 24 Hoffman KE, Penson DF, Zhao Z, Huang L-C, Conwill R, Laviana AA *et al.* Patient-Reported Outcomes Through 5 Years for Active Surveillance, Surgery, Brachytherapy, or External Beam Radiation With or Without Androgen Deprivation Therapy for Localized Prostate Cancer. *JAMA* 2020; **323**: 149–163.

## Supplementary Material

**Supplement Table 1:** Characteristics of the 13 patients with upgrading

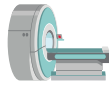
	Age (years)	PSA (ng/ml)	PSA- Density (ng/ml/ml)	PI- RADS	MRI targeted biopsy ISUP GG	Systematic biopsy ISUP GG	SUV- max	PSMA targeted biopsy ISUP GG
<b>1</b>	54	5.04	0.17	2	NA	1	5.79	2
<b>2</b>	65	4.86	0.20	1	NA	1	8.50	3
<b>3</b>	66	4.08	0.16	2	NA	1	5.10	3
<b>4</b>	70	5.80	0.16	1	NA	1	5.10	2
<b>5</b>	56	6.31	0.16	4	1	1	5.5	2
<b>6</b>	81	4.23	0.07	4	Benign	1	4.60	2
<b>7</b>	70	7.39	0.18	2	NA	1	4.60	2
<b>8</b>	76	9.80	0.18	5	Benign	2	17.40	5
<b>9</b>	78	4.75	0.14	4	1	1	6.90	2
<b>10</b>	63	10.40	0.25	5	Benign	1	9.60	2
<b>11</b>	75	7.80	0.08	4	1	NA	9.90	4
<b>12</b>	78	7.20	0.12	2	NA	1	15.60	2
<b>13</b>	61	5.00	0.19	4	Benign	1	6.20	2

PSA = Prostate Specific Antigen, PSAD = Prostate Specific Antigen Density, PI-RADS = Prostate Imaging-Reporting and Data System, ISUP GG= International Society of Urologic Pathology Grade Group, PSMA-PET/CT = Prostate-specific Membrane Antigen Positron Emission Tomography Computed Tomography, SUV = Standardised Uptake Value

## PSMA PET/CT scan bij patiënten met prostaatkanker waarvoor een actief afwachtend beleid

### Achtergrond

Bij het kiezen tussen actief afwachtend beleid en actieve behandeling voor prostaatkanker zijn de huidige methoden die gebruik maken van MRI, niet perfect. Extra beeldvorming met PSMA PET/CT scan kan deze keuze verbeteren door juistere risico-inschatting.



### Centrale vraag

Kan een PSMA PET/CT scan in combinatie met extra gerichte prostaatbipten agressievere vormen van prostaatkanker vinden die eerder niet zijn gevonden bij patiënten die onlangs zijn begonnen met actief afwachtend beleid voor gunstiger risico prostaatkanker

### Interventie(s)

Prostaatkankerpatiënten die werdengevolgd door actief afwachtend beleid kregen een extra PSMA PET/CT scan en eventueel gerichte bipten voor alle verdachte plekken die niet eerder waren gebipteerd om zo te kijken of er agressieve prostaatkanker was gemist in het eerste diagnostische traject.

### Onderzoeksteam

Roderick van den Bergh (Uroloog), Jules Lavalaye (Nucleair geneeskundige), Harm van Melick (uroloog), Joris Heetman (ANIOS en arts-onderzoeker urologie)

### Wie deden mee aan het onderzoek?

In deze studie werden **141** recent gediagnosticeerde prostaatkankerpatiënten die AS volgden, geïncludeerd in het St. Antonius Ziekenhuis.



### Publicatie

Het is recent gepubliceerd <https://authors.elsevier.com/a/1H03q9C1v-xp0D>

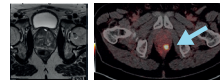
### Financiering

Dit onderzoek is met een bedrag van € 80.000 gefinancierd door het

**ST ANTONIUS**  
Onderzoeksfonds

### Resultaat

Een PSMA PET/CT scan levert bij 1 op 11 (9%) alsnog een agressievere kanker op. Van de 13 patiënten met een agressievere vorm van kanker na de PSMA PET/CT scan, konden er 5 worden vervolgd door middel van een actief afwachtend beleid, bij 7 patiënten bleek operatie of bestraling nodig.



MRI = negatief PSMA PET/CT scan = positief  
Bipten = hoog risico kanker

### Conclusie

PSMA PET/CT scan in combinatie met extra gerichte prostaat bipten kan agressievere vormen van prostaatkanker vinden die eerder over het hoofd zijn gezien bij patiënten die onlangs zijn begonnen met afwachtend beleid voor gunstiger-risico prostaatkanker. Zo kunnen patiënten die dit nodig hebben sneller de juiste behandeling krijgen. Daarnaast kan de PSMA PET/CT scan mogelijk worden gebruikt om bij meer patiënten een veilig actief afwachtend beleid te voeren.

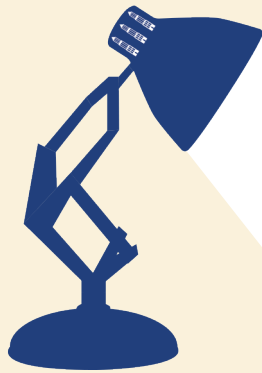
Netherlands Trial Register NL69880.100.19

Samen zorgen  
voor kwaliteit van  
leven

Dit onderzoek is een voorbeeld van hoe het St. Antonius Ziekenhuis zijn ambitie Samen zorgen voor kwaliteit van leven in de praktijk brengt.

RESEARCH & DEVELOPMENT  
**ST ANTONIUS**

**Supplement figure:** Dutch infographic



# CHAPTER 5

## CLINICALLY SIGNIFICANT PROSTATE CANCER DIAGNOSIS WITHOUT HISTOLOGICAL PROOF: A POSSIBILITY IN THE PROSTATE- SPECIFIC MEMBRANE ANTIGEN ERA?

J.G. Heetman

L. Wever

L.J. Paulino Pereira

R.C.N. van den Bergh

Eur Urol Open Sci. 2022 Aug 20;44:30-32. doi: 10.1016/j.euros.2022.06.013.

## Abstract

Magnetic resonance imaging (MRI) has resulted in a reduction in the number of patients indicated for prostate biopsy. Prostate-specific membrane antigen (PSMA) positron emission tomography/computed tomography (PET/CT) has recently shown additional value in detecting clinically significant prostate cancer (csPCa). Combining these imaging modalities allows such specific prediction of the presence of csPCa that the need for histological confirmation may be obsolete. We retrospectively analysed PSMA PET/CT scans performed in the primary staging of PCa in the past 2 years in our centre ( $n = 451$ ). All 74 patients with a maximum standardised uptake value (SUVmax) of 16 had csPCa (Grade Group  $\geq 2$ ). Of the 185 patients with a combination of a Prostate Imaging-Reporting and Data System score  $\geq 4$  and SUVmax  $\geq 8$ , 98% had csPCa. A nomogram combining predictive factors should be developed to identify patients in whom biopsy could theoretically be avoided. Nevertheless, biopsy will remain indispensable in patients with indefinite risk of csPCa and can provide important additional information.

*Patient summary:* Using patient data from our centre, we found that addition of a special type of scan based on prostate-specific membrane antigen could help in the diagnosis of clinically significant prostate cancer without the need for prostate biopsy. Direct therapy without biopsy confirmation of cancer might be possible for a highly select group of patients.



The introduction of magnetic resonance imaging (MRI) recently improved the pathway for the diagnosis of clinically significant prostate cancer (csPCa), resulting in recommendation of prostate MRI before a prostate biopsy.<sup>1</sup> However, this imaging technique cannot confirm csPCa without histological biopsy, with 17% of the biopsies performed for lesions with a Prostate Imaging-Reporting and Data System (PI-RADS) maximum score of 5 confirming nonsignificant PCa or benign tissue.<sup>2</sup>

The PRIMARY trial has recently proved the added value of prostate-specific membrane antigen (PSMA) positron emission tomography/computed tomography (PET/CT) in detecting csPCa lesions in the primary diagnostic setting by showing an improvement in the negative predictive value and sensitivity of MRI when combined.<sup>3</sup> Furthermore, the authors suggested a PRIMARY score for local activity on PSMA PET/CT.<sup>4</sup> Besides detecting csPCa not visible on MRI, prostatic lesions with a high maximum standardised uptake value (SUVmax) on PSMA PET/CT and a PI-RADS score on MRI resulted in high probability of csPCa.<sup>5</sup> This raises the question of whether histological confirmation of suspected lesions is still needed if both aging techniques are combined in an accurate “*virtual biopsy*”:<sup>6</sup> If the chance of csPCa is close to 100% and treatment with radical prostatectomy is planned, a prostate biopsy for histological confirmation could be seen as redundant. A case series of patients who refused prostate biopsy illustrated that this unusual diagnostic pathway might be optional.<sup>7</sup> This pathway for diagnosing csPCa without histological proof could be a future option to reduce the 1 million prostate biopsies performed in Europe each year.<sup>8</sup> Therapy without histological confirmation is already in practice for other malignancies such as renal cell carcinoma, for which histological proof is only used for radiologically indeterminate renal masses.<sup>9</sup> Omission of prostate biopsy in the diagnostic pathway results in a lower burden for the patient, as even the transperineal approach has complications and may be painful.<sup>10</sup>

We hypothesize that it is only feasible to omit biopsy if the combination of prebiopsy parameters can highly specifically predict the presence of csPCa. Ideally, not only International Society of Urological Pathology (ISUP) Grade Group (GG)  $\geq 2$  but also GG  $\geq 3$  can be identified, because active therapy is generally recommended for all of these cases.<sup>1</sup> To test whether prediction of csPCa is indeed feasible with combined MRI information and PSMA PET/CT activity, we analysed a prospectively maintained database of patients with MRI and PSMA PET/CT results available for initial staging, and biopsy-proven PCa diagnosed in the past 2 yr in our institution. Owing to an ongoing prospective trial in our center in which the <sup>68</sup>Ga-PSMA PET/CT is performed for patients starting active surveillance, our data set includes patients with low-, intermediate-, and high-risk PCa. Our centre has extensive experience with both <sup>68</sup>Ga-PSMA PET/CT and MRI of the prostate. The analysis was performed using R v4.1.2 (R Foundation for Statistical Computing, Vienna, Austria); the rpart package was used to create a decision tree for SUVmax thresholds, in addition to the SUVmax of 4 suggested in the PRIMARY study as a threshold for csPCa.<sup>3</sup>

A total of 451 patients were included in the analysis. The baseline characteristics are presented in Table 1. Figure 1 shows ISUP Grade Groups by SUVmax threshold for PI-RADS 1–3 and 4–5 groups. Of the 74 patients with SUVmax  $\geq 16$ , all had GG  $\geq 2$  and 89% had GG  $\geq 3$  disease. The combination of PI-RADS 4 or 5 with SUVmax  $\geq 8$  resulted in GG  $\geq 2$  rate of 98%.

**Table 1:** Baseline imaging characteristics

	Overall ( <i>n</i> = 451)	ISUP Group Grade $\geq 2$ ( <i>n</i> = 336)	ISUP Grade Group $\geq 3$ ( <i>n</i> = 230)
Median age, yr (IQR)	70 (65, 74)	71 (66, 75)	71 (66, 75)
Median PSA, ng/ml (IQR)	8.5 (5.5, 15.5)	10.0 (6.4, 17.6)	10.6 (6.4, 19.6)
Median PSA density, ng/ml/ml (IQR)	0.19 (0.12, 0.33)	0.24 (0.15, 0.38)	0.27 (0.16, 0.41)
MRI T stage, <i>n</i> (%)			
T0	42 (9)	23 (7)	8 (4)
T2	238 (53)	149 (44)	94 (41)
T3	161 (36)	154 (46)	120 (52)
T4	10 (2)	10 (3)	8 (4)
PI-RADS score, <i>n</i> (%)			
1	12 (3)	6 (2)	2 (1)
2	29 (6)	16 (5)	5 (2)
3	32 (7)	15 (4)	9 (4)
4	145 (32)	86 (26)	46 (20)
5	233 (52)	213 (63)	165 (73)
ISUP Grade Group, <i>n</i> (%)			
1	115 (25)	–	–
2	106 (24)	106 (32)	–
3	89 (20)	89 (26)	89 (39)
4	103 (23)	103 (31)	103 (45)
5	38 (8)	38 (11)	38 (17)
Median SUVmax, (IQR)	6.9 (4.2, 12.2)	8.8 (5.4, 14.9)	10.3 (6.4, 17.1)

IQR = interquartile range; PSA = prostate-specific antigen; MRI = magnetic resonance imaging; PI-RADS = Prostate Imaging-Reporting and Data System; ISUP = International Society of Urological Pathology; SUVmax = maximum standardised uptake value.

These results illustrate that PSMA activity on PET/CT is highly indicative of the presence of csPCa. On combination with other parameters, more accurate prediction of GG  $\geq 3$  may be possible. In the PRIMARY trial, the specificity for detection of GG  $\geq 2$  was 50% for SUVmax  $\geq 4$  alone and 40% when combined with MRI. These specificity results are lower than the 57% and 70%, respectively, in our analysis.<sup>3</sup> The specificity increases to 96% and 97%, respectively, when a threshold of 8 is applied to our data. Unlike the PRIMARY trial, patients

underwent PSMA PET/CT after their diagnosis of PCa, resulting in possible overestimation of the predictive accuracy.<sup>3</sup> Initiation of treatment for suspicion of PCa without histological confirmation remains controversial. Performing initial PSMA PET/CT in all patients to decide on the indication for biopsy would not be cost-effective. However, in a select group with high risk of csPCa, upfront PSMA may be performed and biopsy may be omitted if the clinical characteristics and imaging are highly suggestive. However, biopsy may provide more information than ISUP GG only, including specific tumour characteristics, any need for DNA testing, and useful data for planning radical or focal surgery.

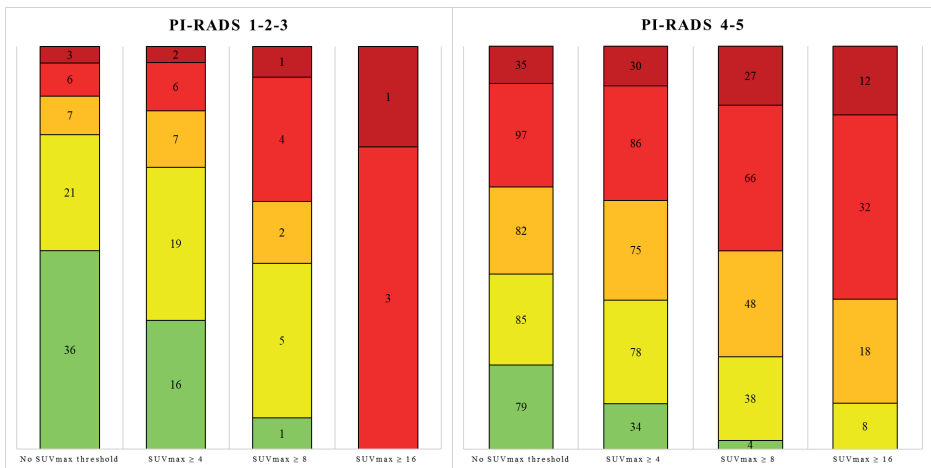


**Figure 1:** ISUP Grade Groups by prostate-specific membrane antigen SUVmax threshold for PI-RADS 1–3 and 4–5 groups. Numbers within the bars denote the number of patients. ISUP = International Society of Urological Pathology; PI-RADS = Prostate Imaging-Reporting and Data System; SUVmax = maximum standardised uptake value.

Further research will focus on a model that combines prebiopsy parameters, possibly with the PRIMARY score<sup>4</sup>, for accurate prediction of csPCa. Only then could treatment without histological confirmation be considered for selected patients.

## References

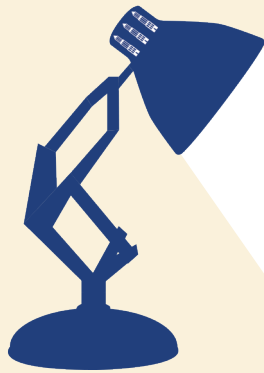
- 1 Mottet N, van den Bergh RCN, Briers E, Van den Broeck T, Cumberbatch MG, De Santis M *et al.* EAU-EANM-ESTRO-ESUR-SIOG Guidelines on Prostate Cancer-2020 Update. Part 1: Screening, Diagnosis, and Local Treatment with Curative Intent. *Eur Urol* 2021; **79**: 243–262.
- 2 Kasivisvanathan V, Rannikko AS, Borghi M, Panebianco V, Mynderse LA, Vaarala MH *et al.* MRI-Targeted or Standard Biopsy for Prostate-Cancer Diagnosis. *N Engl J Med* 2018; **378**: 1767–1777.
- 3 Emmett L, Buteau J, Papa N, Moon D, Thompson J, Roberts MJ *et al.* The Additive Diagnostic Value of Prostate-specific Membrane Antigen Positron Emission Tomography Computed Tomography to Multiparametric Magnetic Resonance Imaging Triage in the Diagnosis of Prostate Cancer (PRIMARY): A Prospective Multicentre Study. *Eur Urol* 2021; **80**: 682–689.
- 4 Emmett LM, Papa N, Buteau J, Ho B, Liu V, Roberts M *et al.* The PRIMARY Score: Using intra-prostatic PSMA PET/CT patterns to optimise prostate cancer diagnosis. *J Nucl Med* 2022; : jnumed.121.263448.
- 5 Ptasznik G, Papa N, Kelly BD, Thompson J, Stricker P, Roberts MJ *et al.* High PSMA PET SUVmax in PI-RADS 4 or 5 men confers a high probability of significant prostate cancer. *BJU Int* 2022. doi:10.1111/bju.15736.
- 6 Murray JM, Wiegand B, Hadaschik B, Herrmann K, Kleesiek J. Virtual Biopsy: Just an AI Software or a Medical Procedure? *J Nucl Med* 2022; **63**: 511–513.
- 7 Meissner VH, Rauscher I, Schwamborn K, Neumann J, Miller G, Weber W *et al.* Radical Prostatectomy Without Prior Biopsy Following Multiparametric Magnetic Resonance Imaging and Prostate-specific Membrane Antigen Positron Emission Tomography. *Eur Urol* 2021; : S0302-2838(21)02194-1.
- 8 Kasivisvanathan V, Emberton M, Moore CM. There Is No Longer a Role for Systematic Biopsies in Prostate Cancer Diagnosis. *Eur Urol Open Sci* 2022; **38**: 12–13.
- 9 Ljungberg B, Albiges L, Abu-Ghanem Y, Bedke J, Capitanio U, Dabestani S *et al.* European Association of Urology Guidelines on Renal Cell Carcinoma: The 2022 Update. *Eur Urol* 2022; : S0302-2838(22)01676-1.
- 10 Tan J-L, Papa N, Hanegbi U, Snow R, Grummet J, Mann S *et al.* Predictors of erectile dysfunction after transperineal template prostate biopsy. *Investig Clin Urol* 2021; **62**: 159–165.





# PART II

THE ADEQUATE STAGING  
OF PROSTATE CANCER





# CHAPTER 6

## EXTERNAL VALIDATION OF NOMOGRAMS INCLUDING MRI FEATURES FOR THE PREDICTION OF SIDE-SPECIFIC EXTRAPROSTATIC EXTENSION

J.G. Heetman

E.J.R.J. van der Hoeven

P. Rajwa

F. Zattoni

C. Kesch

S. Shariat

F. Dal Moro

G. Novara

G. La Bombara

F. Sattin

N. von Ostau

N. Pötsch

P.A.T. Baltzer

L. Wever

J.P.A. van Basten

H.H.E. van Melick

R.C.N. van den Bergh

G. Gandaglia

T.F.W. Soeterik

European Association of Urology Young Academic Urologists Prostate Cancer Working Party

Prostate Cancer Prostatic Dis. 2023 Nov 6. doi: 10.1038/s41391-023-00738-3.

## Abstract

*Background:* Prediction of side-specific extraprostatic extension (EPE) is crucial in selecting patients for nerve-sparing radical prostatectomy (RP). Multiple nomograms, which include magnetic resonance imaging (MRI) information, are available predict sidespecific EPE. It is crucial that the accuracy of these nomograms is assessed with external validation to ensure they can be used in clinical practice to support medical decision-making.

*Methods:* Data of prostate cancer (PCa) patients that underwent robot-assisted RP (RARP) from 2017 to 2021 at four European tertiary referral centres were collected retrospectively. Four previously developed nomograms for the prediction of side-specific EPE were identified and externally validated. Discrimination (area under the curve [AUC]), calibration and net benefit of four nomograms were assessed. To assess the strongest predictor among the MRI features included in all nomograms, we evaluated their association with side-specific EPE using multivariate regression analysis and Akaike Information Criterion (AIC).

*Results:* This study involved 773 patients with a total of 1546 prostate lobes. EPE was found in 338 (22%) lobes. The AUCs of the models predicting EPE ranged from 72.2% (95% CI 69.1-72.3%) (Wibmer) to 75.5% (95% CI 72.5-78.5%) (Nyarangi-Dix). The nomogram with the highest AUC varied across the cohorts. The Soeterik, Nyarangi-Dix, and Martini nomograms demonstrated fair to good calibration for clinically most relevant thresholds between 5 and 30%. In contrast, the Wibmer nomogram showed substantial overestimation of EPE risk for thresholds above 25%. The Nyarangi-Dix nomogram demonstrated a higher net benefit for risk thresholds between 20 and 30% when compared to the other three nomograms. Of all MRI features, the European Society of Urogenital Radiology score and tumour capsule contact length showed the highest AUCs and lowest AIC.

*Conclusion:* The Nyarangi-Dix, Martini and Soeterik nomograms resulted in accurate EPE prediction and are therefore suitable to support medical decision-making.

## Introduction

Accurate prediction of extraprostatic extension (EPE) of prostate cancer (PCa) is crucial for preoperative risk assessment, especially in case nerve-sparing surgery is desired. Several previous studies showed that combining multi-parametric resonance imaging (MRI) features with other clinical parameters such as prostate-specific antigen (PSA) serum values and biopsy information, improves the accuracy of EPE risk prediction.<sup>1-3</sup> To further individualize surgical planning, the risk of EPE can be established for both prostate lobes separately; in a side-specific manner. A number of nomograms for side-specific EPE prediction, including MRI parameters, have been recently developed previously.<sup>4-7</sup> The variables used as inputs for these four nomograms are detailed in Supplementary Table 1. To determine whether these nomograms can be safely applied in daily clinical practice, their diagnostic performance should be established using contemporary patient cohorts other than the ones used for model development.<sup>8</sup> As the prediction formula is tailored to the development data, a nomogram may show excellent performance in the development population but can perform poorly in an external cohort. Preferably, a nomogram is externally validated in different cohorts.<sup>9</sup>

The nomograms described by Soeterik *et al.* and Martini *et al.*, include EPE risk prediction respectively in trichotomous (no tumour present on MRI, suspicious lesion on present on MRI, and EPE present on MRI) and dichotomous fashion (EPE present yes or no).<sup>4,6</sup> Both nomograms have been externally validated, showing moderate to good discrimination and moderate to strong calibration respectively.<sup>10-14</sup> The nomograms developed by Nyarangi-Dix *et al.* and Wibmer *et al.* include other MRI features such as tumour capsule contact length (TCCL) on MRI and the European Society of Urogenital Radiology (ESUR) score for EPE.<sup>5,7</sup> In prior studies, these quantification methods for establishing EPE risk have been shown to improve diagnostic accuracy of MRI.<sup>15-18</sup> However, it is unclear if the incorporation of these promising MRI features into nomograms leads to improved EPE risk prediction, as both Nyarangi-Dix and Wibmer nomograms have not yet been externally validated.

It is crucial that the accuracy of these nomograms is assessed in patients that underwent diagnostic evaluation according to the contemporary guidelines, minimizing the risk of discordance between biopsy and surgical pathology.<sup>19</sup> In addition, to minimize inter-reader variability of MRI interpretation, reporting should be done according to the most recent prostate imaging reporting and data system (PI-RADS) version 2.<sup>20</sup> Therefore, the aim of this study is to externally validate four available side-specific EPE nomograms including MRI parameters, by using an international multi-centre contemporary cohort of patients with prostate cancer undergoing radical prostatectomy.

## Materials/Subjects and Methods

### Patient Population and Study Data

Data of consecutive patients undergoing radical prostatectomy at four high-volume European tertiary referral centers, from 2017 to 2021, were used for the analyses. All clinically relevant variables in addition to those included in the four nomograms were retrospectively collected. Prostate biopsy evaluation and histopathological evaluation of the surgical specimens was done according to the International Society of Urogenital Pathology (ISUP) guidelines<sup>21</sup> MRI prostate (either biparametric [bp] or multiparametric [mp]) reading and reporting was done according to PI-RADS version 2.<sup>22</sup> If missing, the ESUR score for EPE and tumour capsule contact length were retrospectively determined by experienced uro-radiologists in a side-specific manner, according to the ESUR guidelines.<sup>23</sup>

### Model Discrimination, Calibration and Clinical Usefulness

External validation of the four nomograms was done according to the transparent reporting of a multivariable prediction model for individual prognosis or diagnosis (TRIPOD) guidelines.<sup>24</sup> Discrimination, which refers to the ability of the nomogram to distinguish a prostate lobe with the endpoint (EPE) from a lobe without EPE, was quantified using the area under the receiver operating characteristic curve (AUC).<sup>24</sup> Furthermore, the AUC of a logistic regression model, comprising PSA and the presence of EPE on MRI (no lesion, no EPE, equivocal, and EPE), was provided to demonstrate the additional value of the nomograms compared to generally used clinical parameters. The Model calibration, which refers to the agreement between observed endpoints and predictions, was assessed using calibration slopes.<sup>24</sup> The net benefit per risk threshold was determined using decision-curve analysis (DCA). The net benefit is calculated as the proportion of “net” true positives (true positives corrected for the false positives weighted by the odds of the risk cutoff, divided by the sample size).<sup>25</sup>

### Association Between the MRI Features and EPE

The predictive value of individual MRI variables included in the nomograms were assessed by multivariate regression analysis. In multivariable analysis, including PSA density and biopsy ISUP Grade Group, value of the five different MRI variables included in the four nomograms (supplement Table 1), was assessed using an AIC (Akaike Information Criterion) to determine the features with the best fit. In addition, the AUC of the ROC was established.

### Missing Data

Missing data patterns were explored using response matrix and correlation plots. Missing data were handled by using multivariate imputation by chained equations including pooling using Rubin’s rules.<sup>26</sup>

## Results

### Baseline Characteristics

A total of 773 patients were included, representing a total of 1546 prostate lobes. Descriptive characteristics of the total cohort are presented in Table 1 and per cohort in supplementary Table 2. A bpMRI was used in 288 (37%) patients, and a mpMRI in 485 (63%). The characteristics per lobe regarding the covariates used in the different nomograms are presented in Table 2. Of all the lobes 338 (22%) had EPE in prostatectomy specimens. In the per lobe analysis, presence of EPE was associated with relatively higher absolute serum PSA levels and PSA density measured in the patient. The lobes with EPE had more PI-RADS 4 or 5 lesions, a higher ESUR score, more tumour involvement in the biopsy cores, a higher percentage of positive systematic biopsy cores, more tumour extend in the systematic biopsy cores, and a higher ISUP Grade Group (GG). In one of the four cohorts, all data regarding tumour core involvement (%) was not available. Due to the extensive amount of missing data, we decided not to impute this variable. Therefore, the prostate lobes containing cancer of this cohort were excluded per analysis. Missing data patterns of other variables showed data to be either missing completely at random or missing at random and were therefore imputed.

### Model Discrimination

The AUCs for the four nomograms are shown in Table 3. The AUC values are comparable between the four nomograms, ranging from 72.2% (95% CI 69.1–75.3%) for the Wibmer nomogram (lowest) to 75.5% (95% CI 75.2–78.5%) for the Nyarangi-Dix nomogram (highest). All nomograms exhibited a higher AUC than the 70.4% (95% CI 67.2–73.6%) of the model with PSA and EPE on MRI. AUCs of all four nomograms per individual hospital are presented in the Supplemental section (Supplementary Table 3); showing in-between-hospital differences of AUC values of all four nomograms.

### Model Calibration

The agreement between predicted and observed probabilities of all four nomograms are shown in Figure 1. For the clinically most relevant thresholds for the risk of EPE of 0 to 40%, calibration was fair to good for the Soeterik, Martini and Nyarangi-Dix nomograms. The Soeterik and Martini nomogram showed slight overestimation, whereas the Nyarangi-Dix nomogram showed slight underestimation of EPE probability. For the Wibmer nomogram, substantial overestimation of the predicted risk was shown for the thresholds of 25% and above. Overall, the Soeterik nomogram showed the highest agreement of the predicted and observed probabilities for thresholds 0–90%.

**Table 1:** Descriptive characteristics on patient level in the overall population

	Overall
No. of patients	773
<u>Age (median, IQR)</u>	67 (62, 71)
<u>PSA (ng/ml)</u> Mean (IQR)	7.5 (5.5, 11.0)
<u>PSA density (ng/ml/ml)</u> Mean (IQR)	0.19 (0.12, 0.28)
<u>Clinical T stage n (%)*</u>	
T1	424 (55)
T2	284 (38)
T3	45 (6)
Missing	20 (3)
<u>MRI T stage n (%)*</u>	
T0	44 (6)
T2	493 (64)
T2/T3 (uncertain EPE)	126 (16)
T3	107 (14)
T4	2 (0)
Missing	1 (0)
<u>Biopsy type n (%)*</u>	
TRUS-guided systematic	168 (22)
MRI-guided	47 (6)
TRUS + MRI-guided	552 (71)
Missing	4 (1)
<u>Biopsy ISUP Grade Group n (%)*</u>	
Benign	5 (1)
1	126 (16)
2	252 (33)
3	171 (22)
4	150 (19)
5	67 (9)
missing	2 (0)
<u>Pathological stage n (%)*</u>	
T0	1 (0)
T2	460 (60)
T3	310 (40)
T4	1 (0)
missing	10 (1)

**Table 1:** Continued

	Overall
<u>Radical prostatectomy ISUP Grade Group <i>n</i> (%)*</u>	
1	60 (8)
2	313 (40)
3	224 (29)
4	79 (10)
5	80 (10)
missing	17 (2)
<u>Postive surgical margin <i>n</i> (%)*</u>	
missing	14 (2)

EPE = extraprostatic extension, PSA = prostate specific antigen, PI-RADS = Prostate Imaging-Reporting and Data System, ISUP = International Society of Urologic Pathology, TRUS = transrectal ultrasound, \*Percentages may not sum to 100% due to rounding

### Clinical Utility

The DCA of the four nomograms are shown in Figure 2. All four nomograms can be regarded as clinically useful for risk thresholds 9–30%. The Nyarangi-Dix nomogram showed slightly lower net benefit compared with the “treat all” approach for risk thresholds 3–11%, respectively. The Wibmer nomogram showed a no benefit from risk threshold 40% and above, leading to a negative net benefit for risk thresholds 40% and above. The Soeterik and Martini nomogram showed comparable net benefit for risk thresholds 0–35%. The Nyarangi-Dix nomogram was associated with a slightly higher net benefit for the risk thresholds 20–30%, compared with the other three nomograms.

### Predictive Value of side-specific MRI Features

In Table 4, an analysis of the different MRI features incorporated in the four models is shown. The dichotomous classification for EPE had a lower AUC 74.2 (95% CI 71.1–77.3) and a higher AIC of 1426 than the trichotomous classification for EPE used by Soeterik (AUC of 75.1 [95% CI 72.0–78.1] and an AIC of 1415) and the classification used by Wibmer 75.2 (95% CI 72.2–78.3) AIC 1414. The continuous variables used by Nyarangi-Dix had the highest AUCs and lowest AIC with an AUC of 76.5 (95% CI 73.6–79.5) and an AIC of 1396 for TCCL and an AUC of 76.3 (95% CI 73.3–79.3) and an AIC 1379 for the ESUR score, respectively.

**Table 2:** Descriptive characteristics on a per lobe level in the total cohort, divided by the presence of extra prostatic extension

Characteristic	No EPE, (n = 1204)	EPE (n = 338)	p-value
Age(years) (IQR)	67 (62, 71)	68 (63, 72)	0.067
PSA (ng/ml) (IQR)	7.2 (5.3, 10.5)	8.6 (5.9, 13.0)	<0.001
Prostate volume(ml) (IQR)	40 (30, 55)	39 (30, 53)	0.3
PSA density (ng/ml/ml) (IQR)	0.18 (0.12, 0.27)	0.22 (0.15, 0.34)	<0.001
Clinical T stadium n(%*)			<0.001
<i>cT1/cT2a</i>	1138 (95)	280 (83)	
<i>cT2b/c</i>	38 (3)	41 (12)	
<i>cT3/4</i>	19 (2)	14 (4)	
<i>Unknown</i>	9(1)	3 (1)	
PI-RADS 4 or 5, n (%*)	602 (50)	264 (78)	<0.001
missing	8 (1)	1 (0)	
EPE on MRI, n (%*)			<0.001
<i>No visible lesion</i>	571 (47)	74 (22)	
<i>No EPE</i>	499 (41)	143 (42)	
<i>Equivocal</i>	90 (7)	58 (17)	
<i>EPE</i>	38 (3)	61 (18)	
<i>Unknown</i>	6(0)	2(1)	
ESUR score (IQR)	0 (0, 1)	1 (1, 5)	<0.001
TCCL(mm) (IQR)	0 (0,10)	12 (5,21)	<0.001
ISUP Grade Group, n (%*)			
<i>Benign</i>	332 (28)	38 (11)	
1	279 (23)	33 (10)	
2	263 (22)	64 (19)	
3	145 (12)	62 (18)	
4	124 (10)	81 (24)	
5	35 (3)	57 (17)	
<i>Unknown</i>	26(2)	3(1)	
Percentage positive SB (%*) (IQR)	20 (0, 50)	50 (17, 83)	<0.001
missing	52	15	
Tumour extent in SB (mm) (IQR)	2 (0, 10)	9 (0, 13)	<0.001
Missing	179	65	
Tumour involvement in biopsy (%*) (IQR)	15 (0, 50)	50 (15,87)	<0.001
missing	80	27	



**Table 2:** Continued

Characteristic	No EPE, (n = 1204)	EPE (n = 338)	p-value
Cohort, n (%)			
1	460 (38)	112 (33)	
2	337 (28)	113 (33)	
3	329 (27)	81 (24)	
4	78 (6)	32 (9)	

EPE = extraprostatic extension, PSA = prostate specific antigen, PI-RADS = Prostate Imaging-Reporting and Data System, MRI= magnetic resonance imaging, ESUR= European Society of Urological Radiology, TCCL= tumour capsule contact length, ISUP = International Society of Urologic Pathology, SB= systematic biopsy. \*Percentages may not sum to 100% due to rounding

**Table 3:** Discrimination of all four nomograms in the overall population

	Overall	
	Lobes	AUC ( 95% CI)
Soeterik	1546 (100%)	74.6% (71.6-77.7%)
Martini	1150 (74%)	74.3% (71.1-77.6%)
Wibmer	1469 (95%)	72.2% (69.1-75.3%)
Nyarangi-Dix	1546 (100%)	75.5% (72.5-78.5%)

AUC= Area Under the Curve

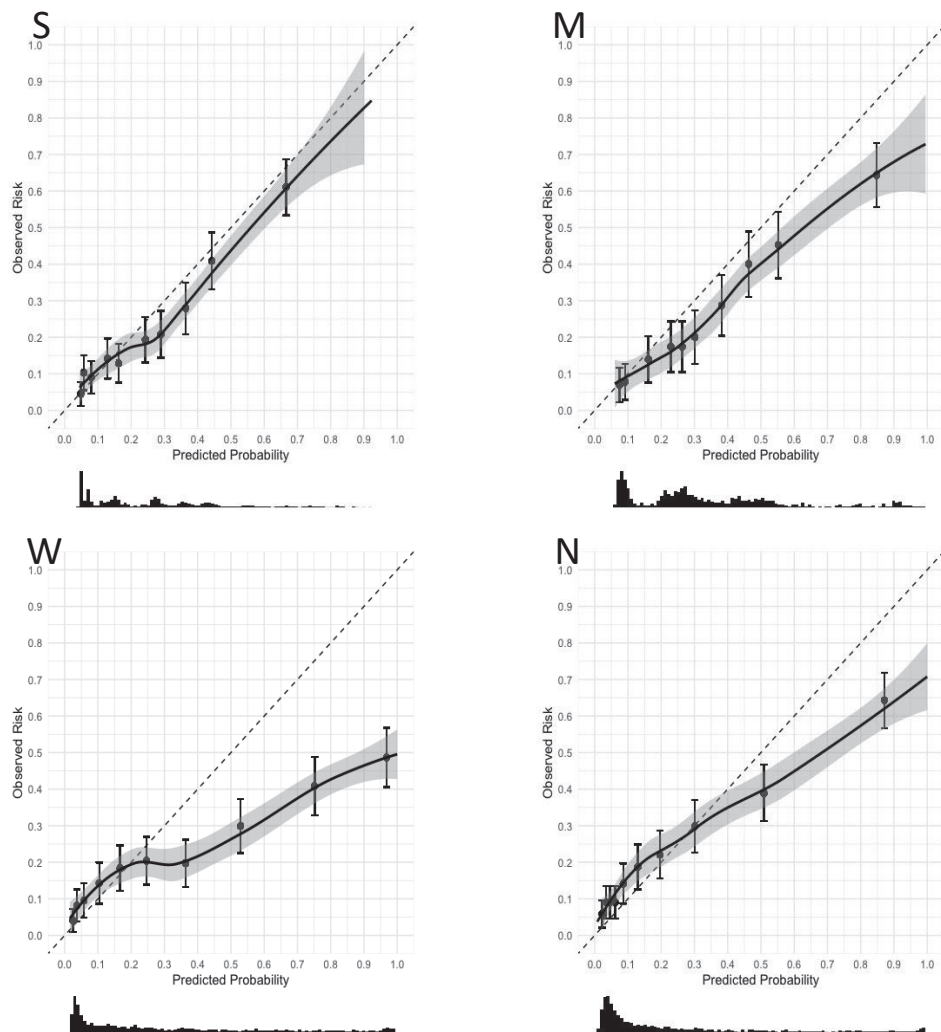


**Figure 1:** Calibration slope for all four models. The Soeterik (S) nomogram, located on the top left, demonstrated fair to good calibration for the clinically most relevant thresholds concerning the risk of extraprostatic extension (EPE) from 0 to 40%. In addition, it showcased the highest concordance between its predictions and observed probabilities across the range of 0–90%. The Martini (M) nomogram, positioned on the top right, also exhibited a fair to good calibration for the 0–40% EPE risk thresholds. The Wibmer (W) nomogram, situated on the bottom left, displayed a more pronounced discrepancy. It substantially overestimated the predicted risk from a threshold of 25% and higher. Lastly, the Nyarangi-Dix (N) nomogram, located on the bottom right, was calibrated as fair to good for the clinically significant 0–40% EPE risk thresholds. Notably, in contrast to the Soeterik and Martini nomograms, it tended to slightly underestimate the EPE probability within this range

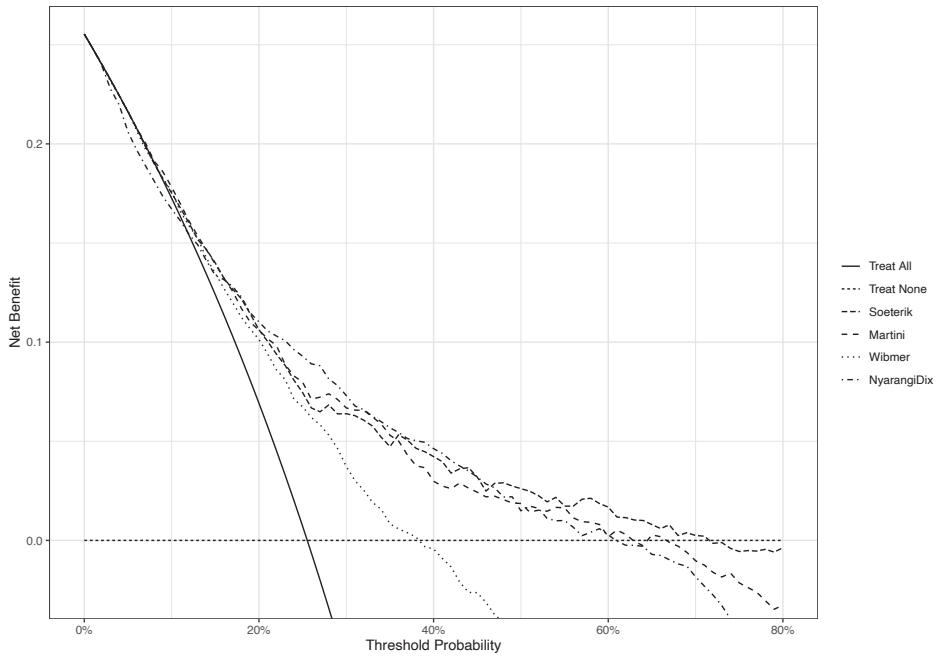


**Figure 2:** Decision-curve analysis for the four models. The Soeterik nomogram showed a net benefit for risk thresholds ranging from 0 to 70%. The Martini nomogram performed comparable to the Soeterik nomogram, in the range from 0 to 35%. The Wibmer nomogram offered no benefit from a risk threshold of 40% and above. The Nyarangi-Dix nomogram while it exhibited slightly lower net benefit than the “treat all” approach for risk thresholds between 3 and 9%, it surpassed the other three models by offering a slightly higher net benefit for thresholds between 20 and 30%.

**Table 4:** Model discrimination of the multivariable logistic regression models including different MRI variables in the overall population

	OR 95% CI	<i>p</i> -value	AUC 95% CI	AIC
Model 1			74.2 (71.1-77.3)	1426
PSAD	2.0 (1.2, 3.3)	0.007		
ISUP				
Benign		Reference		
GG1	1.0 (0.6, 1.6)	>0.9		
GG2	2.1 (1.4, 3.2)	<0.001		
GG3	3.2 (2.0, 5.0)	<0.001		
GG4	5.0 (3.3, 7.8)	<0.001		
GG5	11.0 (6.4, 19.1)	<0.001		
MRI				
No EPE		Reference		
EPE	4.0 (2.5, 6.3)	<0.001		
Model 2			75.1 (72.0-78.1)	1415
PSAD	1.8 (1.1, 3.0)	0.02		
ISUP				
Benign		Reference		
GG1	0.9 (0.5, 1.4)	0.6		
GG2	1.6 (1.0, 2.5)	0.048		
GG3	2.4 (1.5, 3.9)	<0.001		
GG4	3.9 (2.5, 6.2)	<0.001		
GG5	8.7 (5.0, 15.3)	<0.001		
MRI				
No lesion		Reference		
No EPE	1.8 (1.3- 2.5)	<0.001		
EPE	6.0 (3.6, 10.1)	<0.001		
Model 3			75.2 (72.2-78.3)	1414
PSAD	1.8 (1.1, 3.0)	0.02		
ISUP				
Benign		Reference		
GG1	1.0 (0.6, 1.6)	>0.9		
GG2	1.9 (1.2, 2.9)	0.004		
GG3	2.9 (1.8, 4.6)	<0.001		
GG4	4.6 (2.9, 7.1)	<0.001		
GG5	9.5 (5.5, 16.7)	<0.001		
MRI				
No EPE		Reference		
Equivocal	2.1 (1.4, 3.1)	<0.001		
EPE	4.5 (2.8, 7.3)	<0.001		

**Table 4:** Continued

	OR 95% CI <i>p</i> -value	AUC 95% CI	AIC
Model 4		76.5 (73.6-79.5)	1396
PSAD	1.7 (1.0, 2.9) 0.03		
ISUP			
Benign	Reference		
GG1	0.8 (0.5, 1.4) 0.5		
GG2	1.4 (0.9, 2.2) 0.14		
GG3	2.4 (1.5, 3.8) <0.001		
GG4	3.5 (2.3, 5.6) <0.001		
GG5	7.4 (4.2, 13.2) <0.001		
MRI			
TCCL	1.1 (1.0, 1.1) <0.001		
Model 5		76.3 (73.3-79.3)	1379
PSAD	1.6 (1.0, 2.7) 0.08		
ISUP			
Benign	Reference		
GG1	0.9 (0.6, 1.5) 0.8		
GG2	1.6 (1.0, 2.5) 0.045		
GG3	2.6 (1.7, 4.2) <0.001		
GG4	3.7 (2.3, 5.8) <0.001		
GG5	7.1 (4.0, 12.6) <0.001		
MRI			
ESUR	1.3 (1.2, 1.4) <0.001		

PSAD = prostate specific antigen density, ISUP = International Society of Urologic Pathology, MRI= magnetic resonance imaging TCCL= tumour capsule contact length, ESUR= European Society of Urogenital Radiology EPE = extraprostatic extension, Area Under the Curve, AIC = Akaike Information Criterion,

## Discussion

In this study, we present the results of the external validation of four MRI-based nomograms for the prediction of side specific EPE in a European dataset consisting of 773 patients with a total of 1546 prostate lobes. We observed a fair discriminative ability of all four nomograms, with AUC's ranging from 72.2 to 75.5%. The calibration of the Soeterik, Martini, and Nyarangi-Dix nomograms was fair to good for the clinically most relevant risk thresholds of 0–40%. The Wibmer nomogram showed substantial overestimation of the predicted EPE risk for risk thresholds from 25% and above. DCA showed that the Soeterik, Martini and the NyarangiDix nomograms are all clinically useful for risk thresholds 8 to 40%. We conclude that the Soeterik, Martini and the Nyarangi-Dix nomograms are well suitable for use in clinical practice. Based on this study, the Wibmer nomogram should be used which caution due to substantial miscalibration and limited clinical usefulness for risk thresholds above 25%.

Our findings regarding model performance of the Soeterik and Martini nomograms are consistent to those reported in previous external validation studies. The study of Blas *et al.* reported an AUC of 81% for the Soeterik nomogram and 75% for the Martini nomogram, respectively.<sup>13</sup> Another external validation study of the Martini nomogram reported an AUC of 78%.<sup>14</sup> The study of Veerman *et al* reported an AUC of 80% for the Soeterik nomogram.<sup>12</sup> A different study by Diamand *et al.* presented an AUC of 71% for the Soeterik nomogram and 73% for the Martini nomogram.<sup>11</sup> With regard to calibration, these prior studies all reported moderate to good agreement of predicted and observed probabilities for both the Martini and the Soeterik nomogram.

To our knowledge, this is the first study in which the Wibmer and Nyarangi-Dix nomograms are externally validated. On external validation, they both showed substantially lower AUCs compared to the AUCs reported for the development cohorts; respectively 76% versus 87% for Nyarangi-Dix and 72.2% versus 82.8% for the Wibmer nomogram.<sup>5,7</sup> In this study, the Wibmer nomogram showed the relatively lowest AUC of all validated nomograms of respectively 72.2%, substantial underestimation of the predicted EPE risk from thresholds above 25% and a negative net benefit on DCA for thresholds above 40%. The Nyarangi-Dix nomogram showed more favourable results, with an AUC of 75.5%, fair agreement between predicted and observed probabilities and the highest net benefit on DCA compared with the other nomograms (for the clinically most relevant risk thresholds between 10 to 40%).

The reason the Nyarangi-Dix nomogram showed slightly better model performance compared to the other nomograms could be due to the inclusion of the potentially more robust MRI predictors: TCCL and the ESUR score. Due to the scaling of these variables, they may have to potential to explain more variance compared to MRI predictors including solely

two or three subclasses. This hypothesis is supported by our multivariable analysis for the prediction of EPE; showing that inclusion of TCCL and the ESUR score on multivariable logistic regression leads to overall best model fit in terms of AIC as well as most favourable discrimination in terms of AUC. The suggested higher predictive potential is countered by the additional effort required to document these features (in a side specific manner) during routine clinical care making the nomogram potentially less easy-to-use in daily practice. Besides TCCL and the ESUR score, other methods have been proposed to improve EPE risk prediction. For instance, the use of artificial intelligence and radiomics features could potentially further improve EPE risk prediction. Hou *et al.* showed an excellent AUC of 86% for their developed artificial intelligent model, showing the outperform the radiologist (AUC of 72%) for the prediction of EPE.<sup>27</sup> In another study, combined use of MRI index lesion radiomics in a machine learning model was demonstrated to have a high accuracy for EPE detection, reaching an overall accuracy of 83% in the training set.<sup>28</sup> In addition, a prior study by Solari and colleagues showed that PSMA PET/MR radiomics could further improve prostate cancer staging in addition to MRI radiomics. The authors evaluated 9 support vector machine models with PET and/or MRI radiomics features including the apparent diffusion coefficient (ADC). The authors concluded that the best performing model included both PET and ADC radiomics; suggesting their complementary value.<sup>29</sup>

Moving forward, it is also crucial to evaluate if the use of sidespecific EPE nomograms leads to improved patient selection for nerve sparing RP. Such an approach could potentially enhance functional outcomes owing to the benefits of more nerve preservation without risking a PSM.<sup>30,31</sup> However, studies on this topic are scarce. To our best knowledge, one prior singlecentre prospective study was performed on this subject and showed that the use of a side-specific EPE MRI-based nomogram for preoperative planning results in comparable rates of full nervesparing (45% vs. 30%;  $p = 0.083$ ), but relatively lower rates of PSM on lobes with histological EPE (45% vs. 85%;  $p < 0.05$ ).<sup>32</sup> Future prospective multicentre trials are needed to further evaluate if the use of nomograms for preoperative planning improve clinical outcomes for the patient.

Although our study has a number of strengths such as being a multicentre international study including a contemporary population of patients treated at tertiary referral centers, it is not exempt from limitations. First, due to the retrospective collection of data there is a risk of information bias. In addition, although MRI review was performed by dedicated high-volume uro-radiologists, the lack of central review is a limitation. However, interobserver variability is unavoidable in daily clinical practice and thus, on the other hand, our study reflects a real-world clinical situation. It should also be noted that we used both bpMRI and mpMRI in this study. However, we do not consider this as a major limitation as both modalities have been shown to be comparably effective in detecting EPE.<sup>33</sup>

## Conclusion

The external validation of four side-specific nomograms including MRI features showed that three of four nomograms (Nyarangi-Dix, Soeterik and Martini) showed fair to good model discrimination, calibration, and net benefit. Based on this study data, these nomograms can be used in clinical practice to support medical decision-making.



## References

- 1 Feng TS, Sharif-Afshar AR, Wu J, Li Q, Luthringer D, Saouaf R *et al.* Multiparametric MRI Improves Accuracy of Clinical Nomograms for Predicting Extracapsular Extension of Prostate Cancer. *Urology* 2015; **86**: 332–337.
- 2 Rayn KN, Bioom JB, Gold SA, Hale GR, Baiocco JA, Mehralivand S *et al.* Added Value of Multiparametric Magnetic Resonance Imaging to Clinical Nomograms for Predicting Adverse Pathology in Prostate Cancer. *The Journal Of Urology* 2019; **200**: 1041–1047.
- 3 Gandaglia G, Ploussard G, Valerio M, Mattei A, Fiori C, Roumiguié M *et al.* The Key Combined Value of Multiparametric Magnetic Resonance Imaging, and Magnetic Resonance Imaging–targeted and Concomitant Systematic Biopsies for the Prediction of Adverse Pathological Features in Prostate Cancer Patients Undergoing Radical Prostatectomy. *European Urology* 2020; **77**: 733–741.
- 4 Martini A, Gupta A, Lewis SC, Kumarasamy S, Haines KG, Briganti A *et al.* Development and internal validation of a side-specific, multiparametric magnetic resonance imaging-based nomogram for the prediction of extracapsular extension of prostate cancer. *BJU International* 2018; **122**: 1025–1033.
- 5 Nyarangi-Dix J, Wiesenfarth M, Bonekamp D, Hithaler B, Schütz V, Dieffenbacher S *et al.* Combined Clinical Parameters and Multiparametric Magnetic Resonance Imaging for the Prediction of Extraprostatic Disease—A Risk Model for Patient-tailored Risk Stratification When Planning Radical Prostatectomy. *European Urology Focus* 2020; **6**: 1205–1212.
- 6 Soeterik TFW, Van Melick HHE, Dijkman LM, Küsters-Vandeveldel HVN, Stomps S, Schoots IG *et al.* Development and External Validation of a Novel Nomogram to Predict Side-specific Extraprostatic Extension in Patients with Prostate Cancer Undergoing Radical Prostatectomy. *European Urology Oncology* 2020; **S2588–9311**.
- 7 Wibmer AG, Kattan MW, Alessandrino F, Baur ADJ, Boesen L, Franco FB *et al.* International multi-site initiative to develop an mri-inclusive nomogram for side-specific prediction of extraprostatic extension of prostate cancer. *Cancers* 2021; **13**. doi:10.3390/cancers13112627.
- 8 Bleeker SE, Moll HA, Steyerberg EW, Donders ART, Derksen-Lubsen G, Grobbee DE *et al.* External validation is necessary in prediction research: A clinical example. *Journal of Clinical Epidemiology* 2003; **56**: 826–832.
- 9 Siontis GCM, Tzoulaki I, Castaldi PJ, Ioannidis JPA. External validation of new risk prediction models is infrequent and reveals worse prognostic discrimination. *Journal of Clinical Epidemiology* 2015; **68**: 25–34.
- 10 Soeterik TFW, van Melick HHE, Dijkman LM, Küsters-Vandeveldel H, Stomps S, Schoots IG *et al.* Development and External Validation of a Novel Nomogram to Predict Side-specific Extraprostatic Extension in Patients with Prostate Cancer Undergoing Radical Prostatectomy. *European urology oncology* 2022; **5**: 328–337.
- 11 Diamand R, Roche JB, Lievore E, Lacetera V, Chiacchio G, Beatrice V *et al.* External Validation of Models for Prediction of Side-specific Extracapsular Extension in Prostate Cancer Patients Undergoing Radical Prostatectomy. *European Urology Focus* 2022. doi:10.1016/j.euf.2022.09.006.
- 12 Veerman H, Heymans MW, van der Poel HG. External Validation of a Prediction Model for Side-specific Extraprostatic Extension of Prostate Cancer at Robot-assisted Radical Prostatectomy. *European Urology Open Science* 2022; **37**: 50–52.

- 13 Blas L, Shiota M, Nagakawa S, Tsukahara S, Matsumoto T, Lee K *et al.* Validation of user-friendly models predicting extracapsular extension in prostate cancer patients. *Asian Journal of Urology* 2023; **10**: 81–88.
- 14 Soeterik TFW, van Melick HHE, Dijkstra LM, Küsters-Vandeveldel HVN, Biesma DH, Witjes JA *et al.* External validation of the Martini nomogram for prediction of side-specific extraprostatic extension of prostate cancer in patients undergoing robot-assisted radical prostatectomy. *Urologic Oncology: Seminars and Original Investigations* 2020; **38**: 372–378.
- 15 Baco E, Rud E, Vlatkovic L, Svindland A, Eggesbø HB, Hung AJ *et al.* Predictive value of magnetic resonance imaging determined tumor contact length for extracapsular extension of prostate cancer. *Journal of Urology* 2015; **193**: 466–472.
- 16 Eurboonyanun K, Pisuchpen N, O’Shea A, Lahoud RM, Atre ID, Harisinghani M. The absolute tumor-capsule contact length in the diagnosis of extraprostatic extension of prostate cancer. *Abdominal Radiology* 2021; **46**: 4014–4024.
- 17 Li W, Dong A, Hong G, Shang W, Shen X. Diagnostic performance of ESUR scoring system for extraprostatic prostate cancer extension: A meta-analysis. *European Journal of Radiology* 2021; **143**: 109896.
- 18 Asfuroğlu U, Asfuroğlu BB, Özer H, Gönül İl, Tokgöz N, İnan MA *et al.* Which one is better for predicting extraprostatic extension on multiparametric MRI: ESUR score, Likert scale, tumor contact length, or EPE grade? *European Journal of Radiology* 2022; **149**. doi:10.1016/j.ejrad.2022.110228.
- 19 Ahdoot M, Wilbur AR, Reese SE, Lebastchi AH, Mehralivand S, Gomella PT *et al.* MRI-Targeted, Systematic, and Combined Biopsy for Prostate Cancer Diagnosis. *New England Journal of Medicine* 2020; **382**: 917–928.
- 20 Padhani AR, Weinreb J, Rosenkrantz AB, Villeirs G, Turkbey B, Barentsz J. Prostate Imaging-Reporting and Data System Steering Committee: PI-RADS v2 Status Update and Future Directions. *European Urology* 2019; **75**: 385–396.
- 21 Epstein JI, Egevad L, Amin MB, Delahunt B, Srigley JR, Humphrey PA. The 2014 international society of urological pathology (ISUP) consensus conference on gleason grading of prostatic carcinoma definition of grading patterns and proposal for a new grading system. *American Journal of Surgical Pathology* 2016; **40**: 244–252.
- 22 Turkbey B, Rosenkrantz AB, Haider MA, Padhani AR, Villeirs G, Macura KJ *et al.* Prostate Imaging Reporting and Data System Version 2.1: 2019 Update of Prostate Imaging Reporting and Data System Version 2. *European Urology* 2019; **76**: 340–351.
- 23 Barentsz JO, Richenberg J, Clements R, Choyke P, Verma S, Villeirs G *et al.* ESUR prostate MR guidelines 2012. *European Radiology* 2012; **22**: 746–757.
- 24 Collins GS, Reitsma JB, Altman DG, Moons KGM. Transparent reporting of a multivariable prediction model for individual prognosis or diagnosis (TRIPOD): The TRIPOD Statement. *European Urology* 2015; **67**: 1142–1151.
- 25 Van Calster B, Wynants L, Verbeek JFM, Verbakel JY, Christodoulou E, Vickers AJ *et al.* Reporting and Interpreting Decision Curve Analysis: A Guide for Investigators. *European Urology* 2018; **74**: 796–804.
- 26 Van Buuren S, Groothuis-Oudshoorn K. Multivariate Imputation by Chained Equations in R. *Journal of statistical software* 2011; **45**: 1–67.
- 27 Hou Y, Zhang Y-H, Bao J, Bao M-L, Yang G, Shi H-B *et al.* Artificial intelligence is a promising prospect for the detection of prostate cancer extracapsular extension with mpMRI: a two-center comparative study. *Eur J Nucl Med Mol Imaging* 2021; **48**: 3805–3816.

- 28 Cuocolo R, Stanzione A, Faletti R, Gatti M, Callaris G, Fornari A *et al.* MRI index lesion radiomics and machine learning for detection of extraprostatic extension of disease: a multicenter study. *European Radiology* 2021; **31**: 7575–7583.
- 29 Solari EL, Gafita A, Schachoff S, Bogdanović B, Villagrán Asiares A, Amiel T *et al.* The added value of PSMA PET/MR radiomics for prostate cancer staging. *European Journal of Nuclear Medicine and Molecular Imaging* 2022; **49**: 527–538.
- 30 Nguyen LN, Head L, Witiuk K, Punjani N, Mallick R, Clossen S *et al.* The Risks and Benefits of Cavernous Neurovascular Bundle Sparing during Radical Prostatectomy: A Systematic Review and Meta-Analysis. *J Urol* 2017; **198**: 760–769.
- 31 Soeterik TFW, van Melick HHE, Dijksman LM, Stomps S, Witjes JA, van Basten JPA. Nerve Sparing during Robot-Assisted Radical Prostatectomy Increases the Risk of Ipsilateral Positive Surgical Margins. *J Urol* 2020; **204**: 91–95.
- 32 Heetman JG, Soeterik TFW, Wever L, Meyer AR, Nuininga JE, van Soest RJ *et al.* A side-specific nomogram for extraprostatic extension may reduce the positive surgical margin rate in radical prostatectomy. *World Journal of Urology* 2022; **40**: 2919–2924.
- 33 Christophe C, Montagne S, Bourrelier S, Roupret M, Barret E, Rozet F *et al.* Prostate cancer local staging using biparametric MRI: assessment and comparison with multiparametric MRI. *European Journal of Radiology* 2020; **132**: 109350.

## Supplementary Material

**Supplement Table 1:** Input variables for the four different nomograms

Soeterik	Martini	Wibmer	Nyarangi-Dix
PSAD	PSA	Age	Clinical T stadium
ISUP GG per side (Benign, 1,2,3,4,5)	ISUP GG per side (1,2,3,4,5)	PSAD	(cT1a/cT2a, cT2b/c, cT3/4)
<b>MRI (no lesion, no EPE, EPE)</b>	Percent highest biopsy tumour involvement (>50%, ≤50%) <b>MRI (no EPE, EPE)</b>	ISUP GG per side (1,2,3,4,5) Percentage positive SB cores per side Tumour extent in SB PI-RADS 4-5 lesion (y/n) <b>MRI (no EPE, equivocal, EPE)</b> <b>TCCL</b>	PSA Prostate volume ISUP GG per side (1,2,3,4,5) <b>ESUR score</b> <b>TCCL</b>

PSAD = prostate specific antigen density, ISUP = International Society of Urologic Pathology, MRI= magnetic resonance imaging, EPE = extraprostatic extension, TCCL= tumour capsule contact length, ESUR= European Society of Urogenital Radiology

**Supplement Table 2.** Descriptive characteristics in the different cohorts

	Cohort 1	Cohort 2	Cohort 3	Cohort 4
No. of patients	288	225	205	55
Age (median, IQR)	68 (63, 70)	67 (61, 72)	66 (62, 70)	66 (61, 70)
<u>PSA (ng/ml)</u> Mean (IQR)	8.1 (5.6, 13.0)	7.10 (5.2, 10.4)	7.00 (5.28, 9.42)	8.60 (5.45, 12.90)
<u>PSA density (ng/ml/ml)</u> Mean (IQR)	0.20 (0.14, 0.34)	0.21 (0.15, 0.31)	0.14 (0.10, 0.21)	0.19 (0.14, 0.27)
<u>Clinical T stage n (%)*</u>				
T1	139 (48)	124 (55)	135 (66)	25 (45)
T2	101 (35)	90 (40)	68 (33)	25 (45)
T3	29 (10)	11 (5)	0 (0)	5 (9)
Missing	18 (6)	0 (0)	2 (1)	0 (0)
<u>MRI T stage n (%)*</u>				
T0	12 (4)	2 (1)	29 (14)	1 (2)
T2	195 (68)	141 (63)	121 (59)	36 (65)
T2/T3 (uncertain EPE)	47 (16)	46 (20)	33 (16)	0 (0)
T3	34 (13)	34 (15)	21 (10)	18 (33)
T4	0 (0)	2 (1)	0 (0)	0 (0)
Missing	0 (0)	0 (0)	1 (0)	0 (0)

**Supplement Table 2.** Continued

	Cohort 1	Cohort 2	Cohort 3	Cohort 4
<u>Biopsy type n (%)*</u>				
TRUS-guided systematic	70 (24)	38 (17)	43 (21)	17 (31)
MRI-guided	29 (10)	18 (8)	0 (0)	0 (0)
TRUS + MRI-guided	183 (64)	169 (75)	162 (79)	38 (69)
Missing	4 (1)	0 (0)	0 (0)	0 (0)
<u>Biopsy ISUP Grade Group n (%)*</u>				
Benign	2 (1)	1 (0)	2 (1)	0 (0)
1	48 (17)	21 (9)	54 (26)	3 (5)
2	102 (35)	68 (30)	60 (29)	22 (40)
3	65 (23)	61 (27)	38 (19)	7 (13)
4	57 (20)	46 (20)	36 (18)	11 (20)
5	14 (5)	27 (12)	14 (7)	12 (22)
missing	0 (0)	1 (0)	1 (0)	0 (0)
<u>Pathological stage on RP specimen n (%)*</u>				
T0	0 (0)	0 (0)	1 (0)	0 (0)
T2	179 (62)	126 (56)	125 (61)	30 (55)
T3	98 (34)	99 (44)	79 (39)	25 (45)
T4	1 (0)	0 (0)	0 (0)	0 (0)
missing	10 (3)	0 (0)	0 (0)	0 (0)
<u>Pathology ISUP Grade Group on RP specimen n (%)*</u>				
1	19 (7)	18 (8)	21 (10)	2 (4)
2	136 (47)	79 (35)	74 (36)	24 (44)
3	83 (29)	63 (28)	58 (28)	20 (36)
4	23 (8)	28 (12)	26 (13)	2 (4)
5	11 (4)	37 (16)	25 (12)	7 (13)
missing	16 (6)	0 (0)	1 (0)	0 (0)
<u>Positive surgical margin n (%)*</u>				
missing	11 (4)	3 (1)	0 (0)	0 (0)

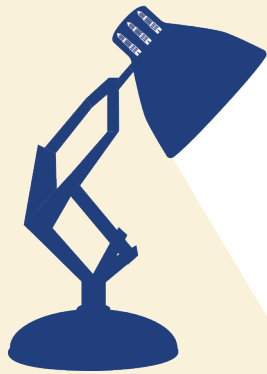
EPE = extraprostatic extension, PSA = prostate specific antigen, MRI= magnetic resonance imaging, TRUS = transrectal ultrasound, ISUP = International Society of Urologic Pathology, RP= radical prostatectomy, \*Percentages may not sum to 100% due to rounding, \*Percentages may not sum to 100% due to rounding

**Supplement Table 3:** Discriminating performance of each nomogram in the different hospitals and the number of lobes the nomogram could be completed on after imputation.

	Cohort 1		Cohort 2	
	lobes	AUC (95%CI)	lobes	AUC (95%CI)
Soeterik	576 (100%)	73.0% (67.6-78.3%)	450 (100%)	<b>74.1% (68.5-79.8%)</b>
Martini	416 (72%)	73.8% (68.2-79.3%)	352 (78%)	73.7% (67.7-79.6%)
Wibmer	576 (100%)	70,0% (64.7-75.2%)	450 (100%)	72.7% (67.2-78.2%)
Nyarangi-Dix	576 (100%)	<b>76.0% (70.8-81.3%)</b>	450 (100%)	73.7% (68.0-79.4%)
	Cohort 3		Cohort 4	
	lobes	AUC (95%CI)	lobes	AUC (95%CI)
Soeterik	410 (100%)	<b>77.9% (72.4-83.4%)</b>	110 (100%)	<b>78.9% (68.7-89.0%)</b>
Martini	302 (78%)	75.5% (69.0-82.0%)	81 (74%)	76.4% (65.6-87.2%)
Wibmer	410 (100%)	76.0% (70.2-82.8%)	33 (30%)	75.7% (59.0-92.4%)
Nyarangi-Dix	410 (100%)	77.6% (72.0-83.2%)	110 (100%)	78.1% (68.2-88.1%)

AUC = Area Under the Curve







# CHAPTER 7

## A SIDE-SPECIFIC NOMOGRAM FOR EXTRAPROSTATIC EXTENSION MAY REDUCE THE POSITIVE SURGICAL MARGIN RATE IN RADICAL PROSTATECTOMY

J.G. Heetman  
T.F.W. Soeterik  
L. Wever  
A.R. Meyer  
J.E. Nuininga  
R.J. van Soest  
H.H.E. van Melick  
J.P.A. van Basten  
R.C.N. van den Bergh

## Abstract

*Purpose:* Nomograms predicting side-specific extraprostatic extension (EPE) may be applied to reduce positive surgical margin (PSM) rates in patients planned for radical prostatectomy (RP). This study evaluates the impact of implementing an externally validated nomogram for side-specific EPE on PSM rate and degree of nerve-sparing.

*Methods:* In patients planned for RP, the side-specific nomogram predictions (based on MRI, ISUP Grade Group and PSA density), with an advised threshold of 20% for safe nerve-sparing, were presented preoperatively to the urological surgeon. The surgeon completed a survey before RP about the planning with respect to side-specific nerve-sparing and change of management due to the result of the nomogram. PSM rates and degree of nerve-sparing were compared to a retrospective control group treated in the months prior to the introduction of the nomogram.

*Results:* A total of 100 patients were included, 50 patients in both groups representing 200 prostate lobes. Of the patients, 37% had histologically confirmed EPE, and 40% a PSM. In 12% of the 100 lobes planned after nomogram presentation, a change in management due to the nomogram was reported. A per-prostate lobe analysis of all the lobes showed comparable rates of full nerve-sparing (45% vs. 30%;  $p = 0.083$ ) and lower rates of PSM on the lobes with histological EPE (45% vs. 85%;  $p < 0.05$ ) in the intervention (nomogram) group versus the control group.

*Conclusion:* Implementing a predictive nomogram for side-specific EPE in the surgical planning for nerve-sparing leads to lower rates PSM on the side of the histological EPE without compromising nerve-sparing.

## Introduction

Radical prostatectomy (RP) is the most adopted treatment for localised prostate cancer; it has been shown to significantly increase life expectancy compared with expectative management in a randomized trial setting.<sup>1</sup> However, RP is associated with substantial morbidity, including postoperative erectile dysfunction and urinary incontinence.<sup>2</sup>

To improve the functional outcome of RP, nerve-sparing techniques have been introduced.<sup>3</sup> Although nerve-sparing can reduce the risk of erectile dysfunction<sup>4</sup>, it is independently associated with an increased risk of positive surgical margins (PSM).<sup>5</sup> Since PSM increases the risk of disease recurrence and even cancer-specific mortality, nerve-sparing with an adverse oncological outcome may impair the long-term prognosis.<sup>6</sup>

The European Association of Urology guidelines advise against nerve-sparing in case of a high risk of extraprostatic extension (EPE).<sup>7</sup> In most cases (85%), EPE is only present on one side<sup>8</sup>; therefore, contralateral nerve-sparing can be presumed as an oncologically safe option. EPE prediction is often based on nomograms such as the Partin tables<sup>9</sup> and the Memorial Sloan Kettering Cancer Center nomogram<sup>10</sup>, but these do not include magnetic resonance imaging (MRI) information and the laterality of the expected EPE. Although MRI has a high specificity for the detection of EPE (80–85%), its per-prostate sensitivity is low (57%). Therefore, the MRI information alone is unreliable to exclude the presence of EPE.<sup>11</sup> Hence, a side-specific approach guided by a nomogram that includes MRI parameters is recommended.<sup>7,12</sup>

With the aim of providing a side-specific prediction of EPE, a nomogram was developed by Soeterik *et al.*<sup>13</sup>, using combined data from the Dutch hospital network, Santeon. This nomogram was validated in two different Dutch populations, showing an excellent Area Under the Curve (AUC) ranging from 0.77 to 0.83 in the two cohorts.<sup>13</sup> Besides the side-specific MRI result, it includes side-specific ISUP Group Grade (GG) as well as PSA density. Aside from this nomogram, multiple other side-specific nomograms with incorporated MRI parameters have recently been developed in different institutions.<sup>14–17</sup> However, studies addressing the impact in clinical practice of implementing the use of a side-specific nomogram for EPE before robot-assisted radical prostatectomy (RARP) are, to this date, not available.

The present study assesses the impact of preoperative application of a side-specific nomogram on the PSM rate, the amount and degree of nerve-sparing performed with RARP, and the change of management.

## Patients and Methods

### Data Source and Patient Selection

The study protocol was reviewed by the local ethical board and registered under W21.217. From June to November 2021, patients undergoing RARP with or without extended pelvic lymph node dissection were consecutively included in a Dutch teaching hospital. Surgeons were presented with side-specific nomogram-derived predictions for EPE when planning for nerve-sparing. The control group consisted of a retrospective control group of men who were successively operated on in the same hospital from February to June 2021 before the introduction of the nomogram. Patients were excluded if they were previously treated with enucleation of the prostate or for prostate cancer.

### MRI and Biopsy Protocol

All patients underwent a pre-biopsy 3-Tesla multiparametric MRI (Magnetom Skyra, Siemens Nederland B.V., The Hague, The Netherlands). The scanner used a body coil. Sequences consisted of sagittal, coronal, and axial T2-weighted images; axial diffusion weighted images; and axial dynamic contrast enhanced images. MRI scans were evaluated by experienced uro-radiologists (>1000 MRI prostate) using the PI-RADS 2.1 classification.<sup>18</sup> The prostate biopsy cores were taken transrectally or transperineally by a urologist. Cognitive target biopsies<sup>19</sup> were performed if a suspected area was seen on the pre-biopsy MRI. When no biopsy was performed on the side contralateral to the MRI index lesion (only target biopsies), the outcome was classified as benign for input in the nomogram.

### Implementation of the Nomogram

Before implementation of the nomogram, the indication for nerve-sparing was not standardised and at the discretion of the urological surgeon. From the start of the study, all urological surgeons were presented with information regarding the nomogram. This nomogram uses the following variables: last measured PSA prior to RARP, prostate volume measured using the MRI, side-specific radiological T stage, and highest ISUP GG per side determined on biopsy cores. This nomogram is online available using the following link: <https://evidencio.com/models/show/2142>.

The results of the nomogram per side were presented preoperatively to the urological surgeon in the electronic patient file of all patients planned for RARP with no regard to pre-operative erectile function. A maximum threshold of 20% risk of EPE was advised for performing nerve-sparing, as suggested by Soeterik *et al.*<sup>13</sup> Because if the risk of EPE was less than 20%, it was assumed that nerve-sparing could be performed safely. To test the added value of the nomogram, the urological surgeon was asked to fill out a survey before the procedure, consisting of the strategy per side concerning nerve-sparing (minimal/partial/full) before and after they saw the result of the nomogram, and change of management due to the nomogram.

## Radical Prostatectomy

Three experienced urological surgeons (R.v.B., A.M., and J.N.) performed the RARP procedures. R.v.B performed 350 RARPs before the start of the study and A.M. and J.N. more than 500. From July 2021 onward, they were joined by one dedicated prostate cancer fellow (R.v.S), who did not perform any RARPs independently before the start of the study and was always directly supervised. The RARP was conducted with either the Da Vinci Si, X or Xi robotic surgical system (Intuitive Surgical, Sunnyvale, CA). Nerve-sparing strategy was divided into three groups: minimal, partial, and full, as suggested by the Pasadena Consensus Panel.<sup>20</sup>

## Pathology

A dedicated uro-pathologist examined both the biopsy cores before the operation and the RP specimens according to the prevailing ISUP classification.<sup>21</sup> A PSM was defined as the tumour cells present at the inked margin.<sup>22</sup>

## Primary and Secondary Outcomes

PSM rates were compared between the retrospective control group and the prospective intervention group on a per-lobe basis. Likewise, was done for all lobes with histological EPE. This analysis was performed because our hypothesis was that the implementation of the nomogram could only benefit the lobes with histological EPE. This is due to the ability of the nomogram to predict EPE and therefore per design could not reduce the PSM rate in the lobes without histological EPE. The secondary outcomes are the amount of nerve-sparing, the change of management due to the result of the nomogram, and performance of the nomogram and MRI. Due to the side-specific approach of the nomogram, a per-prostate lobe analysis was performed.

## Statistical Analysis

To determine the effect of the nomogram on PSM rate, the side-specific pathology results after RARP were compared between the control and intervention group incorporating a chi-squared test and logistic regression, using ISUP GG, PSA density, and EPE on MRI as co-variables.<sup>13</sup> For the difference in the side-specific degree of nerve-sparing, the operation report was consulted and compared between both groups using descriptive statistics, chi-squared test, and logistic regression with the same variables as in the previous logistic regression. Data were collected using REDcap hosted at our institution.<sup>23</sup> The analysis was performed using R version 4.1.2(R foundation for Statistical Computing, Vienna, Austria). To support the regression model, we performed an analysis where we matched control and intervention patients on three variables: ISUP GG, PSA density, and EPE on MRI with the use of the Matchit package for R.<sup>24</sup> For matching, the cardinal method with the standard GPLK solver was used. Robust standard errors were determined using the sandwich package.<sup>25</sup> All tests had a significance level set at  $p < 0.05$ .

## Results

### Baseline Characteristics

A total of 100 consecutive patients were included, representing 200 prostate lobes. Fifty patients were prospectively enrolled and compared to 50 controls. Baseline patient's characteristics are shown in Supplement Table 1; no statistically significant differences were observed.

The per-prostate lobe analysis (Table 1) showed 111 (56%) lobes with a visible lesion on the MRI. Eighty-seven (44%) lobes had a PI-RADS 1 or 2, 8 (4%) a PI-RADS 3 and 105 (52%) PI-RADS 4-5. Forty-six (23%) lobes had a suspicion of EPE on the MRI. Forty-three patients had an ISUP GG  $\geq$  3: 27% in the control group versus 16% in the intervention group ( $p = 0.058$ ). A total of 42 (21%) lobes had histological EPE: 20% in the control group and 26% in the intervention group ( $p = 0.7$ ).

### Positive Surgical Margin Rate

Of all the patients, 40% had a PSM. Of the 62 patients with a pT2, 26% had a PSM and of the 38 with a pT3, 63% had a PSM. Of the 200 lobes, there was a PSM in 55 (28%) lobes: 29% in the control group and 26% in the intervention group. The distribution of the PSM rate between the lobes with no EPE versus EPE per group is shown in Supplement Figure 1. There was a non-significant increase in PSM rate on lobes with no histological EPE in the intervention group 21% versus 15% in the control group ( $p = 0.4$ ). Table 2 shows a significantly lower PSM rate on the lobes with histological EPE in the intervention group (45%) versus the control group (85%) ( $p = 0.008$ ). A logistic regression model was built to test the relationship between the introduction of the nomogram and the lower PSM rate using PSA density, EPE on MRI, and ISUP GG  $\geq$  3. All models are shown in the Supplement Table 2. PSA density provided the best fit and the relationship remained significant: OR 0.18 (CI 0.03, 0.77)  $p = 0.029$ . To support the logistic regression model, a matched model was created (Supplement Table 3). This resulted in a full match with  $n = 32$  (16 intervention, 16 control). In this model, a significantly lower PSM rate remained on the ipsilateral side of the EPE, with an estimated effect of -1.98 (SE 0.87,  $p = 0.024$ ), supporting the effect of the logistic regression model.

### Degree of Nerve-sparing, Performance MRI and Nomogram

Full nerve-sparing was performed in 30% of the control group versus 45% of the intervention group. This was significant in the univariate analysis ( $p = 0.028$ ), but it did not remain significant in the logistic regression model, correcting for the higher ISUP GG ( $p = 0.083$ ) (Supplement Table 4).

The sensitivity and specificity of the MRI in detecting EPE per lobe overall was 50.0% (CI 34.2–65.2) and 84.2% (CI 77.5–89.5). The sensitivity was 60.0% (CI 36.1–80.9) and the specificity was 85.0% (CI 75.3–92.0) in the control group versus 40.9% (CI 20.7–63.7) and 84.2% (CI 73.2–90.8) in the intervention group.

**Table 1:** Baseline characteristics per lobe

	Overall <i>n</i> = 200	Control <i>n</i> = 100	Intervention <i>n</i> = 100	<i>p</i> -value
PSA density ( $\mu\text{g}/\text{ml}^2$ )	0.20 (0.13, 0.38)	0.21 (0.11, 0.40)	0.20 (0.15, 0.34)	0.9
PI-RADS 2.1				0.4
1-2	87 (44%)	42 (42%)	45 (45%)	
3	8 (4%)	6 (6%)	2 (2%)	
4-5	105 (52%)	52 (52%)	53 (53%)	
EPE visible on MRI	46 (23%)	24 (24%)	22 (22%)	0.7
Highest ISUP Grade Group in biopsy				0.041
No biopsy	8 (4%)	0 (0%)	8 (8%)	
Benign	41 (20%)	20 (20%)	21 (21%)	
1	40 (20%)	22 (22%)	18 (18%)	
2	68 (34%)	31 (31%)	37 (37%)	
3	20 (10%)	13 (13%)	7 (7%)	
4	19 (10%)	12 (12%)	7 (7%)	
5	4 (2%)	2 (2%)	2 (2%)	
Degree of nerve sparing preformed				0.006
Minimal	84 (42%)	41 (41%)	43 (43%)	
Partial	41 (20%)	29 (29%)	12 (12%)	
Full	75 (38%)	30 (30%)	45 (45%)	
Histological EPE <i>n</i> (%)	42 (21%)	20 (20%)	22 (22%)	0.7
Positive surgical margin <i>n</i> (%)	55 (28%)	29 (29%)	26 (26%)	0.6

Median (IQR); *n* (%) Wilcoxon rank sum test; Pearson's Chi-squared test; Fisher's exact test

PSA = Prostate Specific Antigen, PI-RADS = Prostate Imaging-Reporting and Data System, EPE = extraprostatic extension, ISUP = International Society of Urologic Pathology

The sensitivity of the nomogram in detecting EPE per lobe in the intervention group with the threshold of 20% was 90.9% (CI 70.8–98.9) and had a specificity of 57.7% (CI 46.0–68.8), the positive predictive value was 37.7% (CI 31.2–44.8) and the negative predictive value was 95.7% (CI 85.6–98.8) A PSM was observed in 38% in the group with a predicted change of  $\geq$  20% versus 13% with less than 20%. There was a management change in 12% of the lobes

due to the use of the nomogram. Of those, eight had a lower degree of nerve-sparing and four had a higher degree. Those with a higher degree of nerve-sparing had no histological EPE or PSM. Of the eight with a lower degree of nerve-sparing, two had a PSM and one histological EPE.

**Table 2:** Baseline characteristics per lobe of the lobes with all histological extraprostatic extension

	Overall <i>n</i> = 42	Control <i>n</i> = 20	Intervention <i>n</i> = 22	<i>p</i> -value
PSA density ( $\mu\text{g}/\text{ml}^2$ )	0.28 (0.17, 0.42)	0.34 (0.19, 0.56)	0.20 (0.17, 0.39)	0.2
PI-RADS 2.1				0.2
1-2	3 (7%)	0 (0%)	3 (14%)	
3	1 (2%)	1 (5%)	0 (0%)	
4-5	38 (90%)	19 (95%)	19 (86%)	
EPE visible on MRI	21 (50%)	12 (60%)	9 (41%)	0.2
ISUP Grade Group $\geq 3$	21 (50%)	12 (60%)	9 (41%)	0.2
Positive Surgical Margin	27 (64%)	17 (85%)	10 (45%)	0.008

*n* (%) Wilcoxon rank sum test; Pearson's Chi-squared test; Fisher's exact test

PSA = Prostate Specific Antigen, PI-RADS = Prostate Imaging-Reporting and Data System, EPE = extraprostatic extension, ISUP = International Society of Urologic Pathology



## Discussion

This study investigated the added value of implementing a nomogram for predicting side-specific EPE. We showed an added clinical value of the nomogram in reducing the PSM on the ipsilateral side of the histological EPE. This is, to our knowledge, the first prospective study conducted to evaluate the clinical impact of a side-specific nomogram for predicting EPE.

Our overall PSM rate per side of 28% is in line with results found in the literature of 33% per side.<sup>5</sup> Likewise, the sensitivity of the MRI is comparable to the results found in the literature of 57% (CI 0.47–0.68)<sup>11</sup> per patients versus our overall of 50% (CI 34.19–65.18) per side. These values make our result more generalisable.

The lower PSM rate on the ipsilateral of the EPE in the intervention group, despite the limited change of management, could also be explained because the surgeon interpreted the results of the nomogram prior to RARP and might, therefore, become better aware of the exact location of the tumour.

Another approach in predicting EPE is the use of artificial intelligence and deep learning models. Hou *et al.*<sup>26</sup> showed an excellent AUC of 0.860 with their artificial intelligent model outperforming the radiologist with an AUC of 0.715. However, this approach is limited due to the use of licensed and complex software, making this nomogram that is free of charge and available online directly useable in daily practice. Furthermore, there is increasing evidence that the PSMA PET/CT information could be valuable in predicting EPE. The systematic review from Woo *et al.*<sup>27</sup> including 12 studies showed a pooled sensitivity of 72% (CI 0.56–0.84) and a specificity of 87% (CI 0.72–0.94). Addition of the PSM PET/CT information to the nomogram could possibly enhance its performance.

A way to omit the need for predicting EPE for guiding nerve-sparing is the neurovascular structure-adjacent frozen-section examination (NeuroSAFE) procedure introduced by Martini Klinik from Hamburg, Germany.<sup>28</sup> It uses frozen section examination to determine if there is a PSM. Although effective in reducing the PSM rate, it leads to a prolonged operation time of at least one hour and, subsequently, more costs.<sup>29</sup> Moreover, the long-term oncological safety and impact on functional outcomes still must be evaluated.

Our study has limitations. Firstly, our hospital was one of the validation cohorts for the nomogram.<sup>13</sup> This may explain the excellent results and may make the results less generalizable. Secondly, the 20% threshold was advised but not binding to the surgeon. Furthermore, we did not correct for surgeon experience, as this would result in small patient

groups. The experience of the surgeon has an impact on achieving trifecta outcomes after RARP.<sup>30</sup> A PSM was found to be correlated with increase in BCR after RARP, one part of the trifecta outcomes.<sup>6</sup> Finally, the result of the nomogram was presented directly before the operation and not used for counselling patients.

This study has multiple strengths. First, several nomograms concerning EPE prediction with the uses of MRI have been recently published<sup>14-17</sup>, but to our knowledge, this is the first study that prospectively evaluates a side-specific nomogram's clinical impact. Secondly, there is a low chance of selection bias because of the consecutive inclusion from patients from the same hospital.

Future directions could be the use of this nomogram for counselling patient for a (unilateral) nerve-sparing approach. Another use for the nomogram could be to select patients for the NeuroSAFE procedure<sup>28</sup> and making it more cost-efficient by only selecting those patients for whom the procedure is beneficial. Furthermore, the step from a side-specific to a lesion-specific approach could result in a better prediction for EPE.

## Conclusions

A side-specific approach toward the prediction of extraprostatic extension using a nomogram result in comparable rates of nerve-sparing but lower rates of positive surgical margins on the side of histological extraprostatic extension. Applying a side-specific nomogram may help counselling patients for nerve-sparing without compromising the oncological outcome.

## References

- 1 Bill-Axelsson A, Holmberg L, Garmo H, Taari K, Busch C, Nordling S *et al.* Radical Prostatectomy or Watchful Waiting in Prostate Cancer - 29-Year Follow-up. *N Engl J Med* 2018; **379**: 2319–2329.
- 2 Holze S, Bräunlich M, Mende M, Arthanareeswaran V-K-A, Neuhaus P, Truss MC *et al.* Age-stratified outcomes after radical prostatectomy in a randomized setting (LAP-01): do younger patients have more to lose? *World J Urol* 2022. doi:10.1007/s00345-022-03945-0.
- 3 Walsh PC. The discovery of the cavernous nerves and development of nerve sparing radical retropubic prostatectomy. *J Urol* 2007; **177**: 1632–1635.
- 4 Nguyen LN, Head L, Witiuk K, Punjani N, Mallick R, Cnossen S *et al.* The Risks and Benefits of Cavernous Neurovascular Bundle Sparing during Radical Prostatectomy: A Systematic Review and Meta-Analysis. *J Urol* 2017; **198**: 760–769.
- 5 Soeterik TFW, van Melick HHE, Dijkman LM, Stomps S, Witjes JA, van Basten JPA. Nerve Sparing during Robot-Assisted Radical Prostatectomy Increases the Risk of Ipsilateral Positive Surgical Margins. *J Urol* 2020; **204**: 91–95.
- 6 Morizane S, Yumioka T, Makishima K, Tsounapi P, Iwamoto H, Hikita K *et al.* Impact of positive surgical margin status in predicting early biochemical recurrence after robot-assisted radical prostatectomy. *Int J Clin Oncol* 2021; **26**: 1961–1967.
- 7 Mottet N, van den Bergh RCN, Briers E, Van den Broeck T, Cumberbatch MG, De Santis M *et al.* EAU-EANM-ESTRO-ESUR-SIOG Guidelines on Prostate Cancer-2020 Update. Part 1: Screening, Diagnosis, and Local Treatment with Curative Intent. *Eur Urol* 2021; **79**: 243–262.
- 8 Ohori M, Kattan MW, Koh H, Maru N, Slawin KM, Shariat S *et al.* Predicting the presence and side of extracapsular extension: a nomogram for staging prostate cancer. *J Urol* 2004; **171**: 1844–1849; discussion 1849.
- 9 Tosoian JJ, Chappidi M, Feng Z, Humphreys EB, Han M, Pavlovich CP *et al.* Prediction of pathological stage based on clinical stage, serum prostate-specific antigen, and biopsy Gleason score: Partin Tables in the contemporary era. *BJU Int* 2017; **119**: 676–683.
- 10 Prostate Cancer Nomograms: Pre-Radical Prostatectomy | Memorial Sloan Kettering Cancer Center. [https://www.mskcc.org/nomograms/prostate/pre\\_op](https://www.mskcc.org/nomograms/prostate/pre_op) (accessed 21 Jan 2022).
- 11 de Rooij M, Hamoen EHJ, Witjes JA, Barentsz JO, Rovers MM. Accuracy of Magnetic Resonance Imaging for Local Staging of Prostate Cancer: A Diagnostic Meta-analysis. *Eur Urol* 2016; **70**: 233–245.
- 12 Sighinolfi MC, Rocco B. Re: EAU Guidelines: Prostate Cancer 2019. *European Urology* 2019; **76**: 871.
- 13 Soeterik TFW, van Melick HHE, Dijkman LM, Küsters-Vandeveldel H, Stomps S, Schoots IG *et al.* Development and External Validation of a Novel Nomogram to Predict Side-specific Extraprostatic Extension in Patients with Prostate Cancer Undergoing Radical Prostatectomy. *Eur Urol Oncol* 2020; : S2588-9311(20)30133–4.
- 14 Martini A, Gupta A, Lewis SC, Kumarasamy S, Haines KG, Briganti A *et al.* Development and internal validation of a side-specific, multiparametric magnetic resonance imaging-based nomogram for the prediction of extracapsular extension of prostate cancer. *BJU Int* 2018; **122**: 1025–1033.
- 15 Diamand R, Ploussard G, Roumiguié M, Oderda M, Benamran D, Fiard G *et al.* External Validation of a Multiparametric Magnetic Resonance Imaging-based Nomogram for the Prediction of Extracapsular Extension and Seminal Vesicle Invasion in Prostate Cancer Patients Undergoing Radical Prostatectomy. *Eur Urol* 2021; **79**: 180–185.

- 16 Nyarangi-Dix J, Wiesenfarth M, Bonekamp D, Hitthaler B, Schütz V, Dieffenbacher S *et al.* Combined Clinical Parameters and Multiparametric Magnetic Resonance Imaging for the Prediction of Extraprostatic Disease-A Risk Model for Patient-tailored Risk Stratification When Planning Radical Prostatectomy. *Eur Urol Focus* 2020; **6**: 1205–1212.
- 17 Wibmer AG, Kattan MW, Alessandrino F, Baur ADJ, Boesen L, Franco FB *et al.* International Multi-Site Initiative to Develop an MRI-Inclusive Nomogram for Side-Specific Prediction of Extraprostatic Extension of Prostate Cancer. *Cancers (Basel)* 2021; **13**: 2627.
- 18 Turkbey B, Rosenkrantz AB, Haider MA, Padhani AR, Villeirs G, Macura KJ *et al.* Prostate Imaging Reporting and Data System Version 2.1: 2019 Update of Prostate Imaging Reporting and Data System Version 2. *Eur Urol* 2019; **76**: 340–351.
- 19 Wegelin O, Exterkate L, van der Leest M, Kummer JA, Vreuls W, de Bruin PC *et al.* The FUTURE Trial: A Multicenter Randomised Controlled Trial on Target Biopsy Techniques Based on Magnetic Resonance Imaging in the Diagnosis of Prostate Cancer in Patients with Prior Negative Biopsies. *Eur Urol* 2019; **75**: 582–590.
- 20 Montorsi F, Wilson TG, Rosen RC, Ahlering TE, Artibani W, Carroll PR *et al.* Best practices in robot-assisted radical prostatectomy: recommendations of the Pasadena Consensus Panel. *Eur Urol* 2012; **62**: 368–381.
- 21 van Leenders GJLH, van der Kwast TH, Grignon DJ, Evans AJ, Kristiansen G, Kweldam CF *et al.* The 2019 International Society of Urological Pathology (ISUP) Consensus Conference on Grading of Prostatic Carcinoma. *Am J Surg Pathol* 2020; **44**: e87–e99.
- 22 Fine SW, Amin MB, Berney DM, Bjartell A, Egevad L, Epstein JI *et al.* A contemporary update on pathology reporting for prostate cancer: biopsy and radical prostatectomy specimens. *Eur Urol* 2012; **62**: 20–39.
- 23 Harris PA, Taylor R, Minor BL, Elliott V, Fernandez M, O'Neal L *et al.* The REDCap consortium: Building an international community of software platform partners. *J Biomed Inform* 2019; **95**: 103208.
- 24 Randolph J, Falbe K, Manuel A, Balloun J. A Step-by-Step Guide to Propensity Score Matching in R. *Practical Assessment, Research, and Evaluation* 2019; **19**. doi:<https://doi.org/10.7275/n3pv-tx27>.
- 25 Zeileis A. Object-Oriented Computation of Sandwich Estimators. *J Stat Soft* 2006; **16**. doi:10.18637/jss.v016.i09.
- 26 Hou Y, Zhang Y-H, Bao J, Bao M-L, Yang G, Shi H-B *et al.* Artificial intelligence is a promising prospect for the detection of prostate cancer extracapsular extension with mpMRI: a two-center comparative study. *Eur J Nucl Med Mol Imaging* 2021; **48**: 3805–3816.
- 27 Woo S, Ghafoor S, Becker AS, Han S, Wibmer AG, Hricak H *et al.* Prostate-specific membrane antigen positron emission tomography (PSMA-PET) for local staging of prostate cancer: a systematic review and meta-analysis. *Eur J Hybrid Imaging* 2020; **4**: 16.
- 28 Schlomm T, Tennstedt P, Huxhold C, Steuber T, Salomon G, Michl U *et al.* Neurovascular structure-adjacent frozen-section examination (NeuroSAFE) increases nerve-sparing frequency and reduces positive surgical margins in open and robot-assisted laparoscopic radical prostatectomy: experience after 11,069 consecutive patients. *Eur Urol* 2012; **62**: 333–340.
- 29 Dinneen E, Haider A, Grierson J, Freeman A, Oxley J, Briggs T *et al.* NeuroSAFE frozen section during robot-assisted radical prostatectomy: peri-operative and histopathological outcomes from the NeuroSAFE PROOF feasibility randomized controlled trial. *BJU Int* 2021; **127**: 676–686.
- 30 Anceschi U, Galfano A, Luciani L, Misuraca L, Albinetti S, Dell'oglio P *et al.* Analysis of predictors of early trifecta achievement after robot-assisted radical prostatectomy for trainers and expert surgeons: the learning curve never ends. *Minerva Urol Nephrol* 2022; **74**: 133–136.

## Supplementary Material

**Supplement Table 1:** Baseline characteristics

	Overall <i>n</i> = 100	Control <i>n</i> = 50	Intervention <i>n</i> = 50	<i>p</i> -value
Age (years)	68.5 (65.0, 72.0)	69.0 (65.0, 73.0)	68.0 (64.3, 72.0)	0.6
BMI (kg/m <sup>2</sup> )	26.1 (24.3, 27.9)	25.8 (24.7, 27.3)	26.4 (24.2, 30.2)	0.3
PSA (µg/ml)	8.8 (6.2, 15.3)	10.5 (6.1, 19.6)	8.1 (6.2, 11.9)	0.2
Prostate volume(ml)	43.7 (31.0, 60.5)	44.5 (33.3, 64.6)	42.7 (31.0, 55.8)	0.5
PSA density(µg/ml <sup>2</sup> )	0.20 (0.13, 0.38)	0.21 (0.11, 0.40)	0.20 (0.15, 0.34)	>0.9
PI-RADS 2.1				0.2
1-2	10 (10%)	7 (14%)	3 (6%)	
3	4 (4%)	3 (6%)	1 (2%)	
4-5	86 (86%)	40 (80%)	46 (92%)	
MRI T-stadium				0.4
T0	10 (10%)	7 (14%)	3 (6%)	
T2	49 (49%)	22 (44%)	27 (54%)	
T3	41 (41%)	21 (42%)	20 (40%)	
T4	0 (0%)	0 (0%)	0 (0%)	
Seminal vesicle invasion on MRI	7 (7.0%)	5 (10%)	2 (4.0%)	0.4
Highest ISUP Group Grade in biopsy				
1	9 (9.0%)	6 (12%)	3 (6.0%)	
2	55 (55%)	24 (48%)	31 (62%)	
3	18 (18%)	10 (20%)	8 (16%)	
4	15 (15%)	9 (18%)	6 (12%)	
5	5 (5.0%)	2 (4.0%)	3 (6.0%)	
PLND Performed	39 (39%)	23 (46%)	16 (32%)	0.2
Histological EPE	37 (37%)	18 (36%)	19 (38%)	0.8
Highest ISUP Grade Group in prostatectomy pathology				
1	3 (3%)	2 (4%)	1 (2%)	
2	56 (56%)	24 (48%)	32 (64%)	
3	28 (28%)	17 (34%)	11 (22%)	
4	8 (8%)	5 (10%)	3 (6%)	
5	5 (5%)	2 (4%)	3 (6%)	
Positive Surgical Margin	55 (28%)	29 (29%)	26 (26%)	0.6

Median (IQR); *n* (%) Wilcoxon rank sum test; Pearson's Chi-squared test; Fisher's exact test  
 BMI = Body Mass Index. PSA = Prostate Specific Antigen, PI-RADS = Prostate Imaging-Reporting and Data System, ISUP = International Society of Urologic Pathology, PLND = Pelvic Lymph Node Dissection, EPE = extraprostatic extension

**Supplement Table 2:** The different logistic regression models built for the effect of the introduction of the nomogram on positive surgical margins on prostate lobes with histological extraprostatic extension

	OR <sup>1</sup>	95% CI	p-value
Model 1			
Control group	-	-	
Intervention group	0.14	0.03, 0.59	0.012
ISUP Grade Group $\geq 3$	0.86	0.20, 5.53	0.8
AIC		53.2	
Model 2			
Intervention group	0.18	0.03, 0.77	0.029
PSA density ( $\mu\text{g}/\text{ml}^2$ )	2.04	0.88, 2,98	0.14
AIC		49.7	
Model 3			
Intervention group	0.16	0.03, 0.64	0.015
EPE on MRI	1.44	0.35, 6.03	0.6
AIC		53.0	
Model 4			
Intervention group	0.17	0.03, 0.75	0.027
PSA density ( $\mu\text{g}/\text{ml}^2$ )	2.34	0.91, 4,11	0.14
ISUP Grade group $\geq 3$	0.75	0.16, 3,28	0.7
AIC		51.6	
Model 5			
Intervention group	0.15	0.03, 0.62	0.015
ISUP Grade Group $\geq 3$	0.75	0.16, 3,30	0.7
EPE on MRI	1.57	0.35, 7,15	0.6
AIC		54.8	
Model 6			
Intervention group	0.18	0.03, 0.77	0.029
PSA density ( $\mu\text{g}/\text{ml}^2$ )	2.08	0.80, 3.30	0.2
EPE on MRI	0.97	0.20, 4,40	>0.90
AIC		51.7	
Model 7			
Intervention group	0.17	0.03, 0.76	0.028
PSA density ( $\mu\text{g}/\text{ml}^2$ )	2.26	0.80, 4,09	0.2
ISUP Grade Group $\geq 3$	0.73	0.14, 3,55	0.7
EPE on MRI	1.09	0.21, 5,56	>0.9
AIC		53.6	

<sup>1</sup> OR = Odds Ratio, CI = Confidence Interval, AIC = Akaike information Criterion, PSA = Prostate Specific Antigen, ISUP = International Society of Urologic Pathology, EPE = extraprostatic extension

**Supplement Table 3:** Matched model using cardinality matching for the effect of the introduction of the nomogram on positive surgical margins on prostate lobes with histological extraprostatic extension

	Overall <i>n</i> = 32	Control <i>n</i> = 16	Intervention <i>n</i> = 16	<i>p</i> -value
PSA density ( $\mu\text{g}/\text{ml}^2$ )	0.32 (0.16, 0.41)	0.28 (0.14, 0.43)	0.32 (0.19, 0.41)	0.9
ISUP Grade Group $\geq 3$	16 (50%)	8 (50%)	8 (50%)	>0.9
EPE on MRI	18 (56%)	9 (56%)	9 (56%)	>0.9
Positive Surgical Margin	19 (59%)	13 (81%)	6 (38%)	0.012

Median (IQR); *n* (%) Wilcoxon rank sum test; Pearson's Chi-squared test; Fisher's exact test

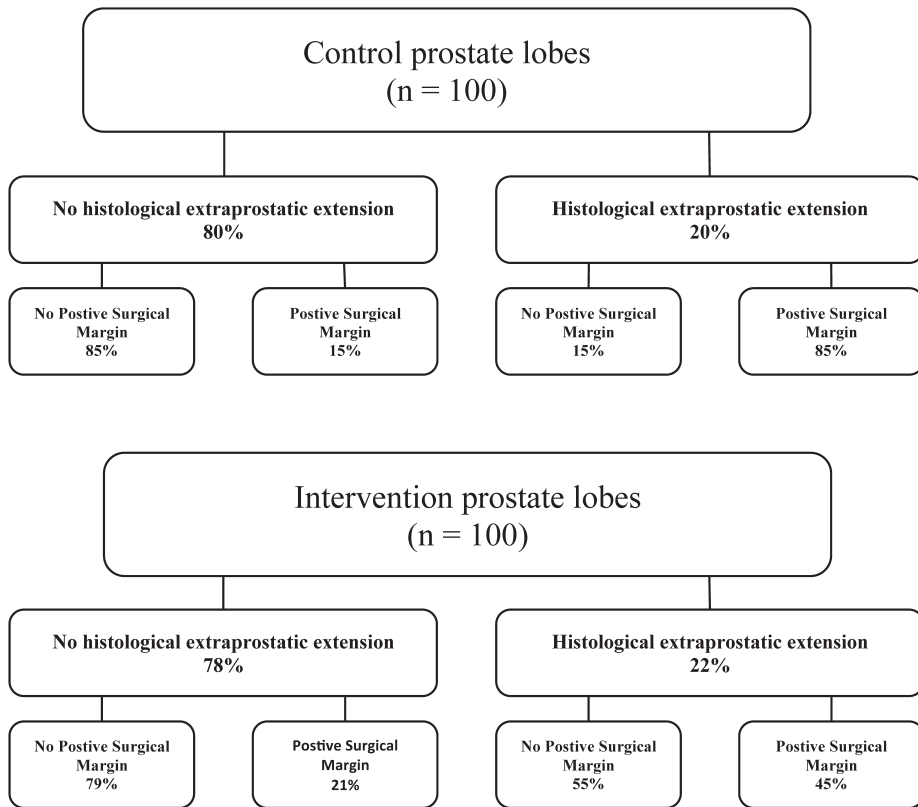
PSA = Prostate Specific Antigen, ISUP = International Society of Urologic Pathology, EPE = extraprostatic extension



**Supplement Table 4:** The different logistic regression models built for the effect of the introduction of the nomogram on full nerve-sparing per prostate lobe

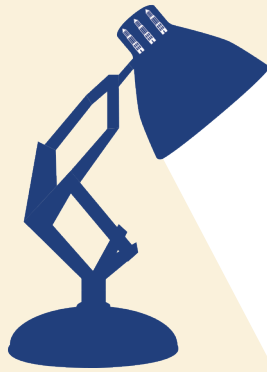
	OR <sup>1</sup>	95% CI	p-value
Model 1			
Control group	-	-	
Intervention group	1.71	1.17, 3.14	0.083
ISUP Grade Group $\geq 3$	0.17	0.06, 0.43	<0.001
AIC		250	
Model 2			
Intervention group	1.92	1.08, 3.47	0.028
PSA density ( $\mu\text{g}/\text{ml}^2$ )	0.93	0.58, 1.30	0.7
AIC		266	
Model 3			
Intervention group	2.01	1.08, 3.77	0.028
EPE on MRI	0.08	0.02, 0.23	<0.001
AIC		236	
Model 4			
Intervention group	1.70	0.93, 3.14	0.085
PSA density ( $\mu\text{g}/\text{ml}^2$ )	1.02	0.65, 1.48	>0.9
ISUP Grade Group $\geq 3$	0.17	0.06, 0.43	<0.001
AIC		252	
Model 5			
Intervention group	1.86	0.99, 3.53	0.054
ISUP Grade Group $\geq 3$	0.30	0.09, 0.79	0.022
EPE on MRI	0.10	0.02, 0.31	<0.001
AIC		232	
Model 6			
Intervention group	2.03	1.09, 3.82	0.026
PSA density ( $\mu\text{g}/\text{ml}^2$ )	0.93	0.62, 1.33	0.7
EPE on MRI	0.08	0.02, 0.23	<0.001
AIC		238	
Model 7			
Intervention group	1.86	0.99, 3.54	0.055
PSA density ( $\mu\text{g}/\text{ml}^2$ )	1.00	0.66, 1.46	>0.9
ISUP Grade Group $\geq 3$	0.30	0.09, 0.80	0.024
EPE on MRI	0.10	0.02, 0.31	<0.001
AIC		234	

<sup>1</sup> OR = Odds Ratio, CI = Confidence Interval, AIC = Akaike information Criterion, PSA = Prostate Specific Antigen, ISUP = International Society of Urologic Pathology, EPE = extraprostatic extension



**Supplement Figure 1:** Distribution of Positive Surgical Margins and histological extraprostatic extension per prostate lobe in the control and the intervention group





# CHAPTER 8

## IS CRIBRIFORM PATTERN IN PROSTATE BIOPSY A RISK FACTOR FOR METASTATIC DISEASE ON $^{68}\text{Ga}$ -PSMA-11 PET/CT?

J.G. Heetman

R. Versteeg

L. Wever

L.J. Paulino Pereira

T.F.W. Soeterik

J. Lavalaye

P.C. de Bruin

R.C.N. van den Bergh

H.H.E. van Melick

## Abstract

*Introduction:* Cribriform growth pattern (CP) in prostate cancer (PCa) has been associated with different unfavourable oncological outcomes. This study addresses if CP in prostate biopsies is an independent risk factor for metastatic disease on PSMA PET/CT.

*Methods:* Treatment-naïve patients with ISUP GG  $\geq 2$  staged with  $^{68}\text{Ga}$ -PSMA-11 PET/CT diagnosed from 2020–2021 were retrospectively enrolled. To test if CP in biopsies was an independent risk factor for metastatic disease on  $^{68}\text{Ga}$ -PSMA PET/CT, regression analyses were performed. Secondary analyses were performed in different subgroups.

*Results:* A total of 401 patients were included. CP was reported in 252 (63%) patients. CP in biopsies was not an independent risk factor for metastatic disease on the  $^{68}\text{Ga}$ -PSMA PET/CT ( $p = 0.14$ ). ISUP Grade Group (GG) 4 ( $p = 0.006$ ), GG 5 ( $p = 0.003$ ), higher PSA level groups per 10 ng/ml until  $> 50$  ( $p$ -value between 0.02 and  $> 0.001$ ) and clinical EPE ( $p > 0.001$ ) were all independent risk factors. In the subgroups with GG 2 ( $n = 99$ ), GG 3 ( $n = 110$ ), intermediate-risk group ( $n = 129$ ) or the high-risk group ( $n = 272$ ), CP in biopsies was also not an independent risk factor for metastatic disease on  $^{68}\text{Ga}$ -PSMA PET/CT. If the EAU guideline recommendation for performing metastatic screening was applied as threshold for PSMA PET/CT imaging, in 9(2%) patients, metastatic disease was missed, and 18% less PSMA PET/CT was performed.

*Conclusion:* This retrospective study found that CP in biopsies was not an independent risk factor for metastatic disease on  $^{68}\text{Ga}$ -PSMA PET/CT.

## Introduction

Cribriform pattern (CP) is one of the four growth patterns of Gleason 4 prostate cancer (PCa). Cribriform or perforated, as in the manner of a sieve, refers to the appearance of a tumour when viewed under a microscope. Presence of this growth pattern is associated with an increased risk of unfavourable oncological outcomes. First, presence of CP in prostatectomy specimens has been associated with an increased risk of metastatic recurrence during follow-up and a shorter time to biochemical recurrence.<sup>1-5</sup> Furthermore, patients with CP have a higher risk of positive lymph nodes at pelvic lymph node dissection.<sup>6</sup> Due to this increased risk, the International Society of Urologic Pathology (ISUP) recommends stating the presence of CP in the pathological report for both prostate biopsies and prostatectomy specimens independent of the ISUP Grade Group (GG).<sup>7,8</sup>

The European Association of Urology (EAU) Guidelines recommend additional metastatic screening for patients with ISUP GG 3 or with high-risk disease.<sup>9</sup> Conventionally, this is done using cross-sectional abdominopelvic imaging and a bone-scan. Prostate-specific membrane antigen positron emission tomography/computed tomography (PSMA-PET/CT) is increasingly used as a staging tool to detect lymph node and distant metastases. The proPSMA trial found that this imaging modality has a superior diagnostic accuracy in comparison to conventional imaging.<sup>10</sup>

In the present study, we assess if CP found in prostate biopsy is independently associated with an increased risk of metastases on PSMA PET/CT.

## Methods

### Data Source and Patient Selection

The study protocol was reviewed by the local ethical board and was registered under W22.013. All treatment-naïve patients with ISUP GG  $\geq 2$  who received a PSMA PET/CT for initial staging in 2020 and 2021 in a single Dutch expert centre for prostate cancer were included in the study. EAU Guidelines recommendations were applied to indicate metastatic screening and were performed to standard by PSMA PET/CT imaging.<sup>9</sup> Because of the expected adverse impact of CP in prostate biopsy tissue, our local protocol recommended that patients with GG 2 should also receive PSMA in case CP was reported in the biopsy tissue. Patients who were treated for PCa before the PSMA PET/CT were excluded. Clinical variables were retrospectively collected.

### Biopsy and Pathological Protocol

Prostate biopsies were performed transperineally or transrectally by experienced urologists. Cognitive targeted biopsies (at least 3 cores per lesion) were taken from suspicious (PI-RADS  $\geq 3$ ) areas on MRI.<sup>11</sup> For systematic biopsies, a volume-dependent approach was applied.

A dedicated uropathologist examined the biopsies according to the prevailing ISUP classification.<sup>7</sup> The presence of CP in biopsy was reported dichotomously as yes/no. The extent of CP was not recorded in detail in the pathological report, which is in accordance with guidelines.

### PSMA PET/CT Protocol

<sup>68</sup>Ga-PSMA-11 was prepared using a GMP-grade <sup>68</sup>Ge/<sup>68</sup>Ga generator and a semi-automated synthesis module (Eckert & Ziegler, Berlin, Germany and ITG, Munich, Germany). The dose of <sup>68</sup>Ga-PSMA was 1.5 MBq/kg. Patients received 10 mg of furosemide at the time of radiotracer injection. PET images were acquired 60 minutes post-injection. Immediately after the PET imaging, a low dose CT was performed. Scans were made using a Biograph mCT40 scanner (Siemens, Erlangen, Germany) or a Gemini ToF 64 slice scanner (Philips, Best, The Netherlands). Image reconstruction and reporting were made according to the prevailing European Association Nuclear Medicine guidelines.<sup>12</sup> Metastatic disease on the PSMA PET/CT was defined as suspicious lesions with PSMA uptake in lymph nodes, bone, or soft tissue, which indicated the presence of prostate cancer metastasis.

### Outcomes and Statistical Testing

Our primary research question was if CP in biopsy is an independent risk factor for metastatic disease on PSMA PET/CT. To address this, two logistic regression analyses with backward selection were performed. The aim of the first analysis was to assess whether CP



had additional value over the main histological predictor ISUP GG for metastatic disease on PSMA PET/CT. The aim of the second analysis was to assess whether CP had additional value over both histological and clinical predictive factors; thereby impacting the indication for performing a PSMA PET. The second analysis included the following covariates: prostate specific antigen (PSA), clinical extra prostatic extension (EPE) and ISUP GG.

As a secondary outcome, the relation between CP in biopsies and metastatic disease on the PSMA PET/CT was analysed in multiple subgroups: ISUP GG 2, 3 and the EAU intermediate risk group.<sup>9</sup> These groups were chosen, because they were the lower limit for an indication for a PSMA PET/CT according to different guidelines. Lastly, EAU high-risk patients were analysed to analyse the value of CP in biopsy in this subgroup.

Data were collected using REDCap hosted at our institution and analysis was performed using R version 4.2.2 (R foundation for Statistical Computing, Vienna, Austria). All tests were two-sided and the significance level was set at  $p < 0.05$ . Missing data for the primary outcome was imputed using the mice package for R. An Akaike Information Criterion (AIC) was provided for all logistic regression analysis.

## Results

### Baseline Characteristics

A total of 401 patients were included in the study. Baseline patient's characteristics are shown in Table 1. In total, 150 patients had metastatic disease on the PSMA PET/CT (37%). These patients were significantly older ( $p < 0.001$ ), had significantly higher PSA levels ( $p < 0.001$ ), and had higher rates of CP present in biopsies ( $p < 0.001$ ). Furthermore, the patients who had metastatic disease on the PSMA PET/CT had higher rates of clinical EPE, 46 (22%) versus 82 (55%) ( $p < 0.001$ ). Additionally, there were more patients without MRI information in the group with metastatic disease on the PSMA PET/CT, 52 (35%) versus 14 (6%). Lastly, there was a significant difference in biopsy strategy and ISUP GG between the two groups. In the group with metastatic disease on PSMA PET/CT, more patients were diagnosed with PCa using only systematic biopsies ( $p < 0.001$ ).

The PSMA PET/CT results of the patients with or without CP per ISUP GG are shown in Figure 1; PSA level and clinical T-stage stratification are shown in supplement Figure 1. In both figures, the univariate significant relation between the variables and metastatic disease on the PSMA PET/CT is visualized.

### Cribiform Pattern

In the first logistic regression analysis, ISUP GG as the only covariable was performed. The relation between CP and metastatic disease on PSMA PET/CT remained significant ( $p = 0.001$ ) (Table 2). In the second regression analysis, clinical EPE and PSA level groups were added as covariables resulting in CP no longer being an independent risk factor for metastatic disease on PSMA PET/CT ( $p = 0.14$ ). In this analysis, ISUP GG 4 ( $p = 0.006$ ), ISUP GG 5 ( $p = 0.003$ ), higher PSA level groups ( $p$ -value between 0.02 and  $> 0.001$ ) and clinical EPE ( $p > 0.001$ ) were all independent risk factors.

### Subgroup Analyses

Among the 129 (32%) patients in the EAU intermediate-risk group, 19 (15%) had metastatic disease on the PSMA PET/CT. Twelve (63%) of these patients had CP compared to 66 (60%) in the group without metastatic disease on the PSMA PET/CT ( $p > 0.9$ ). Of 99 patients with ISUP GG 2, 19 (19%) had metastatic disease on PSMA PET/CT. Eleven (58%) of these had CP, compared to 46 (57%) of the 80 patients without metastatic disease on PSMA PET/CT ( $p > 0.9$ ). Of the 110 patients with a ISUP GG 3, 35 (32%) had metastatic disease on the PSMA PET/CT. Of these patients, 26 (74%) had CP, and of the patients without metastatic disease on the PSMA PET/CT, 43 (57%) had CP ( $p = 0.10$ ).

**Table 1:** Baseline characteristics

	Overall (n = 401)	PSMA PET/CT no metastatic disease (n = 251)	PSMA PET/CT metastatic disease (n = 150)	p-value
Cribriform pattern	252 (63%)	142 (57%)	110 (73%)	<0.001
Age (years)	72 (67, 75 IQR)	71 (66, 75 IQR)	73 (68, 77 IQR)	0.007
PSA (ng/ml)	12.7 (7.2, 25.0 IQR)	9.5 (6.0, 16.3IQR)	25.1 (11.8, 58.3 IQR)	<0.001
Clinical T stadium				<0.001
cT1	140 (35%)	123 (49%)	17 (11%)	
cT2	123 (31%)	74 (29%)	49 (33%)	
cT3	111 (28%)	46 (18%)	65 (43%)	
cT4	17 (4%)	0 (0%)	17 (11%)	
Unknown	10 (3%)	8 (3%)	2(1%)	
MRI T stadium				<0.001
rT0	18 (5%)	15 (6%)	3 (3%)	
rT2	145 (43%)	125 (53%)	20 (20%)	
rT3	160 (48%)	97 (41%)	63 (63%)	
rT4	12 (4%)	0 (0%)	12 (12%)	
Unknown	66	14	52	
Biopsy strategy				<0.001
Systematic only	146 (36%)	55 (22%)	90 (60%)	
Targeted only	46 (11%)	38 (15%)	8 (5%)	
Systematic + Targeted	210 (52%)	158(63%)	52 (35%)	
ISUP Grade Group				<0.001
2	99 (25%)	80 (32%)	19 (13%)	
3	110 (27%)	75 (30%)	35 (23%)	
4	142 (35%)	74 (29%)	68 (45%)	
5	50 (12%)	22 (9%)	28 (19%)	
EAU risk group				<0.001
High	272 (68%)	141 (56%)	131 (87%)	
Intermediate	129 (32%)	110 (44%)	19 (12%)	
PSMA mi Stage				
miN0	251 (63%)	251 (100%)	-	
miN1	47 (12%)	-	47 (31%)	
miM1a	18 (5%)	-	18 (12%)	
miM1b	75 (19%)	-	75 (50%)	
miM1c	10 (2%)	-	10 (7%)	

Median (IQR)= Inter quantile range; n (%) Wilcoxon -rank sum test; Pearson's Chi-squared test; Fisher's exact test

PSMA PET/CT = Prostate-specific Membrane Antigen Positron Emission Tomography Computed Tomography. PSA = Prostate Specific Antigen, ISUP = International Society of Urologic Pathology, MRI= Magnetic Resonance Imaging

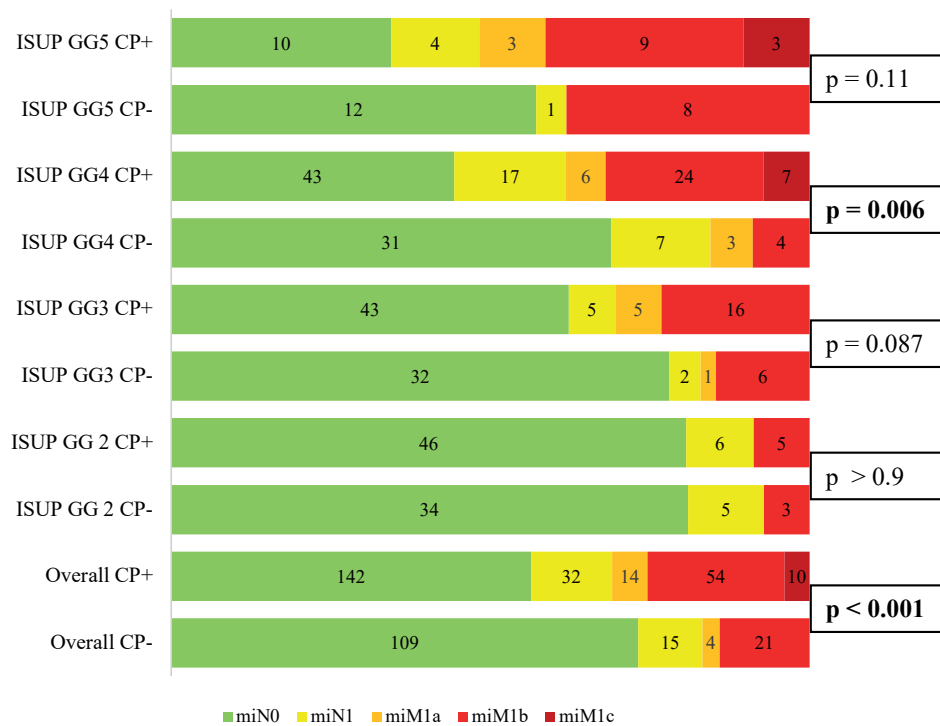


**Figure 1:** Distribution of PSMAPET/CT results per ISUP Grade Group with and without cribriform pattern (CP),  $p$ -values calculated using Pearson's Chi-squared test between

Of the 272 patients with high-risk disease, 131 (48%) had metastatic disease on the PSMA PET/CT. Of those patients, 98 (75%) had CP in biopsy versus 76 (54%) in the patients without metastatic disease on the PSMA PET/CT, and this was significant in the univariable logistic regression ( $p < 0.001$ ). This did not remain significant in the multivariable logistic regression analysis including ISUP GG, PSA and clinical EPE ( $p = 0.2$ ).

If the EAU high-risk or ISUP GG 3 had been applied as the threshold for a PSMA PET/CT instead of the full cohort in this cohort as recommended by the EAU guidelines, metastatic disease on PSMA PET/CT would have been missed in nine (2%) patients and would have led to a reduction of 74 (18%) patients indicated for PSMA PET/CT.

**Table 2:** Regression analysis for the relation of the variables and metastatic disease on the PSMA PET/CT

	Regression analysis 1		Regression analysis 2	
	OR (CI95%)	<i>p</i> -value	OR (CI95%)	<i>p</i> -value
Cribriform pattern				
No	reference	-	reference	-
Yes	2.11 (1.34, 3.36)	0.001	1.47 (0.89, 2.47)	0.14
ISUP Grade Group				
2	reference	-	reference	-
3	1.92 (1.01, 3.73)	0.048	1.23 (0.59, 2.58)	0.6
4	3.70 (2.05, 6.92)	<0.001	2.59 (1.32, 5.22)	0.006
5	5.61 (2.65, 12.2)	<0.001	3.66 (1.58, 8.69)	0.003
Clinical EPE				
No			reference	-
Yes			2.90 (1.73,4.89)	<0.001
PSA (ng/ml)				
0-10			reference	-
10-20			2.21 (1.22, 4.02)	0.011
20-30			3.02 (1.34, 6.77)	0.005
30-40			3.29 (1.28, 8.66)	0.02
40-50			13.0 (3.14, 65.8)	<0.001
50+			12.2 (5.32, 30.6)	<0.001
	AIC 499		AIC 427	

ISUP = International Society of Urologic Pathology, PSA = Prostate Specific Antigen, EPE = extraprostatic extension, AIC = Akaike information Criterion

## Discussion

The present study assesses if CP in prostate biopsy is an independent risk factor for metastatic disease on PSMA PET/CT. We found that CP in biopsy was not an independent risk factor. Furthermore, CP was not a significant risk factor for metastatic disease on PSMA PET/CT in subgroup analyses: neither in the intermediate- or high-risk group, nor in subgroups with ISUP GG 2 or 3. When a threshold of high-risk disease or ISUP GG3 was applied in conformance to the EAU guideline, nine (2%) of the patients with metastatic disease on PSMA PET/CT were missed, and this resulted in a 18% reduction in the number of PSMA PET/CT performed in our cohort. In clinical practice, the indication to perform PSMA-PET/CT does not differ between men with or without CP in their prostate biopsy. To our knowledge, this is the first study addressing the relation of CP in biopsies with metastatic disease on PSMA PET/CT.

The present results are inconsistent with those reported in literature on the relation of CP in prostatectomy specimens with metastatic recurrence.<sup>1-5</sup> Contrary to our results, Downes *et al.* found that CP in biopsy was a strong predictor for lymph node metastasis at prostatectomy.<sup>6</sup> This could be due to small metastatic lymph nodes being missed by the PSMA PET/CT as a result of the partial-volume effect.<sup>13</sup>

Detection of intraprostatic lesions with CP using the combination of MRI and targeted biopsy is challenging. Cai *et al.* found that MRI visualized nearly all intraprostatic lesions with CP (96%). However, only 55% were detected by targeted biopsy when compared to prostatectomy specimen.<sup>14</sup> In contrast, Truong *et al.* found that intraprostatic lesions with CP had a significantly lower visibility on MRI (36%) when compared to other growth patterns of Gleason 4 (83%).<sup>15</sup> Both groups comprised of a small number of intraprostatic lesions with CP; therefore, no strong conclusions can be drawn. As a result, the diagnostic pathway with MRI and targeted biopsy could possibly result in missed CP lesions and incorrect patient selection for active surveillance strategy.<sup>16</sup> To predict the chance of CP, Goa *et al.* developed a nomogram using MRI variables with a 79.2% sensitivity.<sup>17</sup> Furthermore, the activity on a PSMA PET/CT may be more accurate in detecting intraprostatic lesions with CP than MRI.<sup>18</sup> This could mean that a prebiopsy PSMA PET/CT could be of additional value in the detection of lesions with CP.

Another challenge in the detection of CP is the high interobserver variability among pathologists.<sup>19</sup> To counter this problem and aid pathologists, an artificial intelligence software was developed for automatic detection of CP.<sup>20</sup> This software showed potential additional value; however, it has not yet been applied to patients.

Selecting patients for additional imaging for the screening of metastatic disease remains challenging. In our cohort, CP did not provide additional predictive information for selecting patients for screening of metastatic disease. A different approach to applying risk group stratification for the selection of patients for additional imaging is to use nomograms that predict lymph node invasion.<sup>21,22</sup> These nomograms could help select patients in the intermediate-risk group for additional imaging. Adding the presence of CP/IDC in biopsy to these nomograms did not improve the lymph node invasion prediction underlining our current study's finding of a lack of predictive value of CP.<sup>23</sup>

The present study had some limitations. First, a retrospective study design was used. Second, a large number of patients had no MRI information available; therefore, this information could not be included in the analysis. Third, due to a difference in biopsy protocols, not all patients received targeted biopsy, possibly resulting in missed lesions with a higher ISUP GG or CP. Fourth, no central pathology review was performed. Fifth, not all patients who were suspected of having metastatic disease received a PSMA PET/CT. Some patients with exceptional high PSA or symptomatic metastatic disease received conventional imaging outside of our centre's standard of care. These patients were not included in the analysis. Finally, the poor sensitivity of prostate needle biopsy in detecting CP was a limitation to our hypothesis. Ericson *et al.* and Downes *et al.* found a sensitivity of 56.3% and 43.8% respectively, of biopsy for detecting CP and/or intraductal carcinoma (IDC) in prostatectomy specimens and a significantly higher specificity of 87.2% and 95%, respectively.<sup>6,24</sup> Likewise, Van der Slot *et al.* found a poor sensitivity of 45.1% and a higher specificity of 92.6% of biopsy for detecting CP/IDC in prostatectomy specimens in patients with a ISUP GG2 in biopsy.<sup>25</sup>

The present study also has some strengths. This is the first known study assessing if presence of CP in biopsies is a risk factor for metastatic disease on a PSMA PET/CT. Furthermore, the study used real data from the largest teaching hospital in The Netherlands with extensive experience in PSMA PET/CT.

Future research should focus on factors that identify patients who are most at risk of metastases to individualize indication for additional imaging. In our cohort of 401 patients, CP was not an independent risk factor for metastatic disease on the PSMA PET/CT. This could be as a result of low sensitivity of biopsies to detect CP. Moving forward, a future study could address the relationship between CP in radical prostatectomy specimens and metastatic disease on the PSMA PET/CT. Alternatively, a study may be conducted on the increase in sensitivity for detection of CP in biopsies with a prebiopsy PSMA PET/CT. Furthermore, the relation of IDC in biopsies on metastatic disease on PSMA PET/CT could be clarified. IDC, as well as CP, has an increased risk of metastatic disease.<sup>26</sup>

## Conclusion

This single-centre retrospective study found that presence of CP in biopsies is not an independent risk factor for lymph node or distant metastatic disease, as visualized on the PSMA PET/CT. Consequently, in retrospect, the presence of CP did not warrant adapting additional imaging indications in this cohort.

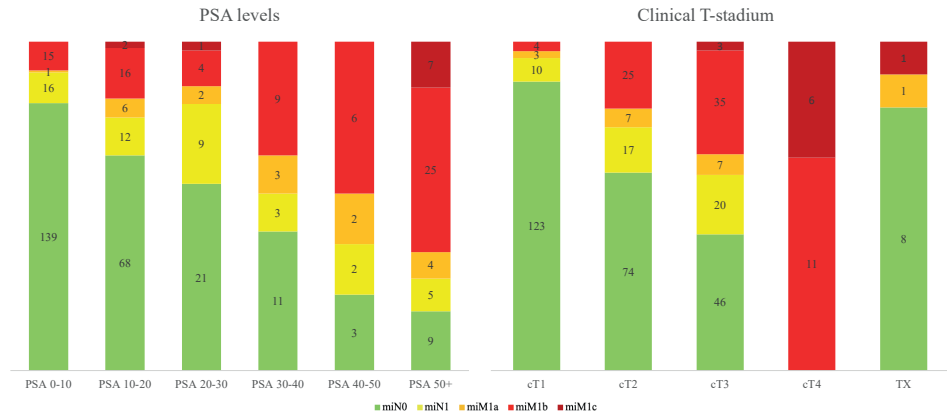


## References

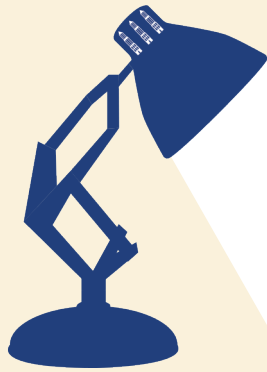
- 1 Kweldam CF, Wildhagen MF, Steyerberg EW, Bangma CH, van der Kwast TH, van Leenders GJLH. Cribriform growth is highly predictive for postoperative metastasis and disease-specific death in Gleason score 7 prostate cancer. *Mod Pathol* 2015; **28**: 457–464.
- 2 Dong F, Yang P, Wang C, Wu S, Xiao Y, McDougal WS *et al*. Architectural heterogeneity and cribriform pattern predict adverse clinical outcome for Gleason grade 4 prostatic adenocarcinoma. *Am J Surg Pathol* 2013; **37**: 1855–1861.
- 3 Hollemans E, Verhoef EI, Bangma CH, Rietbergen J, Roobol MJ, Helleman J *et al*. Clinical outcome comparison of Grade Group 1 and Grade Group 2 prostate cancer with and without cribriform architecture at the time of radical prostatectomy. *Histopathology* 2020; **76**: 755–762.
- 4 Hollemans E, Verhoef EI, Bangma CH, Rietbergen J, Osanto S, Pelger RCM *et al*. Cribriform architecture in radical prostatectomies predicts oncological outcome in Gleason score 8 prostate cancer patients. *Mod Pathol* 2021; **34**: 184–193.
- 5 Remmers S, Hollemans E, Nieboer D, Luiting HB, van Leenders GJLH, Helleman J *et al*. Improving the prediction of biochemical recurrence after radical prostatectomy with the addition of detailed pathology of the positive surgical margin and cribriform growth. *Ann Diagn Pathol* 2022; **56**: 151842.
- 6 Downes MR, Xu B, van der Kwast TH. Cribriform architecture prostatic adenocarcinoma in needle biopsies is a strong independent predictor for lymph node metastases in radical prostatectomy. *Eur J Cancer* 2021; **148**: 432–439.
- 7 van Leenders GJLH, van der Kwast TH, Grignon DJ, Evans AJ, Kristiansen G, Kweldam CF *et al*. The 2019 International Society of Urological Pathology (ISUP) Consensus Conference on Grading of Prostatic Carcinoma. *Am J Surg Pathol* 2020; **44**: e87–e99.
- 8 van der Kwast TH, van Leenders GJ, Berney DM, Delahunt B, Evans AJ, Iczkowski KA *et al*. ISUP Consensus Definition of Cribriform Pattern Prostate Cancer. *Am J Surg Pathol* 2021; **45**: 1118–1126.
- 9 Mottet N, van den Bergh RCN, Briers E, Van den Broeck T, Cumberbatch MG, De Santis M *et al*. EAU-EANM-ESTRO-ESUR-SIOG Guidelines on Prostate Cancer-2020 Update. Part 1: Screening, Diagnosis, and Local Treatment with Curative Intent. *Eur Urol* 2021; **79**: 243–262.
- 10 Hofman MS, Lawrentschuk N, Francis RJ, Tang C, Vela I, Thomas P *et al*. Prostate-specific membrane antigen PET-CT in patients with high-risk prostate cancer before curative-intent surgery or radiotherapy (proPSMA): a prospective, randomised, multicentre study. *Lancet* 2020; **395**: 1208–1216.
- 11 Wegelin O, Exterkate L, van der Leest M, Kummer JA, Vreuls W, de Bruin PC *et al*. The FUTURE Trial: A Multicenter Randomised Controlled Trial on Target Biopsy Techniques Based on Magnetic Resonance Imaging in the Diagnosis of Prostate Cancer in Patients with Prior Negative Biopsies. *Eur Urol* 2019; **75**: 582–590.
- 12 Ceci F, Oprea-Lager DE, Emmett L, Adam JA, Bomanji J, Czernin J *et al*. E-PSMA: the EANM standardized reporting guidelines v1.0 for PSMA-PET. *Eur J Nucl Med Mol Imaging* 2021; **48**: 1626–1638.
- 13 Soret M, Bacharach SL, Buvat I. Partial-volume effect in PET tumor imaging. *J Nucl Med* 2007; **48**: 932–945.
- 14 Cai Q, Costa DN, Metter CK, Goldberg K, Roehrborn CG, Cadeddu J *et al*. Sensitivity of multiparametric MRI and targeted biopsy for detection of adverse pathologies (Cribriform gleason pattern 4 and intraductal carcinoma): Correlation of detected and missed prostate cancer foci with whole mount histopathology. *Urol Oncol* 2022; **40**: 452.e1–452.e8.

- 15 Truong M, Hollenberg G, Weinberg E, Messing EM, Miyamoto H, Frye TP. Impact of Gleason Subtype on Prostate Cancer Detection Using Multiparametric Magnetic Resonance Imaging: Correlation with Final Histopathology. *J Urol* 2017; **198**: 316–321.
- 16 Bernardino RM, Carvalho R, Severo L, Alves M, Papoila AL, Pinheiro LC. Prostate cancer with cribriform pattern: Exclusion criterion for active surveillance? *Arch Ital Urol Androl* 2020; **92**. doi:10.4081/aiua.2020.3.235.
- 17 Gao J, Zhang Q, Fu Y, Wang W, Zhang C, Kan Y *et al*. Combined clinical characteristics and multiparametric MRI parameters for prediction of cribriform morphology in intermediate-risk prostate cancer patients. *Urol Oncol* 2020; **38**: 216–224.
- 18 Gao J, Zhang C, Zhang Q, Fu Y, Zhao X, Chen M *et al*. Diagnostic performance of 68Ga-PSMA PET/CT for identification of aggressive cribriform morphology in prostate cancer with whole-mount sections. *Eur J Nucl Med Mol Imaging* 2019; **46**: 1531–1541.
- 19 Kweldam CF, Nieboer D, Algaba F, Amin MB, Berney DM, Billis A *et al*. Gleason grade 4 prostate adenocarcinoma patterns: an interobserver agreement study among genitourinary pathologists. *Histopathology* 2016; **69**: 441–449.
- 20 Ambrosini P, Hollemans E, Kweldam CF, Leenders GJLH van, Stallinga S, Vos F. Automated detection of cribriform growth patterns in prostate histology images. *Sci Rep* 2020; **10**: 14904.
- 21 Prostate Cancer Nomograms: Dynamic Prostate Cancer Nomogram: Coefficients | Memorial Sloan Kettering Cancer Center. [https://www.mskcc.org/nomograms/prostate/pre\\_op/coefficients](https://www.mskcc.org/nomograms/prostate/pre_op/coefficients) (accessed 22 Jul2022).
- 22 Briganti A, Larcher A, Abdollah F, Capitanio U, Gallina A, Suardi N *et al*. Updated Nomogram Predicting Lymph Node Invasion in Patients with Prostate Cancer Undergoing Extended Pelvic Lymph Node Dissection: The Essential Importance of Percentage of Positive Cores. *European Urology* 2012; **61**: 480–487.
- 23 de Barros HA, Remmers S, Luiting HB, van Leenders GJLH, Roobol MJ, Bekers EM *et al*. Predictive value of Cribriform and Intraductal Carcinoma for the Nomogram-Based Selection of Prostate Cancer Patients for Pelvic Lymph Node Dissection. *Urology* 2022; : S0090-4295(22)00537–4.
- 24 Ericson KJ, Wu SS, Lundy SD, Thomas LJ, Klein EA, McKenney JK. Diagnostic Accuracy of Prostate Biopsy for Detecting Cribriform Gleason Pattern 4 Carcinoma and Intraductal Carcinoma in Paired Radical Prostatectomy Specimens: Implications for Active Surveillance. *J Urol* 2020; **203**: 311–319.
- 25 van der Slot MA, Seyrek N, Kweldam CF, den Bakker MA, Busstra MB, Gan M *et al*. Percentage Gleason pattern 4 and PI-RADS score predict upgrading in biopsy Grade Group 2 prostate cancer patients without cribriform pattern. *World J Urol* 2022; **40**: 2723–2729.
- 26 Pantazopoulos H, Diop M-K, Grosset A-A, Rouleau-Gagné F, Al-Saleh A, Boblea T *et al*. Intraductal Carcinoma of the Prostate as a Cause of Prostate Cancer Metastasis: A Molecular Portrait. *Cancers (Basel)* 2022; **14**: 820.

## Supplementary Material



**Supplement Figure 2:** Distribution of PSMA PET/CT results per PSA level clinical T-stage



# CHAPTER 9

GENERAL SUMMARY



## General Summary

Prostate cancer (PCa) represents a common malignancy characterized by a significant discrepancy between incidence and mortality rates. This variance indicates that not all forms of PCa significantly affect life expectancy, as the disease spectrum ranges from indolent to aggressive forms. Accurate detection and staging of PCa are essential for providing patients with optimal treatment strategies, aimed at enhancing both life expectancy and quality of life while minimizing unnecessary diagnoses and treatments. The integration of advanced imaging techniques in the diagnosis and staging of PCa has significantly improved the precision of detecting and staging clinically significant (cs)PCa. This thesis explores new developments in this rapidly evolving field of research.

### Part I: The Detection of Clinically Significant Prostate Cancer

The findings in the **Part I** of this thesis add to the growing body of evidence supporting the role of local gland Prostate Specific Membrane Antigen (PSMA) activity in the detection and characterisation of prostate cancer (PCa).

In **Chapter 2** the efficacy of the  $^{18}\text{F}$ -PSMA-1007 tracer for characterizing intraprostatic PCa, significant correlations were observed between the maximum standardised uptake value (SUVmax) on PET/CT scans and the International Society of Urologic Pathology (ISUP) Grade Group (GG) and the PSMA Immune Reactive Score on histology. This relationship was found to be independent of tumour length. Furthermore, the study affirmed that the risk of missing clinically significant PCa (csPCa) due to the partial-volume effect was not applicable in this cohort, as all csPCa lesions were significantly larger than the voxel size used. Interestingly, when applying a SUVmax threshold of 4, only one csPCa lesion fell below this threshold. Limitations of this study include the inclusion of no low-risk patients, the evaluations of only histological confirmed tumours and the localisation with low-dose CT.

In the evaluation of the added value of the SUVmax of the PSMA PET/CT in predicting ISUP GG  $\geq 2$  and  $\geq 3$  on prostate biopsy in **Chapter 3**, the study demonstrated that SUVmax significantly enhances the predictive capability of both models, especially for GG  $\geq 3$ . This highlights the utility of SUVmax in identifying patients with a high likelihood of harbouring GG  $\geq 3$  PCa. Our findings suggest that a high SUVmax could potential help select patients with a substantial risk of csPCa. The foremost limitations of this study were that the PSMA PET/CT took place after diagnosis, and no patients without the diagnosis PCa were included.

In **Chapter 4** the of adding PSMA PET/CT and targeted biopsy in patient recently started with active surveillance (AS) after MRI at diagnosis revealed that the number needed to scan (NNS) to detect biopsy upgrading was 11. Upgrading was more frequent in patients

with negative MRI findings. Our results suggest that PSMA PET/CT might correct for a portion of understaging noted in traditional MRI and biopsy approaches. A limitation of this study was that not all patients received re-biopsy, but only the patient with a suspected lesions deemed not covered by previous biopsy on PSMA PET/CT.

In **Chapter 5**, the potential treatment for suspected PCa without histological confirmation is discussed, due to the advent of PSMA PET/CT. In our cohort of 451 patients all 74 patients with a SUVmax greater than 16 had csPCa. Additionally, of the 185 patients with a PI-RADS score greater than 4 and an SUVmax over 8, 98% had csPCa. These findings suggest that a diagnostic pathway where patients receive a prostatectomy without biopsy when clinical characteristics and imaging strongly indicated csPCa could be possibility in the future. However, it is crucial to recognize that a biopsy can provide information beyond the ISUP GG, including specific tumour characteristics, the necessity for DNA testing, and essential data for planning radical or focal surgery.

## **Part II: The adequate Staging of Prostate Cancer**

In **Part II** of this thesis explored the challenges in the staging of PCa, highlighting the importance of effectively utilizing available imaging modalities for accurate staging and their strategic implementation in clinical settings.

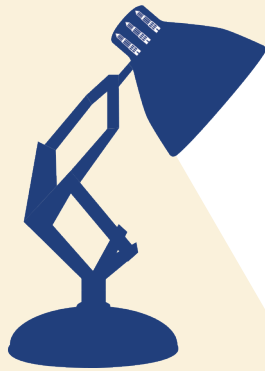
In **Chapter 6**, our focus was on the external validation of four MRI-based nomograms—Soeterik, Martini, Nyarangi-Dix, and Wibmer—for predicting side-specific extraprostatic extension (EPE) in a large European dataset. These nomograms exhibited fair discriminative abilities, with Area Under the Curve (AUC) values ranging from 72% to 75%. For risk thresholds from 0 to 40%, the Soeterik, Martini, and Nyarangi-Dix nomograms showed fair to good calibration. However, the Wibmer nomogram significantly overestimated the EPE risk for thresholds above 25%. Decision Curve Analysis (DCA) indicated the clinical utility of the Soeterik, Martini, and Nyarangi-Dix nomograms for risk thresholds between 8% and 40%. The Nyarangi-Dix nomogram, incorporating robust MRI predictors like tumour capsular contact length and the European Society of Urogenital Radiology score, displayed superior performance. Yet, the additional time required for documenting these variables and their general absence in routine clinical care may limit the nomogram's practicality. The retrospective study presented in **Chapter 6** faced limitations, including potential information bias due to retrospective design and no central MRI review.

**Chapter 7** detailed the implementation of the Soeterik nomogram in 50 patients, demonstrating its clinical value in reducing positive surgical margins (PSM) on the ipsilateral side of histological EPE. Despite no significant management changes in nerve-sparing techniques, this outcome could be due to increased surgeon awareness of tumour



location, as informed by the nomogram. Notably, the surgeons' experience, impacting outcomes after robot-assisted radical prostatectomy (RARP), was not factored into the study. An additional limitation is that the advised 20% threshold for the nomogram was not strictly adhered to by the surgeons.

In **Chapter 8**, we explored whether the presence of cribriform pattern (CP) in prostate biopsy is an independent risk factor for metastatic disease on PSMA PET/CT. Our investigation concluded that CP in biopsy was not an independent risk factor. Additionally, CP did not emerge as a significant risk factor in various subgroup analyses. These included intermediate- or high-risk groups, nor in subgroups with ISUP GG 2 or 3. When a threshold of high-risk disease or ISUP GG 3 was applied, conforming to the European Association of Urology guideline, 2% of the patients with metastatic disease on PSMA PET/CT were missed. This led to an 18% reduction in the number of PSMA PET/CT performed in our cohort.



# CHAPTER 10

GENERAL DISCUSSION  
AND FUTURE PERSPECTIVES



## General Discussion and Future Perspectives

This thesis presents novel insights into the diagnosis, staging and treatment planning of prostate cancer (PCa), highlighting the expanding role of imaging and its optimal implementation. The studies address the additional value of Prostate-specific Membrane Antigen/Positron Emission Tomography/Computed Tomography (PSMA PET/CT) in the detection and treatment selection of PCa, the validation and implementation of Magnetic Resonance Imaging (MRI) based nomograms for PCa staging, and the selection of patients for staging PSMA PET/CT using cribriform pattern (CP) in prostate needle biopsy. As is often the case in the realm of research, the thesis' findings have opened new opportunities for inquiry and future directions for study, more so than at the inception of this thesis.

### Utilising PSMA PET/CT for Clinically Significant Prostate Cancer Detection

Imaging of the prostate fulfils multiple roles, one of which is to assist in identifying candidates for prostate biopsy and to guide the biopsy procedure, thereby ensuring the collection of dependable pathological information. Furthermore, imaging provides prognostic insights and helps identify local tumour characteristics that influence treatment decisions, such as the risk of extraprostatic extension (EPE). The European guidelines recommend using MRI to aid the biopsy decision and strategy.<sup>1</sup> While intended for staging in men with confirmed prostate cancer, PSMA PET/CT can also be applied before diagnosis. Although any added imaging modality to the standard pathway inherently contributes additional information, its value also depends on efficiency and cost-effectiveness, as reflected by metrics like the number needed to scan (NNS).

In **Chapter 2**, the efficacy of the <sup>18</sup>F-PSMA-1007 tracer for characterising intraprostatic prostate cancer (PCa) was highlighted. A significant correlation was observed between the maximum standardised uptake value (SUVmax) on PET/CT scans and the International Society of Urologic Pathology (ISUP) Grade Group (GG), as well as the PSMA Immune Reactive Score on histology. This correlation was independent of tumour length, which was consistent with Woythal *et al.*'s findings using the <sup>68</sup>Ga-PSMA-HBED-CC tracer.<sup>2</sup> Notably, the study demonstrated that clinically significant PCa (csPCa) was reliably detected, with only one csPCa lesion below the SUVmax threshold of 4. This suggests a potential threshold that warrants further research.

**Chapter 4** focused on applying pre-biopsy PSMA PET/CT in patients starting active surveillance (AS). It was found that the NNS to detect biopsy upgrading was 11, with upgrades more common in patients with negative MRI findings. This suggests that PSMA PET/CT might reduce understaging in traditional MRI and biopsy methods. The 9% upgrading rate should be compared against the 17% post-prostatectomy upgrading after MRI and biopsy diagnosis.<sup>3</sup> However, a follow up of this group is needed to determine the effect on long-term oncological outcomes.

**Chapters 2** and **4** collectively highlight the potential of PSMA PET/CT in detecting intraprostatic PCa and its added value for candidates of an AS, who received a pre-biopsy MRI at initial diagnosis. The systematic review and meta-analysis by Kawada *et al.*, which included five prospective studies involving 497 participants, concluded that PSMA PET/CT, when combined with targeted biopsy, demonstrates favourable diagnostic accuracy for the detection of clinically significant prostate cancer (csPCa).<sup>4</sup> The pooled sensitivity, specificity, positive predictive value (PPV), and negative predictive value (NPV) were 0.89 (95% confidence interval [CI]: 0.85–0.93), 0.56 (95% CI: 0.29–0.80), 0.69 (95% CI: 0.58–0.79), and 0.78 (95% CI: 0.50–0.93), respectively. Moreover, this accuracy appears to be enhanced when PSMA PET/CT is combined with MRI; the pooled sensitivity, specificity, PPV, and NPV for csPCa detection were 0.91 (95% CI: 0.77–0.97), 0.64 (95% CI: 0.40–0.82), 0.75 (95% CI: 0.56–0.87), and 0.85 (95% CI: 0.62–0.95), respectively. They also noted that PSMA PET/CT has particularly promising clinical applications in patients with equivocal MRI results (Prostate Imaging-Reporting and Data System [PI-RADS] 3), where the sensitivity, specificity, PPV, and NPV were 0.69, 0.73, 0.48, and 0.86, respectively. However, in the PASPoRT cohort presented in **Chapter 4**, none of the patients who experienced upgrading at PSMA targeted biopsy had a PI-RADS 3 at MRI. A study by Goa *et al.* suggests that PSMA PET/CT may surpass MRI in accurately detecting CP lesions.<sup>5</sup> In this context, the average apparent diffusion coefficient (ADC<sub>mean</sub>) and the tenth percentile ADC (ADC<sub>10%</sub>) measurements from MRI did not show a significant difference between non-CP lesions and CP lesions ( $p > 0.05$ ). Conversely, a higher SUV<sub>max</sub> was significantly different between non-CP and CP lesions ( $p > 0.001$ ). Notably, within the PASPoRT cohort, one patient who did not exhibit upgrading at PSMA-targeted biopsy received active treatment due to the detection of new CP at biopsy. This indicates that PSMA PET/CT may offer additional value compared to MRI in detecting csPCa, opening opportunities for further research and clinical applications.

### Reporting PSMA Activity in the Prostate

A practical issue for reporting PSMA PET/CT is the variation in SUV values between different PSMA ligands, with <sup>18</sup>F-based tracers generally showing higher SUV<sub>max</sub> values than <sup>68</sup>Ga-based tracers. Consequently, SUV<sub>max</sub> values cannot be universally applied across different centres using various PSMA tracers, making it challenging to determine usable cut-off points. To address these challenges, there are multiple initiatives for the standardisation of reporting activity in the prostate. The two most prominent ones are the PRIMARY score (Figure 1) and the PSMA expression score (Figure 2).<sup>6,7</sup> The PRIMARY score, which incorporates both the activity as well as the pattern of activity, has recently demonstrated better interrater reliability ( $\kappa = 0.65$ ) compared to the PI-RADS ( $\kappa = 0.48$ ) in a group of 242 patients<sup>8</sup>. Its diagnostic performance in detecting csPCa is comparable to that of mpMRI (sensitivity, 86% vs. 89%; specificity, 76% vs. 74%; positive predictive value, 88% vs. 88%; negative predictive value, 72% vs. 76%). When combined imaging is used, the sensitivity

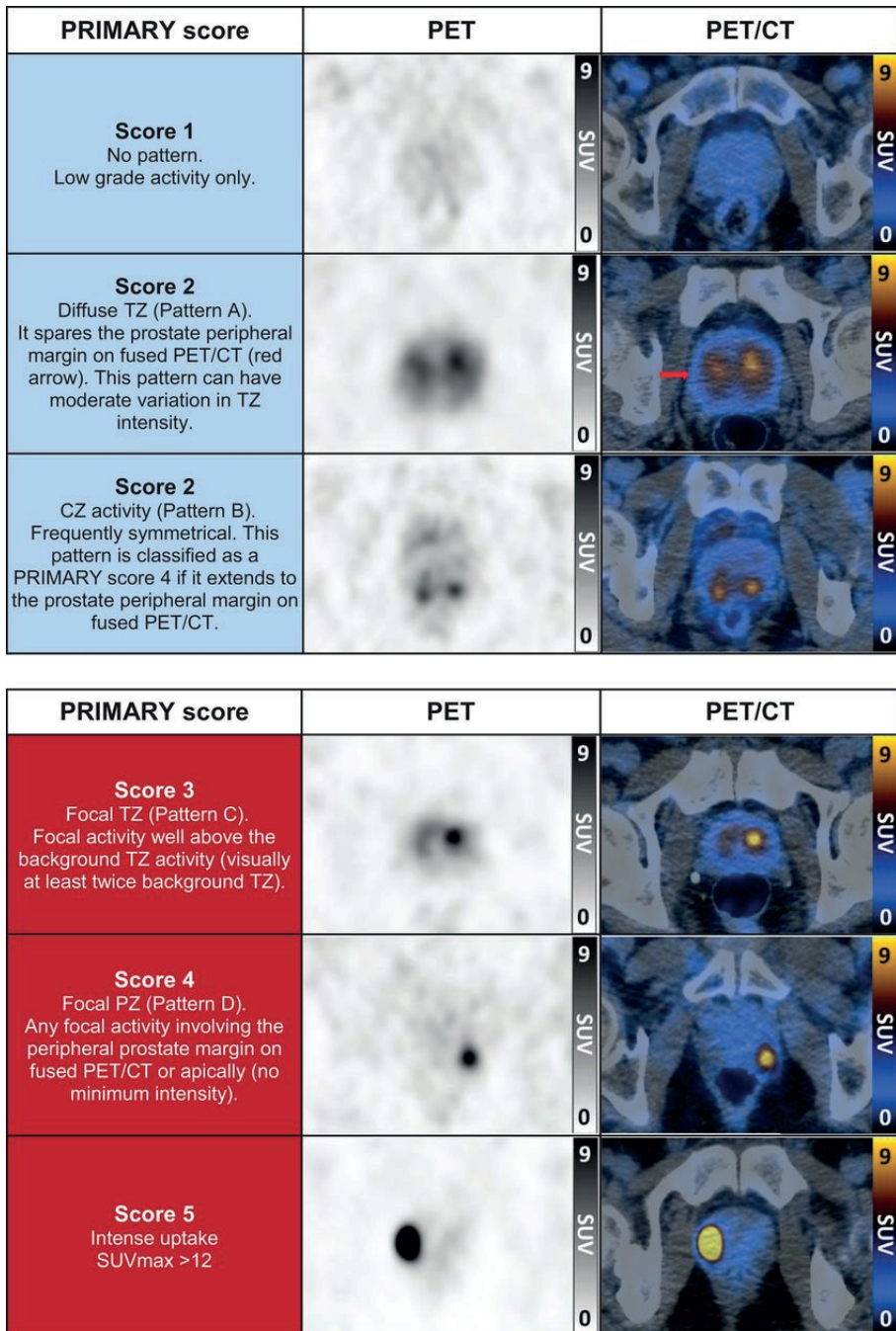
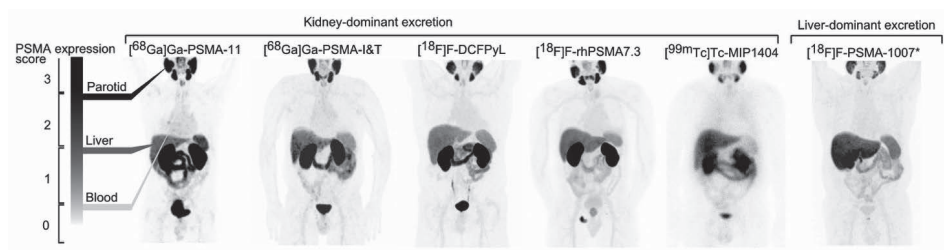


**Figure 1:** PRIMARY score, this figure was originally published in JNM. Emmett LM, Papa N, Buteau J, Ho B, Liu V, Roberts M, et al. The PRIMARY Score: Using intra-prostatic PSMA PET/CT patterns to optimise prostate cancer diagnosis. J Nucl 2022;jnumed.121.263448

increases to 94%, specificity to 68%, PPV to 86%, and NPV to 85%. However, a limitation of this score is its reliance on SUVmax for the highest score of 5, and currently, the available evidence is limited to the <sup>68</sup>Ga-PSMA-11 tracer.

The PSMA expression score compares the activity in the prostate gland to other areas of the body that express PSMA, thus addressing the unreliability of incorporating solely SUVmax.<sup>7</sup> However, the clinical performance of this score is yet to be determined. Both scoring systems were not available when our research for this thesis commenced and therefore, they are not included in our study.

To address the complexities concerning PSMA PET/CT reporting, Artificial Intelligence (AI) with deep learning could be instrumental in aiding the nuclear physician. Such models, encompassing both scan results and patient characteristics, might yield more accurate and generalisable outcomes. While AI models have been implemented in MRI in daily practice, their application in PSMA PET/CT is not utilised.<sup>9</sup>



Score	Reported PSMA Uptake	Uptake (PROMISE V2)
0	No	Equal to or lower than blood pool
1	Low	Equal to or lower than liver <sup>a</sup> and higher than blood pool
2	Intermediate	Equal to or lower than parotid gland and higher than liver <sup>1</sup>
3	High	Higher than parotid gland

a= For PSMA ligands with liver dominant excretion (eg, [18F]F-PSMA-1007), the spleen is recommended as the reference organ instead of the liver.

**Figure 2:** PSMA-expression score: Original publication in European Urology, combination of Table 3 and Supplementary Figure 3 from Seifert R, Emmett L, Rowe SP, Herrmann K, Hadaschik B, Calais J, *et al.* Second Version of the Prostate Cancer Molecular Imaging Standardized Evaluation Framework Including Response Evaluation for Clinical Trials (PROMISE V2). *Eur Urol* 2023;83:405-12. Re-use in line with Creative Commons CC-BY license



### Prospects for Pre-Biopsy PSMA PET/CT Implementation in Clinical Practice

Given the costs and limited availability of PSMA PET/CT, it is impractical to scan all patients with suspected PCa. For effective utilisation of PSMA PET/CT in a pre-biopsy context, two scenarios emerge as particularly interesting: first, the use of PSMA PET/CT in patients with a high suspicion of PCa but with a negative MRI or equivocal MRI. In the PASPoRT study, which is presented in **Chapter 4**, patients with an indication for AS showed significant biopsy upgrading. This was observed in patients with a Prostate-specific antigen (PSA) density greater than 0.15 ng/ml<sup>2</sup> and a negative MRI. In this group, 5 out of 14 patients exhibited upgrading, leading to an NNS of 2.8, compared to the NNS of 11 for the entire group. Thus, although the PASPoRT patients already had the diagnosis PCa, utilising PSMA PET/CT for patients with a negative MRI and elevated PSA density could be an efficient strategy, warranting prospective evaluation. Additionally, the PRIMARY 2 study follows up on the PRIMARY study by investigating the added diagnostic value of PSMA PET/CT in patients with negative multiparametric (mp) MRI and one 'red flag' (such as PSA > 10 ng/ml, PSA density > 0.1 ng/ml<sup>2</sup>, abnormal digital rectal examination, strong family history, PSA doubling time < 36 months, or PSA velocity > 0.75 ng/ml/year) or equivocal mpMRI (PI-RADS 3), versus standard care.<sup>10</sup> This study, whose enrolment is set to conclude in March 2025, plans to recruit 660 patients, with 330 in the control arm and 330 in the intervention arm. The outcomes will be crucial in determining the additional diagnostic value of pre-biopsy PSMA PET/CT in patients with a negative or equivocal mpMRI.

A second approach for the effective implementation of pre-biopsy PSMA PET/CT is in patients with a very high risk of metastatic disease before biopsy. This potential was explored in a study by Bodar and colleagues involving the <sup>18</sup>F-PSMA(DCFPyL) tracer.<sup>11</sup> The study included 60 patients with PSA levels ranging from 20 to 60, all demonstrating tracer uptake in the prostate exceeding that of normal tissue. CsPCa, defined as ISUP GG 2 or higher, was detected in 82% of patients through PSMA-targeted biopsies, increasing to 87% when combined with systematic biopsies. Notably, 45% of these patients were found to have metastatic disease as identified by PSMA PET/CT. This suggests that for patients with PSA levels in the 20–60 ng/ml range, utilising the <sup>18</sup>F-PSMA(DCFPyL) tracer could provide a diagnostic pathway that potentially bypasses MRI, offering a more streamlined process for identifying both localised and metastatic PCa. This approach could also reduce costs by eliminating MRI from the diagnostic pathway in most patients with a PSA higher than 20. However, further research is necessary to confirm these promising results across different tracers and with a validated method for reporting PSMA expression in the prostate.

Despite the various limitations associated with using PSMA PET/CT for detecting and characterising intraprostatic PCa, its capability to detect not only metastatic disease but also intraprostatic disease makes it a potential one-stop shop for selected patients

suspected of having high-risk PCa. Furthermore, it can visualise MRI occult csPCa, as can be seen in **Chapter 4**. These advantages make pre-biopsy PSMA PET/CT a valuable addition to the diagnostic pathway of PCa in selected patients. If the added value of an MRI of the prostate is limited, while direct PSMA provides all necessary information regarding biopsy indication and strategy, disease staging, and treatment decisions, PSMA may be the preferred imaging technique in future diagnostic pathways for some men. Figure 3 presents an example of how such a pathway may look like.

### **Integrating PSMA PET/CT in Active Surveillance**

Additional imaging and targeted biopsies lead to improved grading of the disease, but at the same time, it leads to stage migration.<sup>12</sup> This issue has been discussed mainly after the application of MRI, but it would also further apply when biopsies are performed after adding PSMA.<sup>12</sup> Following a combination of MRI-targeted biopsy, 17% of patients experienced downgrading at prostatectomy.<sup>3</sup> In our cohort of the PASPoRT, 40% of the patients who underwent prostatectomy experienced downgrading, suggesting that the addition of PSMA-targeted biopsy in men already diagnosed after systematic biopsy and MRI-targeted biopsy may potentially further increase the proportion of downgrading. Consequently, additional PSMA PET/CT may result in unjust exclusion from AS and could potentially lead to overtreatment. However, the activity on PSMA PET/CT could be a new biomarker to predict the aggressiveness of a tumour, and the exclusion of these patients could thereby be justified. However long time follow up of low-risk patients with a PSMA PET/CT is not yet available. The data on patients who were treated with a prostatectomy are promising and show activity on PSMA PET/CT, which is an independent prognostic biomarker for biochemical recurrence-free survival.<sup>13</sup> The follow up of our PASPoRT cohort could be a valuable asset in determining the prognostic value of PSMA PET/CT activity in patients with low and favourable intermediate risk PCa.

The evolution of more accurate imaging and biopsy protocols has expanded the inclusion criteria for AS.<sup>14</sup> With the rapid advancements in the field of prostate imaging and biopsy protocols, we anticipate further expansion of these criteria. Favourable PSMA characteristics could also be used as an argument to relax other AS criteria and expand eligibility. This could result in a more heterogeneous group eligible for AS, necessitating a more personalised approach to follow-up. Currently, there is one standardised AS follow-up protocol, but advancements in imaging and a deeper understanding of PCa present an opportunity for tailored follow-up protocols. With a personalised approach, the follow-up for patients with a low risk of upgrading could be de-escalated without jeopardising the success of AS.

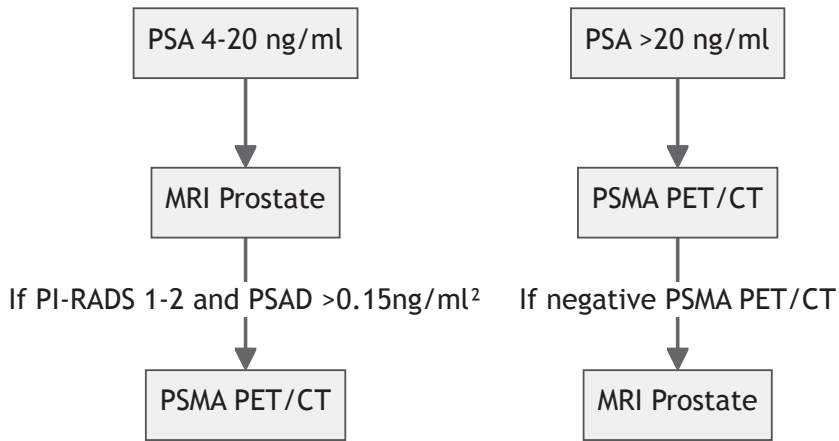


**Figure 3:** Possible future diagnostic pathway for biopsy naïve patients suspected of prostate cancer

Imaging could play a pivotal role in a minimally invasive follow-up protocol. While the role of MRI is established in the initial diagnosis of PCa, its value in subsequent evaluations is not yet clear and should not solely rely upon the need for repeat biopsies.<sup>15</sup> The Prostate Cancer Radiological Estimation of Change in Sequential Evaluation (PRECISE) score, developed to detect the differences between serial MRIs for predicting biopsy upgrading, still has an uncertain value.<sup>16</sup> **Chapter 4** demonstrated the role of the PSMA PET/CT in selecting patients for AS; however, it may also be important in AS follow-up. Combined with other factors, imaging could potentially reduce the number of patients undergoing unnecessary repeat biopsies, creating a less intense but equally effective AS protocol. The reduction of the number of patients indicated for repeat biopsy could result in a decrease in costs, making the introduction of the PSMA PET/CT in an AS protocol economical and valuable. An ongoing follow-up study of the PASPoRT includes patients who remain under AS and had an initial PSMA PET/CT with an SUVmax of 4 or higher. In addition to an MRI, these patients undergo a subsequent PSMA PET/CT after two years. The findings from this study are expected to offer more insights into the utility of follow-up PSMA PET/CT scans within an AS protocol.

### Virtual Biopsy

The recent advances in imaging, coupled with patient characteristics, present the intriguing possibility of a virtual biopsy, potentially eliminating the need for histological confirmation. This concept holds promise for more accurately assessing the potential malignancy of PCa and the necessity for curative treatment compared to traditional invasive prostate biopsies, as imaging can examine the whole prostate without an invasive procedure.

In a prostate needle biopsy, the pathologist's assessment is confined to the tissue sample obtained. As a result, their report can only provide highly accurate information about the specific millimetres of tissue examined. This limited scope means that while the biopsy can offer insights into the malignancy within the sampled area, it cannot conclusively predict the condition of the entire organ. Furthermore, is there a possibility of a false negative because a lesion was missed during the biopsy. That this way of diagnosing is not perfect is shown in the amount of up and downgrading at prostatectomy.<sup>2,17</sup>

The practice of treating malignancies without histological confirmation is not unprecedented. For instance, in the case of renal cell carcinoma, histological proof is reserved for radiologically indeterminate renal masses.<sup>18</sup> Omitting prostate biopsy from the diagnostic pathway could significantly reduce patient burden, considering that even the transperineal approach, though less invasive than the transrectal approach, can still lead to complications and discomfort.<sup>19</sup> As of today, the imaging information is not accurate enough to omit histological confirmation for all patients suspected of PCa. However, the integration of PSMA activity into advanced predictive models might change this in the foreseeable future. In the evaluation of the added value of PSMA PET/CT SUVmax in predicting ISUP GG  $\geq 2$  and  $\geq 3$  on prostate biopsy in **Chapter 3**, the study demonstrated that SUVmax significantly enhances the predictive capability of both models, especially for GG  $\geq 3$ . This highlights the utility of SUVmax in identifying patients with a high likelihood of harbouring GG  $\geq 3$  PCa. These insights complement existing research, such as results from the PRIMARY study, which posited that a combination of negative MRI and a SUVmax below 4 effectively reduces the necessity of prostate biopsy due to the low likelihood of csPCa.<sup>20</sup> Conversely, our findings suggest that a high SUVmax could potentially help select patients with a substantial risk of csPCa. This concept aligns with Ptasznik *et al.*'s observation that patients with a PI-RADS score of 4 or 5 and SUVmax above 8.7 invariably had GG  $\geq 2$ .<sup>21</sup>

The 'Say NO to Biopsy' (SNOTOB) study, a single-centre, single-arm, open-label study, aims to enrol 57 patients to explore a biopsy-free diagnostic pathway.<sup>22</sup> In this study, patients deemed at high risk for csPCa based on an <sup>18</sup>F-PSMA-1007 PET/CT diagnostic model will undergo RARP without prior biopsy. Should the results confirm the feasibility of treating patients without a biopsy, it could potentially lead to a paradigm shift in the diagnosis of patients with suspected PCa. It should however be acknowledged that besides a diagnostic purpose, biopsy information could be used during treatment decision-making or for tissue biomarkers.

### **Detection of Extraprostatic Extension**

After the detection of PCa, accurate staging is crucial for selecting the best treatment for patients. Local staging is particularly important for deciding on nerve-sparing robot-assisted radical prostatectomy (RARP). While nerve-sparing techniques can reduce the

risk of erectile dysfunction, they are associated with an increased risk of positive surgical margins (PSM), which elevates the likelihood of disease recurrence and cancer-specific mortality.<sup>23,24</sup> In **Part II, Chapter 6** validated multiple side-specific nomograms for EPE, while **Chapter 7** highlighted the Soeterik nomogram's effectiveness in reducing PSM in lobes with EPE. However, given the small size of our single-centre cohort, a larger multicentre study is necessary to confirm these initial positive results of the clinical implementation of a side-specific nomogram for EPE. To enhance the accuracy of these nomograms, incorporating additional variables or utilising machine learning and AI could be beneficial. For instance, the application of AI and radiomics features has shown the potential to improve EPE risk prediction.

Hou *et al.* developed an AI model demonstrating an impressive Area Under the Curve (AUC) of 86%, outperforming radiologists who achieved an AUC of 72% in EPE prediction.<sup>25</sup> In another study, the combined use of MRI index lesion radiomics within a machine learning model achieved high accuracy for EPE detection, reaching an overall accuracy of 83% in the training set. Additionally, Solari *et al.* explored the integration of PSMA PET/MR radiomics with MRI radiomics in PCa staging.<sup>26</sup> They evaluated nine support vector machine models incorporating PET and/or MRI radiomics features, including the apparent diffusion coefficient (ADC). Their findings suggested that the best-performing model included both PET and ADC radiomics, highlighting their complementary value. Van den Berg *et al.* demonstrated the development and external validation of an AI-driven MRI-based model for lesion-specific EPE prediction.<sup>27</sup> This model, encompassing a wide range of conventional and novel radiomics, showed excellent discriminative performance. The Random Forest model displayed robust performance in calibration for both internal and external test cohorts, surpassing the radiology interpretations in terms of accuracy, specificity, and positive predictive value in the external test cohort. However, all these innovative models require further validation and clinical testing before they can be reliable enough to be used in clinical practice.

The implementation of advanced models for the prediction of EPE, unlike symbolic AI or simple machine learning models like decision trees or linear regression, presents a notable challenge. These advanced models are not fully understood by people, creating a 'black box', where the factors impacting the model's results are not always clear. This complexity makes their application in daily clinical use more difficult.

### **The Staging of Lymph Node Invasion and Metastatic Disease**

In the staging of lymph node invasion (LNI) and metastatic disease, PSMA PET/CT is used for patients at risk, supported by multiple phase 3 trials.<sup>28–30</sup> However, the impact of this widely adopted imaging modality on disease-specific survival is not fully clear, despite promising

results in surrogate outcomes like biochemical recurrence and treatment failure. The 54-month follow-up of the proPSMA study presented by Kasivisvanathan at the 38th Annual EAU Congress indicated that patients with a negative PSMA PET/CT had a longer period of freedom from treatment failure compared to those with a positive node.<sup>31</sup> Similarly, a study by Meijer *et al.*, involving 145 patients with an LNI identified during extended pelvic lymph node dissection (ePLND), found that patients with lymph nodes not visible on PSMA PET/CT had a median biochemical recurrence (BCR) of 13.7 months, compared to 7.9 months for patients with visible nodes.<sup>32</sup>

Given the increased accuracy of PSMA PET/CT in detecting LNI and metastatic disease compared to conventional CT and bone scans, the necessity of staging ePLND in patients with a negative PSMA PET/CT is in question. The PSMA-SELECT trial is investigating the use of PSMA PET/CT as a tool for deciding between prostatectomy with or without ePLND. The primary outcome is the non-inferiority of BCR at 2 years.<sup>33</sup>

The widespread use of PSMA PET/CT for staging raises a dilemma about which patients should undergo this scarce and costly imaging modality. In **Chapter 8**, we examined whether the presence of a CP in prostate biopsy is an independent risk factor for metastatic disease on PSMA PET/CT, potentially guiding the selection for additional imaging. Our findings indicated that CP in biopsy does not independently predict metastatic disease. For risk group stratification in selecting patients for additional imaging, nomograms predicting lymph node invasion could be employed. However, incorporating the presence of CP/intraductal carcinoma in biopsy into these nomograms did not improve the prediction of LNI, supporting our conclusions about the limited predictive value of CP.<sup>34</sup>

## Conclusion

Imaging plays a crucial role in the detection and staging of PCa, from detecting abnormal lesions within the prostate to guiding biopsies and detecting metastatic disease. This thesis enhances the current knowledge regarding imaging in the primary diagnosis of PCa. Given the disease's spectrum from indolent to aggressive forms, precise detection and staging are essential to ensure that the most effective treatment options are provided. An improved understanding of csPCa risk prior to biopsy enables more accurate patient selection and improved biopsy targeting. In this context, PSMA PET/CT complements MRI, adding value. Although the long-term impact of PSMA PET/CT on disease-specific survival and quality of life remains to be fully clarified, its potential for managing both low, intermediate, and high-risk PCa is enormous, with future studies expected to provide further insights into these vital outcomes. Besides considering long-term outcomes, the costs and availability of pre-biopsy PSMA PET/CT are significant hurdles to its widespread application, particularly in anticipation of an influx of patients with the expected initiation of prostate cancer screening in Europe.<sup>35</sup>

Utilising a validated nomogram for side-specific EPE can enhance patient selection for nerve-sparing RARP and reduce the PSM rate. There is an expectation that future advanced models will significantly improve patient selection for nerve-sparing RARP. The continuous effort to refine patient selection for additional staging with PSMA PET/CT is underway, with the acknowledgement that CP is not an optimal candidate. This effort aims to ensure the optimal utilisation of this powerful, albeit scarce and costly, imaging modality.

## References

- 1 Mottet N, van den Bergh RCN, Briers E, Van den Broeck T, Cumberbatch MG, De Santis M *et al.* EAU-EANM-ESTRO-ESUR-SIOG Guidelines on Prostate Cancer-2020 Update. Part 1: Screening, Diagnosis, and Local Treatment with Curative Intent. *Eur Urol* 2021; **79**: 243–262.
- 2 Woythal N, Arsenic R, Kempkensteffen C, Miller K, Janssen J-C, Huang K *et al.* Immunohistochemical Validation of PSMA Expression Measured by 68Ga-PSMA PET/CT in Primary Prostate Cancer. *Journal of Nuclear Medicine* 2018; **59**: 238–243.
- 3 Schoots IG, Nieboer D, Giganti F, Moore CM, Bangma CH, Roobol MJ. Is magnetic resonance imaging-targeted biopsy a useful addition to systematic confirmatory biopsy in men on active surveillance for low-risk prostate cancer? A systematic review and meta-analysis. *BJU Int* 2018; **122**: 946–958.
- 4 Kawada T, Yanagisawa T, Rajwa P, Sari Motlagh R, Mostafaei H, Quhal F *et al.* Diagnostic Performance of Prostate-specific Membrane Antigen Positron Emission Tomography-targeted biopsy for Detection of Clinically Significant Prostate Cancer: A Systematic Review and Meta-analysis. *Eur Urol Oncol* 2022; : S2588-9311(22)00064–5.
- 5 Gao J, Zhang C, Zhang Q, Fu Y, Zhao X, Chen M *et al.* Diagnostic performance of 68Ga-PSMA PET/CT for identification of aggressive cribriform morphology in prostate cancer with whole-mount sections. *Eur J Nucl Med Mol Imaging* 2019; **46**: 1531–1541.
- 6 Emmett LM, Papa N, Buteau J, Ho B, Liu V, Roberts M *et al.* The PRIMARY Score: Using intra-prostatic PSMA PET/CT patterns to optimise prostate cancer diagnosis. *J Nucl Med* 2022; : jnumed.121.263448.
- 7 Seifert R, Emmett L, Rowe SP, Herrmann K, Hadaschik B, Calais J *et al.* Second Version of the Prostate Cancer Molecular Imaging Standardized Evaluation Framework Including Response Evaluation for Clinical Trials (PROMISE V2). *Eur Urol* 2023; **83**: 405–412.
- 8 Emmett L, Papa N, Counter W, Calais J, Barbato F, Burger I *et al.* Reproducibility and Accuracy of the PRIMARY Score on PSMA PET and of PI-RADS on Multiparametric MRI for Prostate Cancer Diagnosis Within a Real-World Database. *J Nucl Med* 2023; : jnumed.123.266164.
- 9 He M, Cao Y, Chi C, Yang X, Ramin R, Wang S *et al.* Research progress on deep learning in magnetic resonance imaging-based diagnosis and treatment of prostate cancer: a review on the current status and perspectives. *Front Oncol* 2023; **13**: 1189370.
- 10 Buteau JP, Moon D, Fahey MT, Roberts MJ, Thompson J, Murphy DG *et al.* Clinical Trial Protocol for PRIMARY2: A Multicentre, Phase 3, Randomised Controlled Trial Investigating the Additive Diagnostic Value of [68Ga]Ga-PSMA-11 Positron Emission Tomography/Computed Tomography in Men with Negative or Equivocal Multiparametric Magnetic Resonance Imaging for the Diagnosis of Clinically Significant Prostate Cancer. *Eur Urol Oncol* 2023; : S2588-9311(23)00253–5.
- 11 Bodar YJL, Boevé LMS, van Leeuwen PJ, Baars PC, Nieuwenhuijzen JA, van Haarst EP *et al.* Using prostate-specific membrane antigen positron-emission tomography to guide prostate biopsies and stage men at high-risk of prostate cancer. *BJU Int* 2023; **132**: 705–712.
- 12 Vickers A, Carlsson SV, Cooperberg M. Routine Use of Magnetic Resonance Imaging for Early Detection of Prostate Cancer Is Not Justified by the Clinical Trial Evidence. *Eur Urol* 2020; **78**: 304–306.
- 13 Roberts MJ, Morton A, Papa N, Franklin A, Raveenthiran S, Yaxley WJ *et al.* Primary tumour PSMA intensity is an independent prognostic biomarker for biochemical recurrence-free survival following radical prostatectomy. *Eur J Nucl Med Mol Imaging* 2022; **49**: 3289–3294.
- 14 PRIAS project - Active surveillance -. <https://www.prias-project.org/> (accessed 22 Jun2022).



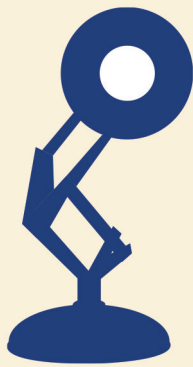
- 15 Rajwa P, Pradere B, Quhal F, Mori K, Laukhtina E, Huebner NA *et al.* Reliability of Serial Prostate Magnetic Resonance Imaging to Detect Prostate Cancer Progression During Active Surveillance: A Systematic Review and Meta-analysis. *Eur Urol* 2021; **80**: 549–563.
- 16 Bhanji Y, Mamawala M, de la Calle CM, Landis P, Epstein JI, Simopoulos DN *et al.* Prostate Cancer Radiological Estimation of Change in Sequential Evaluation (PRECISE) Magnetic Resonance Imaging Scoring to Predict Clinical Outcomes in Active Surveillance for Grade Group 1 Prostate Cancer. *Urology* 2023; **180**: 194–199.
- 17 Ahdoot M, Wilbur AR, Reese SE, Lebastchi AH, Mehralivand S, Gomella PT *et al.* MRI-Targeted, Systematic, and Combined Biopsy for Prostate Cancer Diagnosis. *N Engl J Med* 2020; **382**: 917–928.
- 18 Ljungberg B, Albiges L, Abu-Ghanem Y, Bedke J, Capitanio U, Dabestani S *et al.* European Association of Urology Guidelines on Renal Cell Carcinoma: The 2022 Update. *Eur Urol* 2022; : S0302-2838(22)01676–1.
- 19 Tan J-L, Papa N, Hanegbi U, Snow R, Grummet J, Mann S *et al.* Predictors of erectile dysfunction after transperineal template prostate biopsy. *Investig Clin Urol* 2021; **62**: 159–165.
- 20 Emmett L, Buteau J, Papa N, Moon D, Thompson J, Roberts MJ *et al.* The Additive Diagnostic Value of Prostate-specific Membrane Antigen Positron Emission Tomography Computed Tomography to Multiparametric Magnetic Resonance Imaging Triage in the Diagnosis of Prostate Cancer (PRIMARY): A Prospective Multicentre Study. *Eur Urol* 2021; **80**: 682–689.
- 21 Ptasznik G, Papa N, Kelly BD, Thompson J, Stricker P, Roberts MJ *et al.* High PSMA PET SUVmax in PI-RADS 4 or 5 men confers a high probability of significant prostate cancer. *BJU Int* 2022. doi:10.1111/bju.15736.
- 22 Wang C, Dong Q, Liu X, Ni M, Xie Q, Xiao J *et al.* Protocol for SNOTOB study: radical prostatectomy without prostate biopsy following 18F-PSMA-1007 PET/CT based on a diagnostic model: a single-centre, single-arm, open-label study. *BMJ Open* 2023; **13**: e073983.
- 23 Nguyen LN, Head L, Witiuk K, Punjani N, Mallick R, Cnossen S *et al.* The Risks and Benefits of Cavernous Neurovascular Bundle Sparing during Radical Prostatectomy: A Systematic Review and Meta-Analysis. *J Urol* 2017; **198**: 760–769.
- 24 Soeterik TFW, van MHHE, Dijkstra LM, Stomps S, Witjes JA, van BIPA. Nerve Sparing during Robot-Assisted Radical Prostatectomy Increases the Risk of Ipsilateral Positive Surgical Margins. *Journal of Urology* 2020; **204**: 91–95.
- 25 Hou Y, Zhang Y-H, Bao J, Bao M-L, Yang G, Shi H-B *et al.* Artificial intelligence is a promising prospect for the detection of prostate cancer extracapsular extension with mpMRI: a two-center comparative study. *Eur J Nucl Med Mol Imaging* 2021; **48**: 3805–3816.
- 26 Solari EL, Gafita A, Schachoff S, Bogdanović B, Villagrán Asiares A, Amiel T *et al.* The added value of PSMA PET/MR radiomics for prostate cancer staging. *Eur J Nucl Med Mol Imaging* 2021. doi:10.1007/s00259-021-05430-z.
- 27 van den Berg I, Soeterik TFW, van der Hoeven EJRI, Claassen B, Brink WM, Baas DJH *et al.* The Development and External Validation of Artificial Intelligence-Driven MRI-Based Models to Improve Prediction of Lesion-Specific Extraprostatic Extension in Patients with Prostate Cancer. *Cancers (Basel)* 2023; **15**: 5452.
- 28 Hope TA, Eiber M, Armstrong WR, Juarez R, Murthy V, Lawhn-Heath C *et al.* Diagnostic Accuracy of 68Ga-PSMA-11 PET for Pelvic Nodal Metastasis Detection Prior to Radical Prostatectomy and Pelvic Lymph Node Dissection: A Multicenter Prospective Phase 3 Imaging Trial. *JAMA Oncol* 2021; **7**: 1635–1642.

- 29 Pienta KJ, Gorin MA, Rowe SP, Carroll PR, Pouliot F, Probst S *et al.* A Phase 2/3 Prospective Multicenter Study of the Diagnostic Accuracy of Prostate Specific Membrane Antigen PET/CT with 18F-DCFPyL in Prostate Cancer Patients (OSPREY). *J Urol* 2021; **206**: 52–61.
- 30 Surasi DS, Eiber M, Maurer T, Preston MA, Helfand BT, Josephson D *et al.* Diagnostic Performance and Safety of Positron Emission Tomography with 18F-rhPSMA-7.3 in Patients with Newly Diagnosed Unfavourable Intermediate- to Very-high-risk Prostate Cancer: Results from a Phase 3, Prospective, Multicentre Study (LIGHTHOUSE). *Eur Urol* 2023; **84**: 361–370.
- 31 Kasivisvanathan V, Murphy DG, Link E, Lawrentschuk N, O'Brien J, Buteau JP *et al.* Baseline PSMA PET-CT is prognostic for treatment failure in men with intermediate-to-high risk prostate cancer: 54 months follow-up of the proPSMA randomised trial. *European Urology* 2023; **83**: S1797–S1798.
- 32 Meijer D, Ettema RH, van Leeuwen PJ, van der Kwast TH, van der Poel HG, Donswijk ML *et al.* The prognostic value of lymph node staging with prostate-specific membrane antigen (PSMA) positron emission tomography/computed tomography (PET/CT) and extended pelvic lymph node dissection in node-positive patients with prostate cancer. *BJU Int* 2023; **131**: 330–338.
- 33 Soeterik TFW, Wever L, Dijkman LM, Frederix GWJ, Van Melick HHE, Monninkhof EM *et al.* Clinical Trial Protocol for PSMA-SELECT: A Dutch National Randomised Study of Prostate-specific Membrane Antigen Positron Emission Tomography/Computed Tomography as a Triage Tool for Pelvic Lymph Node Dissection in Patients Undergoing Radical Prostatectomy. *Eur Urol Focus* 2022; **8**: 1198–1203.
- 34 de Barros HA, Remmers S, Luiting HB, van Leenders GJLH, Roobol MJ, Bekers EM *et al.* Predictive value of Cribriform and Intraductal Carcinoma for the Nomogram-Based Selection of Prostate Cancer Patients for Pelvic Lymph Node Dissection. *Urology* 2022; : S0090-4295(22)00537–4.
- 35 Gómez Rivas J, Leenen RCA, Venderbos LDF, Helleman J, de la Parra I, Vasilyeva V *et al.* Navigating through the Controversies and Emerging Paradigms in Early Detection of Prostate Cancer: Bridging the Gap from Classic RCTs to Modern Population-Based Pilot Programs. *Journal of Personalized Medicine* 2023; **13**: 1677.





# APPENDICES



# APPENDIX

DUTCH SUMMARY –  
NEDERLANDSE SAMENVATTING





## Nederlandse Samenvatting

Prostaat­kanker is een veel­voorkomende vorm van kanker die wordt geken­merkt door een aanzienlijk verschil tussen incidentie- en sterft­cijfers. Dit betekent dat niet alle vormen van prostaat­kanker de levens­verwachting beïnvloeden. Er is een groot verschil in ernst van prostaat­kanker: van relatief onschuldige tot agres­sieve vormen. De vorm die invloed kan hebben op de levens­verwachting wordt ‘klinisch significant’ genoemd, en de vorm die dat niet heeft wordt ‘klinisch niet significant’ genoemd. Nauwkeurige detectie en stadiëring van prostaat­kanker zijn hierdoor essentieel om patiënten te voorzien van de optimale behandel­strategieën. Deze strategieën zijn gericht op het verbeteren van de levens­verwachting, met een zo laag mogelijke negatieve impact op de kwaliteit van het leven. Tegelijkertijd moeten onnodige diagnoses en behandel­ingen worden geminimaliseerd. De introductie van geavanceerde beeld­vormingstechnieken in de diagnose en stadiëring van prostaat­kanker heeft het diagnostisch traject aanzienlijk verbeterd. Dit proefschrift draagt hieraan bij door het gebruik van de Prostaat Specifiek Membraan Antigeen Positron Emissie Tomografie/Computertomografie (PSMA PET/CT) en de Magnetic Resonance Imaging (MRI) van de prostaat te onderzoeken bij de diagnose en het bepalen van een behandel­strategie voor prostaat­kanker.

### Deel I: De detectie van klinisch significante prostaat­kanker

In het eerste gedeelte van dit proefschrift ligt de aandacht op het detecteren van prostaat­kanker in de prostaat met de Prostaat Specifiek Membraan Antigeen (PSMA) activiteit die gezien wordt op de PSMA Positron Emissie Tomografie/Computertomografie (PET/CT). Deze beeld­vormingstechniek wordt met name gebruikt voor het detecteren van uitgezaaide prostaat­kanker, maar er is steeds meer bewijs dat het ook gebruikt kan worden om kanker te detecteren in de prostaat. Het eerste gedeelte van dit proefschrift draagt hieraan bij.

In **hoofdstuk 2** wordt de effectiviteit van de <sup>18</sup>F-PSMA-1007 tracer voor het karakteriseren van in de prostaat gelegen prostaat­kanker onderzocht. Voor dit deel van het onderzoek werden prostaten die in verband met prostaat­kanker waren verwijderd met een prostatectomie aanvullend onderzocht door de patholoog. De patholoog kleurde afwijkingen in de prostaat met een PSMA-kleuring en gaf hieraan een PSMA Immunoreactieve Score. Daarnaast is retrospectief de PSMA PET/CT bekeken en zijn alle afwijkingen in de prostaat gemeten op maximale activiteit (SUVmax). Er is een significante correlatie gevonden tussen de SUVmax en de kwaadaardigheid van de prostaat­kanker, via een hogere International Society of Urologic Pathology (ISUP) Grade Group (GG). Verder is er een significant verband gevonden tussen de hoeveelheid PSMA-expressie die zichtbaar was in de tumor bij de pathologie, aangegeven door de PSMA Immunoreactieve Score, en een hogere activiteit op de PSMA PET/CT. Deze

relaties waren beide onafhankelijk van de tumorgrootte. De PSMA PET/ CT heeft als beperking dat zij hele kleine afwijkingen niet detecteert. Voor het cohort van het onderhavige onderzoek was dit echter geen probleem. De klinisch significante prostaatkankers waren namelijk groot genoeg voor detectie door de PSMA PET/CT. Als in het gebruikte cohort een drempel van een SUVmax van 4 was gebruikt om te differentiëren tussen positief en negatief, werd slechts één afwijking met klinisch significante prostaatkanker gemist. Beperkingen van deze studie zijn: (1) het niet includeren van laag-risicopatiënten, (2) de evaluatie van alleen histologisch bevestigde tumoren, en (3) het lokaliseren van afwijkingen met een lage dosis CT.

In **hoofdstuk 3** wordt de toegevoegde waarde van de SUVmax van de PSMA PET/CT in het voorspellen van klinisch significante prostaatkanker bij prostaatbiopsie geanalyseerd. Hiervoor zijn twee definities van klinisch significante prostaatkanker gebruikt: ISUP GG 2 of hoger (dit is de algemeen geaccepteerde grens) en ISUP GG 3 of hoger. Vanaf ISUP GG 3 is een actief afwachtend beleid volgens de richtlijn niet meer mogelijk. Dit werd onderzocht door een model te ontwikkelen voor het voorspellen van klinisch significante prostaatkanker in een retrospectief cohort. Hierin werd de leeftijd van de patiënt, de MRI-uitslag en het PSA-gehalte in het bloed gebruikt. Vervolgens werd het model met alleen deze variabelen vergeleken met een model waarbij, naast de eerder genoemde variabelen, de SUVmax van de PSMA PET/CT werd opgenomen. Deze studie laat zien dat SUVmax de voorspellende capaciteit van modellen met beide definities voor klinisch significante prostaatkanker aanzienlijk verbetert, vooral bij de definitie van ISUP GG 3 of hoger. Dit benadrukt het nut van SUVmax bij het identificeren van patiënten met een hoge kans op het hebben van ISUP GG  $\geq$  3 prostaatkanker. Onze bevindingen suggereren dat een hoge SUVmax kan helpen bij het selecteren van patiënten met een substantieel risico op een kwaadaardige vorm van prostaatkanker. De voornaamste beperkingen van deze studie waren dat de PSMA PET/CT plaatsvond na de diagnose en dat er geen patiënten zonder de diagnose prostaatkanker in het cohort zaten.

**Hoofdstuk 4** gaat in op de toevoeging van PSMA PET/CT en gerichte biopsie bij patiënten die recentelijk waren gestart met actief afwachtend beleid voor laag of laag-intermediair risico prostaatkanker. Deze patiënten hadden bij hun initiële diagnose een MRI gekregen en bij een zichtbare afwijking kregen patiënten MRI-gerichte biopten. Bij dit onderzoek werd er gekeken of aanvullende PSMA-gerichte biopten ervoor zorgden dat er meer kwaadaardige kanker werd gevonden. Uit deze studie bleek dat het aantal benodigde scans om biopsie-upgrading te detecteren 11 is. Deze upgrading kwam vaker voor bij patiënten zonder afwijkingen op de MRI. Onze resultaten lijken erop te wijzen dat PSMA PET/CT met aanvullende biopten een deel van de onderstadiëring in het huidige diagnostische traject kan verminderen. Een beperking van deze studie was dat niet alle patiënten aanvullende biopten ontvingen. Alleen de patiënten met een vermoedelijke laesie die niet gedekt werd door de vorige biopsie op PSMA PET/CT, ontvingen aanvullende biopten.

In **hoofdstuk 5** wordt besproken of het mogelijk is om prostaatbiopten achterwege te laten door de introductie van de PSMA PET/CT. In een cohort van 451 patiënten hadden alle 74 patiënten met een SUVmax groter dan 16, klinisch significante prostaatkanker. Bovendien had van de 185 patiënten met een verdachte MRI, geduid als een PI-RADS 4 of hoger in combinatie met een SUVmax boven 8, 98% klinisch significante prostaatkanker. Deze bevindingen suggereren dat een diagnostisch traject waarbij patiënten een prostatectomie ontvangen zonder biopsie, in de toekomst mogelijk kan zijn als er op de beeldvorming een sterk vermoeden is van klinisch significante prostaatkanker. Dit laat onverlet dat biopsie meer informatie biedt dan alleen een wel of geen klinisch significante prostaatkanker. Andere informatie die onder andere uit biopten wordt bepaald zijn de noodzaak voor DNA-testen, en essentiële gegevens voor het plannen van radicale of focale chirurgie.

## **Deel II: De adequate stadiëring van prostaatkanker**

In deel II van dit proefschrift worden de uitdagingen bij het bepalen van het stadium van prostaatkanker besproken. Hierbij wordt benadrukt hoe belangrijk het is om beschikbare beeldvormingstechnieken effectief te gebruiken en te combineren met andere gegevens, zoals in de vorm van een nomogram.

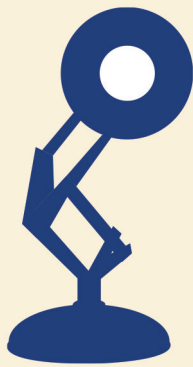
In **hoofdstuk 6** worden de validatie van vier op MRI gebaseerde nomogrammen - Soeterik, Martini, Nyarangi-Dix en Wibmer - voor het voorspellen van zij-specifieke extraprostatie extensie (EPE) in een grote Europese dataset gepresenteerd. Het wel of niet aanwezig zijn van EPE is belangrijk voor het wel of niet uitvoeren van een zenuwsparende prostatectomie. Dit zorgt voor een mogelijk beter behoud van erectiele functie, maar zorgt er ook voor dat het risico op een positief snijvlak hoger wordt. In de richtlijn wordt daarom aanbevolen om niet zenuwsparend te opereren aan de kant van de EPE. Omdat de uitslag van alleen de MRI hiervoor onvoldoende betrouwbaar is, worden nomogrammen gebruikt.

De onderzochte nomogrammen vertoonden een redelijk discriminatoir vermogen, met Area Under the Curve waarden variërend van 72% tot 75%. Voor risicodrempels van 0 tot 40% toonden de Soeterik, Martini en Nyarangi-Dix nomogrammen een redelijke tot goede kalibratie. Echter, het Wibmer nomogram overschatte het risico op EPE vanaf een voorspelde kans van 25%. Decision Curve Analysis gaf de klinische bruikbaarheid van de Soeterik, Martini en Nyarangi-Dix nomogrammen aan voor een voorspelde kans tussen 8% en 40%. Het Nyarangi-Dix nomogram, dat meer gedetailleerde MRI gegevens zoals tumor capsulaire contactlengte en de score van de Europese Vereniging voor Urogenitale Radiologie bevatte, vertoonde de beste prestaties. Toch kan de extra tijd van de radioloog voor het verzamelen van deze variabelen, de praktische bruikbaarheid van het nomogram beperken. Het onderzoek had als beperkingen de potentiële informatiebias vanwege het retrospectieve ontwerp en het ontbreken van een centrale MRI-beoordeling.

**Hoofdstuk 7** beschrijft de implementatie van het Soeterik nomogram in 50 patiënten voor de behandeling van prostaatkanker. Deze groep werd vergeleken met een retrospectief cohort van 50 patiënten die waren geopereerd voorafgaand aan de implementatie van het nomogram. In deze studie keken we of de toevoeging van de uitslag van het nomogram ervoor zorgde dat er meer zenuwsparend werd geopereerd zonder dat het aantal positieve snijvlakken toenam. Wij zagen in dit onderzoek dat er minder positieve snijvlakken waren aan de kant van EPE. Er werd geen verschil gezien in hoe vaak er zenuwsparend werd geopereerd. Dit resultaat zou te wijten kunnen zijn aan verhoogd bewustzijn van de uroloog over de plaats van de tumor en de kans op EPE door het nomogram. Een beperking van dit onderzoek was dat de ervaring van de uroloog, die de uitkomsten na de operatie beïnvloedt, niet in de studie werd meegenomen. Daarnaast werd de aanbevolen drempel van 20% voor het nomogram niet strikt nageleefd door de urologen.

In **hoofdstuk 8** wordt onderzocht of de aanwezigheid van een cribriforme groei in prostaatbiopsie een onafhankelijke risicofactor is voor uitgezaaide prostaatkanker gevonden op de PSMA PET/CT. De PSMA PET/CT wordt door de richtlijn aanbevolen om te gebruiken voor het vinden van metastasen. Omdat er maar beperkte scan capaciteit is, moet er doelmatig worden omgaan met de beschikbare ruimte. Cribriforme groei is een groeipatroon dat gelinkt is aan negatieve uitkomsten na behandeling. Mogelijk kunnen we dit gebruiken voor het selecteren van patiënten voor een aanvullende scan. Uit ons onderzoek kwam naar voren dat cribriforme groei in biopsie geen onafhankelijke risicofactor was. Bovendien kwam cribriforme groei niet naar voren als een significante risicofactor in verschillende subgroep analyses, waaronder die voor intermediaire of hoge risicogroepen, noch in subgroepen met ISUP GG 2 of 3. Toen een drempel van hoog-risicoziekte of ISUP GG 3 werd toegepast, conform de richtlijn van de Europese Vereniging van Urologie, werd 2% van de patiënten met metastatische ziekte op PSMA PET/CT gemist. Dit leidde tot een 18% vermindering in het aantal uitgevoerde PSMA PET/CT's in ons cohort. Cribriforme groei was in ons cohort geen zinvol selectie criterium voor een aanvullende PSMA PET/CT voor het detecteren van gemetastaseerde prostaatkanker.





# APPENDIX

CURRICULUM VITAE AUCTORIS





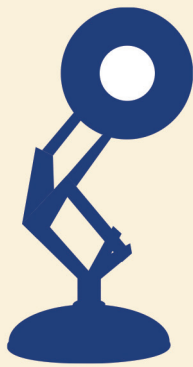
## Curriculum Vitae Auctoris



Joris Heetman was born on the 21st of January 1993 in Assen, the Netherlands. He was raised in Norg by Gies Heetman and Juliette Heetman-Cleton, along with his younger brother, Jelle Heetman. He graduated from athenaeum at the Dr. Nassaucollege in Assen in 2011. After one year of studying aerospace engineering in Delft, he started his studies in Medicine at the University of Utrecht. In his last year of medicine, his interest in urology and academic research began after a clinical clerkship in urology at the Sint Antonius Hospital. Following the clinical clerkship, he published a case series as a letter to the editor concerning prostate-specific membrane

antigen for the detection of prostate cancer in the prostate gland, under the supervision of Dr. van den Bergh.

Once he graduated with a Master of Science in Medicine in 2019, he began working as a resident not in training at the Department of Surgery at the Franciscus Gasthuis in Rotterdam. After one year, he continued as a resident not in training at the Department of Urology at the Sint Antonius Hospital in Nieuwegein. In 2021, after one year of working at the Sint Antonius Hospital, he started a one-year full-time research position under the supervision of Dr. van den Bergh and Dr. van Melick. After this year, he split his time between research and working as a resident not in training. During his research period, he had the opportunity to present his research multiple times at national and international congresses. In March 2024, he started his urology residency training program at the surgical department at the Sint Antonius Hospital in Nieuwegein. He lives happily with Lilian Boer in Utrecht.



# APPENDIX

## LIST OF PUBLICATIONS

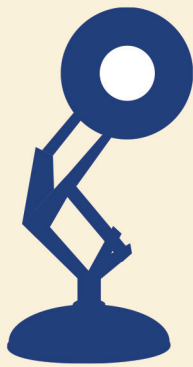


## List of Publications

1. **Heetman JG**, Paulino Pereira LJ, Kelder JC, Soeterik TFW, Wever L, Lavalaye J, van der Hoeven EJ RJ, Lam MGEH, van Melick HHE, van den Bergh RCN. **The additional value of  $^{68}\text{Ga}$ -PSMA PET/CT SUVmax in predicting ISUP GG $\geq$ 2 and ISUP GG $\geq$ 3 prostate cancer in biopsy.** *Prostate*. 2024 May 5. doi: 10.1002/pros.24716. Epub ahead of print. PMID: 38704755.
2. **Heetman JG**, van der Hoeven EJ RJ, Rajwa P, Zattoni F, Kesch C, Shariat S, Dal Moro F, Novara G, La Bombarda G, Sattin F, von Ostau N, Pötsch N, Baltzer PAT, Wever L, Van Basten JPA, Van Melick HHE, Van den Bergh RCN, Gandaglia G, Soeterik TFW; European Association of Urology Young Academic Urologists Prostate Cancer Working Party. **External validation of nomograms including MRI features for the prediction of side-specific extraprostatic extension.** *Prostate Cancer Prostatic Dis*. 2023 Nov 6. doi: 10.1038/s41391-023-00738-3. Epub ahead of print. PMID: 37932522.
3. **Heetman JG**, Hermsen R, Exterkate L, Küsters-Vandevelde HVN, Brouwer LJM, Somford DM, van den Bergh RCN, van Basten JA. **Immunohistochemical and histopathological validation of 18 F-PSMA-1007 PET/CT for intraprostatic cancerous lesions.** *Prostate*. 2023 Oct;83(14):1332-1341. doi: 10.1002/pros.24595. Epub 2023 Jul 16. PMID: 37455399.
4. **Heetman JG**, Versteeg R, Wever L, Paulino Pereira LJ, Soeterik TFW, Lavalaye J, de Bruin PC, van den Bergh RCN, van Melick HHE. **Is cribriform pattern in prostate biopsy a risk factor for metastatic disease on  $^{68}\text{Ga}$ -PSMA-11 PET/CT?** *World J Urol*. 2023 Aug;41(8):2165-2171. doi: 10.1007/s00345-023-04467-z. Epub 2023 Jun 17. Erratum in: *World J Urol*. 2023 Oct;41(10):2877. doi: 10.1007/s00345-023-04615-5. PMID: 37330440.
5. **Heetman JG**, Lavalaye J, Polm PD, Soeterik TFW, Wever L, Paulino Pereira LJ, van der Hoeven EJ RJ, van Melick HHE, van den Bergh RCN. **Gallium-68 Prostate-specific Membrane Antigen Positron Emission Tomography/Computed Tomography in Active Surveillance for Prostate Cancer Trial (PASPoRT).** *Eur Urol Oncol*. 2024 Apr;7(2):204-210. doi: 10.1016/j.euo.2023.05.004. Epub 2023 Jun 7. PMID: 37296065.
6. **Heetman JG**, Soeterik TFW, Wever L, Meyer AR, Nuininga JE, van Soest RJ, van Melick HHE, van Basten JPA, van den Bergh RCN. **A side-specific nomogram for extraprostatic extension may reduce the positive surgical margin rate in radical prostatectomy.** *World J Urol*. 2022 Dec;40(12):2919-2924. doi: 10.1007/s00345-022-04191-0. Epub 2022 Nov 7. PMID: 36344738.

7. Paulino Pereira LJ, **Heetman JG**, van den Bergh RCN, van Melick HHE. **Superfast Magnetic Resonance Imaging-based Diagnostic Pathway for Prostate Cancer.** Eur Urol Open Sci. 2022 Oct 25;46:30-32. doi: 10.1016/j.euros.2022.09.017. PMID: 36310760; PMCID: PMC9615134.
8. **Heetman JG**, Wever L, Paulino Pereira LJ, van den Bergh RCN. **Clinically Significant Prostate Cancer Diagnosis Without Histological Proof: A Possibility in the Prostate-specific Membrane Antigen Era?** Eur Urol Open Sci. 2022 Aug 20;44:30-32. doi: 10.1016/j.euros.2022.06.013. PMID: 36046616; PMCID: PMC9421196.
9. van Grevenstein WMU, van der Linde EM, **Heetman JG**, Lange JF, Ten Cate TJ, Wauben LSG, Dekker-van Doorn CM. **Crew Resource Management Training for Surgical Teams, A Fragmented Landscape.** J Surg Educ. 2021 Nov-Dec;78(6):2102-2109. doi: 10.1016/j.jsurg.2021.05.006. Epub 2021 Jun 13. PMID: 34134934.







# APPENDIX

DANKWOORD



## Dankwoord

De afgelopen jaren heb ik met veel plezier aan dit onderzoek gewerkt. Tijdens mijn promotieonderzoek heb ik veel geleerd, van de analyse van gegevens tot het maken van een goede en haalbare planning. In deze tijd heb ik veel hulp gehad van mensen om mij heen om er iets moois van te maken.

Ik zou graag mijn dank extra willen uitspreken naar een aantal personen in het bijzonder.

Geachte Dr. R.C.N. van den Bergh, Beste Roderick, heel erg bedankt dat jij mij hebt geïnteresseerd voor het vak urologie en voor de wetenschap. Als coassistent vroeg jij aan mij: *“Moet jij geen uroloog worden?”*. Dit heeft mij aan het denken gezet, en ik ben deze weg ingeslagen met veel plezier! Tijdens ditzelfde coschap kreeg ik een patiëntenlijstje dat, met heel veel hulp van jou, uitmondde in mijn eerste publicatie! Ik ben daarnaast erg dankbaar en trots dat ik de PASPoRT-studie, die jij hebt opgezet, heb mogen afmaken en publiceren. Het heeft nu zelfs de richtlijn gehaald!

Geachte Dr. H.H.E. van Melick, Beste Harm, na mijn coschap urologie stond er in mijn beoordeling door jou: *is welkom om in verder traject zich te ontwikkelen*. Bedankt voor die mooie kans, en dat ik mij verder heb kunnen ontwikkelen in het mooiste specialisme dat de geneeskunde te bieden heeft. Als opleider urologie van het Sint Antoniusziekenhuis heb ik veel van jou geleerd, ook al was ik toen nog niet in opleiding tot uroloog.

Geachte prof. M.G.E.H. Lam, Beste Marnix, heel erg bedankt dat ik onder jou mocht promoveren! Jouw kritische blik en begeleiding zorgden ervoor dat het een uiteindelijk mooi haalbaar en samenhangend project is geworden. Ik heb hiervoor nog heel wat ideeën moeten schrappen, maar anders was het nooit afgekomen.

Geachte Dr. T.W.F. Soeterik, Beste Timo, dankzij jou ben ik dit mooie promotietraject gestart. Ik ben verdergegaan met projecten die jij nog had lopen en heb veel aan je hulp gehad. Jouw connecties met de YAU en jouw nomogram hebben geresulteerd in twee hele mooie hoofdstukken in dit boekje. Daarnaast heb ik vaak in jouw boekje gekeken als inspiratie.

Geachte Dr. J.P.A. van Basten, Beste JP, het was mij een waar genoegen om drie artikelen met jou te schrijven. Jouw kritische blik heeft mijn manier van schrijven een stuk beter gemaakt, en bedankt dat je mij hebt benaderd om de PEEP 2 te analyseren en te schrijven! Ik ben erg trots op dat stuk.

Geachte Dr. E.J.R.J. van der Hoeven, Dr. J. Lavalaye en Drs. R. Hermsen, Beste Erik, Jules en Rick. Zonder jullie hulp was dit proefschrift, dat veel beeldvorming behandelt, er nooit gekomen! Erik, jij hebt als radioloog een groot gedeelte van de MRI's die ik heb gebruikt verslagen, waaronder ook een hoop herbeoordelingen in je vrije tijd, waarvoor dank. Jules, jij bent als nucleair geneeskundige de PSMA-expert van het Sint Antonius Ziekenhuis, ik heb veel gehad aan je hulp en je kennis. Rick, samen hebben wij het artikel in hoofdstuk twee geschreven, bedankt voor de fijne samenwerking. Jij hebt als nucleair geneeskundige alle scans nog een keer beoordeeld, wat behoorlijk wat tijd heeft gekost.

Geachte leden van de promotie- en beoordelingscommissie, dank voor het beoordelen van dit proefschrift.

Beste urologen, arts-assistenten, onderzoekers, verpleegkundigen van de F2 en poli medewerkers van de poli urologie. Urologen, bedankt voor alles wat jullie mij hebben geleerd in mijn jaren als ANIOS. Ik had mij geen betere plek kunnen wensen; het was een veilig leerklimaat en altijd gezellig tijdens de lunch! Daarnaast veel dank voor de ruimte die ik heb gekregen om aan mijn onderzoek te werken. Doordat ik een vijftig procent onderzoeksaanstelling kreeg, heb ik dit mooi kunnen afmaken.

Collega-assistenten, bedankt voor jullie collegialiteit. Ik heb het geluk gehad om al die jaren omringd te zijn door fijne collega's; het was mij een waar genoegen om met jullie de poli, de spoed en de zaal te bemannen.

Onderzoekers, toen ik begon met onderzoek in het Antonius moesten Lieke en ik elke dag maar kijken waar we konden zitten, nu is er, door jullie inzet, een echte promovendi kamer en is de groep een stuk groter. Heel erg bedankt voor de koffie- en brainstormmomenten, en natuurlijk de EMUC! Ik kijk nu al uit naar jullie meesterwerken, Lieke, Leonor, Cato, Anne en Rosemarijn!

Verpleegkundigen van de F2, aan het begin moesten jullie even aan mij wennen (en ik aan jullie) maar uiteindelijk hebben we een hele fijne samenwerking gehad! Ik deed met veel plezier de afdeling en dat kwam grotendeels door jullie. De opleidingsplek heb ik grotendeels te danken aan jullie goede maar ook kritische referentie!

Poli medewerkers van de urologie, bedankt voor de fijne samenwerking, het heeft mij flink wat uurtjes op de fiets gekost om al het lekkers dat er stond op de poli weer te verbranden.

Vrienden van de Sweder, Partout, Lans en uit Norg, bedankt voor alle afleiding en hulp! Nu al zin in de borrel.

Lieve mam, bedankt voor alle steun de afgelopen jaren en dat ik af en toe mocht bijkomen in Norg. Het is niet altijd makkelijk geweest om twee eigenwijze puberzonen in je eentje op te voeden nadat papa overleed, maar het is in je eigen woorden toch redelijk gelukt. Ik ben als arts in jouw voetsporen getreden en vind het fijn om met jou te kunnen praten over de zin en onzin in de gezondheidszorg. Je kritische denken en arbeidsethos heb je aan mij overgedragen en hebben ervoor gezorgd dat ik ben wie ik nu ben. Nogmaals dank, mam!

Lief klein broertje, al meer dan 20 jaar toren jij boven mij uit qua lengte. Sorry dat je al die jaren naar dat geneeskunde gepraat hebt moeten luisteren van mam en mij, dit gaat denk ik helaas nog wel even door. Bedankt dat je altijd voor mam en mij klaarstaat, zonder jou hulp tijdens het klussen was ons huis nooit afgekomen! Daarnaast is het ook altijd leuk om met jou te praten over onze gezamenlijke nerdhobby's die we al delen zolang ik mij kan herinneren.

Allerliefste Lil, wij zijn nu al 7 jaar samen. Elke dag ben ik weer superblij om een dag met jou door te brengen. De afgelopen jaren was ik veel met mijn werk en onderzoek bezig. Bedankt dat jij mij die ruimte hebt gegeven. Jij hebt de afgelopen jaren vaak genoeg gevraagd: *"Ben je nou alweer aan het werk?"* Vaak was het antwoord ja, en dit is dan eindelijk het resultaat. Al heb ik er ook veel aan gehad dat jij mij even weg trok van mijn werk om even te genieten. Samen zijn we nu grote stappen aan het maken en hebben we samen ons eigen plekje in Utrecht. Ik ben er volledig van overtuigd dat we samen heel veel mooie herinneringen gaan maken in ons koophuis op de Zandhofsestraat!





